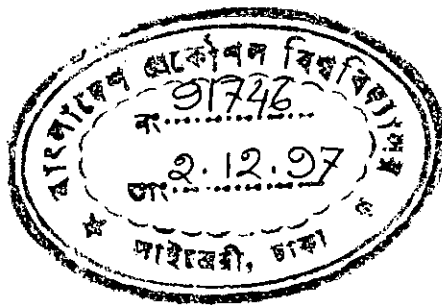


**DETERMINATION OF OPTIMUM TOOL GEOMETRY
OF A CEMENTED CARBIDE TOOL FOR CUTTING
A STAINLESS STEEL MATERIAL**

A Thesis

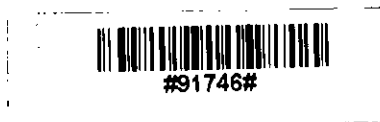
by

AMAL KUMAR NAG



Department of Industrial and Production Engineering
Bangladesh University of Engineering and Technology
Dhaka-1000, Bangladesh

October, 1997



**DETERMINATION OF OPTIMUM TOOL GEOMETRY
OF A CEMENTED CARBIDE TOOL FOR CUTTING
A STAINLESS STEEL MATERIAL**

A Thesis

by

AMAL KUMAR NAG

Submitted to the Department of Industrial and Production Engineering, Bangladesh University of Engineering and Technology, Dhaka in partial fulfillment of the requirement for the degree of MASTER OF ENGINEERING (IP).

October, 1997

Department of Industrial and Production Engineering
Bangladesh University of Engineering and Technology
Dhaka-1000, Bangladesh

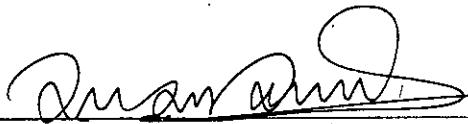
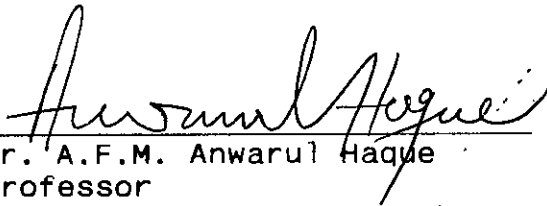

**DETERMINATION OF OPTIMUM TOOL GEOMETRY
OF A CEMENTED CARBIDE TOOL FOR CUTTING
A STAINLESS STEEL MATERIAL**

A Thesis

by

AMAL KUMAR NAG

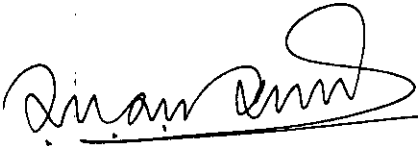
Approved as to the style and content by :

1. 
Dr. A.K.M. Nurul Amin
Professor & Head
Dept. of I.P.E., BUET, Dhaka
Chairman
2. 
Dr. A.F.M. Anwarul Haque
Professor
Dept. of I.P.E., BUET, Dhaka
Member
2. 
Dr. Ahsan Ali Khan
Professor
Dept. of I.P.E., BUET, Dhaka
Member

Department of Industrial and Production Engineering
Bangladesh University of Engineering and Technology
Dhaka-1000, Bangladesh

C E R T I F I C A T E

This is to certify that the thesis work was done by me
and this work has not been submitted elsewhere for award
of any degree or diploma.


Countersigned

Amal Kumar Nag
Author

ACKNOWLEDGEMENT

It is a matter of great pleasure for the author to have an opportunity to acknowledge his indebtedness and profound gratitude to Dr. A.K.M. Nurul Amin, Professor & Head, Department of Industrial and Production Engineering, Bangladesh University of Engineering and Technology (BUET), Dhaka for his inspiration, expert guidance, continuous supervision, proper advice and suggestions regarding experimental works. He also expressing that project and thesis could not have been completed without his hopeful encouragement.

The author wishes to express his heartfelt gratitude to Dr. M. Anwarul Azim, Professor, Department of Industrial and Production Engineering, BUET for providing him all facilities in the department at various stages of the work, during the author's M.Engg. degree.

The author is also indebted to acknowledge to Professor Dr. Ahsan Ali Khan, Professor, Department of Industrial and Production Engineering, BUET for his cordial co-operations, inspirations and valuable advice at different times of the period of M.Engineering.

The author is thankful to Mr. Abu Taleb and Mr. Sankar Das of Machine Tools Lab., Industrial & Production Engineering department, BUET for their extended hand to performe the project work.

Thanks are also given to the Superintendent, Foreman, and to all other Instructors and Operators of the Machine Shop, BUET also all the employees of Metal Cutting Workshop for their hearty assistance to parting the shaft, facing and to helping in tool grinding which was often needed during the project work.

The author gratefully remembers the co-operations and help from all staff of Industrial and Production Engineering Departemnt, BUET.

The author also wishes to thank BUET authority for awarding him a Teaching Assistantship during his study. Lastly, thanks are due to all who helped directly or indirectly at the different stages of the work.

ABSTRACT

In the age of market economy it is essential that the production cost of any part has to be minimum to make competitive in the global market. From this point of view tool geometry plays an important role in manufacturing economy. Tool geometry has influence on wear rate and, therefore, on tool life, also on production costs. The knowledge of selecting appropriate tool geometry and other cutting conditions for various application is almost absent in the relevant industries of our country at different cutting conditions. The cutting speed range was selected to cover the critical cutting speed at which built up edge vanishes from the tool surface during cutting. Tool wear is also found to have minimum value near the critical cutting speed. Experiment were conducted with various parameters of the tool geometry with a view to determining their optimum values. The optimum values of these angles were determined from the condition of minimum intensity of tool wear criterion. It has been established that intensity of tool wear can be reduced quite appreciably (3 to 4 times) by proper selection of tool geometry. In the present work the tool geometry parameters were varied one by one, so there remains a scope for further works by varying two or more parameters together. The present work attempts to present a method of selecting optimum tool geometry for turning stainless steel with cemented carbide cutting tool.

CONTENTS

	<u>Page</u>
NOMENCLATURE	x
LIST OF FIGURES	xiii
LIST OF TABLES AND DATA SHEETS	xviii
1. INTRODUCTION & AIMS AND OBJECTIVES	1
1.1 Introduction	1
1.2 Aims & Objectives	5
2. BACKGROUND STUDY AND GENERAL THEORY	6
2.1 Background study	6
2.2 Theory	13
2.3 Tool Life	13
2.4 Optimization	16
2.4.1 Conditions of Optimization	16
2.4.2 Standard Time And Machining Time During Cutting Operation	16
2.5 Effect of the Cutting Speed	18
2.6 Effect of the Depth of Cut and Rate of Feed	20
2.7 Factor which affect the Tool Geometry	22
2.8 Effect of Cutting Tool Angles	23
2.9 Chip Contraction	31
2.10 Causes of Tool Failure	34
2.11 Optimum Wear Criterion	37

CONTENTS (Contd.)

	<u>Page</u>
3. METHODOLOGY AND CONDITIONS OF EXPERIMENTS	41
3.1 Methodology	41
3.2 Description of Work and Tool Material	46
3.3 Selection of Grinding Wheel	48
3.4 Considering Cutting Angles Ranges	50
3.5 Assumptions and Conditions of the Experiment	51
3.6 Experimental Set Up	52
3.7 Experimental Details	55
3.7.1 Determination of critical cutting speed	55
3.7.2 Selection of Experimental cutting speed to determine the optimum tool geometry	64
3.7.3 Determination of intensity of tool flank wear and optimum tool geometry	64
4. RESULTS AND DISCUSSION	117
4.1 Result	117
4.2 Discussion	119
4.3 Limitation	121
5. CONCLUSION, RECOMMENDATION AND PROSPECT	123
5.1 Conclusion	123
5.2 Recommendation	124
5.3 Prospect	126
REFERENCES	127

NOMENCLATURE

h	-	Tool wear, mm
T_L	-	Tool life, min
r	-	Nose radius, mm
h_t	-	Height of tool point, mm
l	-	Tool point length, mm
ϵ	-	Plan angle
γ	-	Back rake angle
γ_1	-	Side rake angle
α	-	Side relief angle
α_1	-	End relief angle
ϕ	-	Side cutting edge angle
ϕ_1	-	End cutting edge angle
β'	-	Wedge angle
δ	-	Cutting angle
π_c	-	Cutting plane
λ	-	Inclination angle
T_p	-	Standard time (per piece), min.
T_{pr}	-	Processing time, min.
T_h	-	Handling time, min.
T_s	-	Time required for servicing the workpiece, min.
T_f	-	Fatigue allowance (time required for steel and personnel needs) min.
t_m, T_m	-	Machining time, min.
L_c	-	Travel of the tool, m/length of cut
n	-	Speed of the workpiece (spindle), rpm
s	-	Rate of feed mm/rev.
V_c	-	Cutting speed, m/min. (Actual)
n_1	-	Exponent depending upon cutting conditions
C	-	Constant - the cutting speed for a tool life of one minute
F	-	Cycles per second
Y	-	Deflection, mm

NOMENCLATURE (Contd.)

D	-	Workpiece diameter, mm corresponding to the point being considered on the cutting edge of the tool
μ	-	Helix angle
t	-	Depth of cut
F_x, F_y, F_z		Resistive force
P_z	-	Cutting force, in Kgf
τ_s	-	Shear stress
K	-	Chip shrinkage co-efficient
η	-	Frictional angle
β	-	Shear angle
L_0	-	Length of uncut chip, m
L	-	Actual length of the chip, m
V_{c1}, V_{c2}	-	Critical cutting speed, m/min
V_{op1}, V_{op2}	-	Optimum cutting speed, m/min.
HCL	-	Hydro-chloric acid
HNO_3	-	Nitric acid
$HNO_3; HCL = 1:3$		Aqua Regia
σ_t	-	Tensile strength
h_f	-	Tool flank wear
h_c	-	Tool crater wear
C_p	-	Total machining cost/piece
C_1	-	Idle cost/piece
C_c	-	Machining cost/piece
C_{tc}	-	Tool changing cost/piece
C_{tg}	-	Tool regrinding cost/piece
C_{td}	-	Tool depreciation cost/piece
C_t	-	Tool cost/grind
T_c	-	Time of complete a piece
T_i, T_I	-	Idle time/piece
T_{tc}, t_{ct}	-	Tool changing time
P_R	-	Profit rate
I_p	-	Income/piece (Excluding material cost)
T_L^*	-	Maximum tool life available
V_{max}	-	Maximum cutting speed available in machine

NOMENCLATURE (Contd.)

t_{max}	-	Maximum depth of cut available at the cutting edge
P_{max}	-	Maximum power available at the cutting edge
M	-	Total service life, min
K'	-	Number of sharpening allowed by the tip
T	-	Machining time, corresponding to the given amount of wear
x'	-	Layer of removed in grinding the tool face in sharpening, mm
Δ	-	Sharpening tolerance ($\Delta=0.1$ to 0.2 mm)
B	-	Width of the tip
y'	-	Layer removed in grinding the tool flank in sharpening, mm
x,y	-	Exponential which differs for different work, tool, and machining variables.

LIST OF FIGURES

		Page
1.	Figure-12 Determination of critical cutting speed V_c of stainless steel at $S=0.2$ mm/rev, $t=0.1$ mm $r=0$, $\alpha=5^\circ$, $\alpha_1=6^\circ$, $\phi=45^\circ$, $\phi_1=20^\circ$, $\gamma=0^\circ$ & $\gamma_1=0^\circ$ in turning with cemented carbide cutting tool.	63
2.	Figure-13 Effect of cutting length on tool flank wear, h_f at constant $S=0.2$ mm/rev, $t=0.1$ mm $r=0$, $\alpha=5^\circ$, $\alpha_1=6^\circ$, $\phi=45^\circ$, $\phi_1=20^\circ$, $\gamma=0^\circ$ & $\gamma_1=0^\circ$ in turning with stainless steel with cemented carbide cutting tool.	72
3.	Figure-14 Effect of cutting length on tool flank wear, h_f at constant $S=0.2$ mm/rev, $t=0.1$ mm $r=0$, $\alpha=7^\circ$, $\alpha_1=6^\circ$, $\phi=45^\circ$, $\phi_1=20^\circ$, $\gamma=0^\circ$ & $\gamma_1=0^\circ$ in turning with stainless steel with cemented carbide cutting tool.	73
4.	Figure-15 Effect of cutting length on tool flank wear, h_f at constant $S=0.2$ mm/rev, $t=0.1$ mm $r=0$, $\alpha=9^\circ$, $\alpha_1=6^\circ$, $\phi=45^\circ$, $\phi_1=20^\circ$, $\gamma=0^\circ$ & $\gamma_1=0^\circ$ in turning with stainless steel with cemented carbide cutting tool.	74
5.	Figure-16 Effect of cutting length on tool flank wear, h_f at constant $S=0.2$ mm/rev, $t=0.1$ mm $r=0$, $\alpha=11^\circ$, $\alpha_1=6^\circ$, $\phi=45^\circ$, $\phi_1=20^\circ$, $\gamma=0^\circ$ & $\gamma_1=0^\circ$ in turning with stainless steel with cemented carbide cutting tool.	75
6.	Figure-17 Effect of cutting length on tool flank wear, h_f at constant $S=0.2$ mm/rev, $t=0.1$ mm $r=0$, $\alpha=7^\circ$, $\alpha_1=5^\circ$, $\phi=45^\circ$, $\phi_1=20^\circ$, $\gamma=0^\circ$ & $\gamma_1=0^\circ$ in turning with stainless steel with cemented carbide cutting tool.	76
7.	Figure-18 Effect of cutting length on tool flank wear, h_f at constant $S=0.2$ mm/rev, $t=0.1$ mm $r=0$, $\alpha=7^\circ$, $\alpha_1=7^\circ$, $\phi=45^\circ$, $\phi_1=20^\circ$, $\gamma=0^\circ$ & $\gamma_1=0^\circ$ in turning with stainless steel with cemented carbide cutting tool.	77
8.	Figure-19 Effect of cutting length on tool flank wear, h_f at constant $S=0.2$ mm/rev, $t=0.1$ mm $r=0$, $\alpha=7^\circ$, $\alpha_1=9^\circ$, $\phi=45^\circ$, $\phi_1=20^\circ$, $\gamma=0^\circ$ & $\gamma_1=0^\circ$ in turning with stainless steel with cemented carbide cutting tool.	78

LIST OF FIGURES (Contd.)

	Page
9. Figure-20 Effect of cutting length on tool flank wear, h_f at constant $S=0.2$ mm/rev, $t=0.1$ mm $r=0$, $\alpha=7^\circ$, $\alpha_1=11^\circ$, $\phi=45^\circ$, $\phi_1=20^\circ$, $\gamma=0^\circ$ & $\gamma_1=0^\circ$ in turning with stainless steel with cemented carbide cutting tool.	79
10. Figure-21 Effect of cutting length on tool flank wear, h_f at constant $S=0.2$ mm/rev, $t=0.1$ mm $r=0$, $\alpha=7^\circ$, $\alpha_1=7^\circ$, $\phi=30^\circ$, $\phi_1=20^\circ$, $\gamma=0^\circ$ & $\gamma_1=0^\circ$ in turning with stainless steel with cemented carbide cutting tool.	80
11. Figure-22 Effect of cutting length on tool flank wear, h_f at constant $S=0.2$ mm/rev, $t=0.1$ mm $r=0$, $\alpha=7^\circ$, $\alpha_1=7^\circ$, $\phi=40^\circ$, $\phi_1=20^\circ$, $\gamma=0^\circ$ & $\gamma_1=0^\circ$ in turning with stainless steel with cemented carbide cutting tool.	81
12. Figure-23 Effect of cutting length on tool flank wear, h_f at constant $S=0.2$ mm/rev, $t=0.1$ mm $r=0$, $\alpha=7^\circ$, $\alpha_1=7^\circ$, $\phi=50^\circ$, $\phi_1=20^\circ$, $\gamma=0^\circ$ & $\gamma_1=0^\circ$ in turning with stainless steel with cemented carbide cutting tool.	82
13. Figure-24 Effect of cutting length on tool flank wear, h_f at constant $S=0.2$ mm/rev, $t=0.1$ mm $r=0$, $\alpha=7^\circ$, $\alpha_1=7^\circ$, $\phi=60^\circ$, $\phi_1=20^\circ$, $\gamma=0^\circ$ & $\gamma_1=0^\circ$ in turning with stainless steel with cemented carbide cutting tool.	83
14. Figure-25 Effect of cutting length on tool flank wear, h_f at constant $S=0.2$ mm/rev, $t=0.1$ mm $r=0$, $\alpha=7^\circ$, $\alpha_1=7^\circ$, $\phi=50^\circ$, $\phi_1=15^\circ$, $\gamma=0^\circ$ & $\gamma_1=0^\circ$ in turning with stainless steel with cemented carbide cutting tool.	84
15. Figure-26 Effect of cutting length on tool flank wear, h_f at constant $S=0.2$ mm/rev, $t=0.1$ mm $r=0$, $\alpha=7^\circ$, $\alpha_1=7^\circ$, $\phi=50^\circ$, $\phi_1=25^\circ$, $\gamma=0^\circ$ & $\gamma_1=0^\circ$ in turning with stainless steel with cemented carbide cutting tool.	85
16. Figure-27 Effect of cutting length on tool flank wear, h_f at constant $S=0.2$ mm/rev, $t=0.1$ mm $r=0$, $\alpha=7^\circ$, $\alpha_1=7^\circ$, $\phi=50^\circ$, $\phi_1=35^\circ$, $\gamma=0^\circ$ & $\gamma_1=0^\circ$ in turning with stainless steel with cemented carbide cutting tool.	86

LIST OF FIGURES (Contd.)

	Page
17. Figure-28 Effect of cutting length on tool flank wear, h_f at constant $S=0.2$ mm/rev, $t=0.1$ mm $r=0$, $\alpha=7^\circ$, $\alpha_1=7^\circ$, $\phi=50^\circ$, $\phi_1=45^\circ$, $\gamma=0^\circ$ & $\gamma_1=0^\circ$ in turning with stainless steel with cemented carbide cutting tool.	87
18. Figure-29 Effect of cutting length on tool flank wear, h_f at constant $S=0.2$ mm/rev, $t=0.1$ mm $r=0$, $\alpha=7^\circ$, $\alpha_1=7^\circ$, $\phi=50^\circ$, $\phi_1=25^\circ$, $\gamma=-8^\circ$ & $\gamma_1=0^\circ$ in turning with stainless steel with cemented carbide cutting tool.	88
19. Figure-30 Effect of cutting length on tool flank wear, h_f at constant $S=0.2$ mm/rev, $t=0.1$ mm $r=0$, $\alpha=7^\circ$, $\alpha_1=7^\circ$, $\phi=50^\circ$, $\phi_1=25^\circ$, $\gamma=0^\circ$ & $\gamma_1=0^\circ$ in turning with stainless steel with cemented carbide cutting tool.	89
20. Figure-31 Effect of cutting length on tool flank wear, h_f at constant $S=0.2$ mm/rev, $t=0.1$ mm $r=0$, $\alpha=7^\circ$, $\alpha_1=7^\circ$, $\phi=50^\circ$, $\phi_1=25^\circ$, $\gamma=5^\circ$ & $\gamma_1=0^\circ$ in turning with stainless steel with cemented carbide cutting tool.	90
21. Figure-32 Effect of cutting length on tool flank wear, h_f at constant $S=0.2$ mm/rev, $t=0.1$ mm $r=0$, $\alpha=7^\circ$, $\alpha_1=7^\circ$, $\phi=50^\circ$, $\phi_1=25^\circ$, $\gamma=10^\circ$ & $\gamma_1=0^\circ$ in turning with stainless steel with cemented carbide cutting tool.	91
22. Figure-33 Effect of cutting length on tool flank wear, h_f at constant $S=0.2$ mm/rev, $t=0.1$ mm $r=0$, $\alpha=7^\circ$, $\alpha_1=7^\circ$, $\phi=50^\circ$, $\phi_1=25^\circ$, $\gamma=0^\circ$ & $\gamma_1=-7^\circ$ in turning with stainless steel with cemented carbide cutting tool.	92
23. Figure-34 Effect of cutting length on tool flank wear, h_f at constant $S=0.2$ mm/rev, $t=0.1$ mm $r=0$, $\alpha=7^\circ$, $\alpha_1=7^\circ$, $\phi=50^\circ$, $\phi_1=25^\circ$, $\gamma=0^\circ$ & $\gamma_1=0^\circ$ in turning with stainless steel with cemented carbide cutting tool.	93
24. Figure-35 Effect of cutting length on tool flank wear, h_f at constant $S=0.2$ mm/rev, $t=0.1$ mm $r=0$, $\alpha=7^\circ$, $\alpha_1=7^\circ$, $\phi=50^\circ$, $\phi_1=25^\circ$, $\gamma=0^\circ$ & $\gamma_1=5^\circ$ in turning with stainless steel with cemented carbide cutting tool.	94

LIST OF FIGURES (Contd.)

	Page
25. Figure-36 Effect of cutting length on tool flank wear, h_f at constant $S=0.2$ mm/rev, $t=0.1$ mm $r=0$, $\alpha=7^\circ$, $\alpha_1=7^\circ$, $\phi=50^\circ$, $\phi_1=25^\circ$, $\gamma=0^\circ$ & $\gamma_1=10^\circ$ in turning with stainless steel with cemented carbide cutting tool.	95
26. Figure-37 Determination of optimum tool angle α of cemented carbide cutting tool for stainless steel at constant $S=0.2$ mm/rev, $t=0.1$ mm $r=0$ and keeping fixed other angles ($\alpha_1=6^\circ$, $\phi=45^\circ$, $\phi_1=20^\circ$, $\gamma=0^\circ$ & $\gamma_1=0^\circ$)	98
27. Figure-38 Determination of optimum tool angle α_1 of cemented carbide cutting tool for stainless steel at constant $S=0.2$ mm/rev, $t=0.1$ mm $r=0$ and keeping fixed other angles ($\alpha=7^\circ$, $\phi=45^\circ$, $\phi_1=20^\circ$, $\gamma=0^\circ$ & $\gamma_1=0^\circ$)	99
28. Figure-39 Determination of optimum tool angle ϕ of cemented carbide cutting tool for stainless steel at constant $S=0.2$ mm/rev, $t=0.1$ mm $r=0$ and keeping fixed other angles ($\alpha=7^\circ$, $\alpha_1=7^\circ$, $\phi_1=20^\circ$, $\gamma=0^\circ$ & $\gamma_1=0^\circ$)	100
29. Figure-40 Determination of optimum tool angle ϕ_1 of cemented carbide cutting tool for stainless steel at constant $S=0.2$ mm/rev, $t=0.1$ mm $r=0$ and keeping fixed other angles ($\alpha=7^\circ$, $\alpha_1=7^\circ$, $\phi=50^\circ$, $\gamma=0^\circ$ & $\gamma_1=0^\circ$)	101
30. Figure-41 Determination of optimum tool angle γ of cemented carbide cutting tool for stainless steel at constant $S=0.2$ mm/rev, $t=0.1$ mm $r=0$ and keeping fixed other angles ($\alpha=7^\circ$, $\alpha_1=7^\circ$, $\phi=50^\circ$, $\phi_1=25^\circ$, & $\gamma_1=0^\circ$)	102
31. Figure-42 Determination of optimum tool angle γ_1 of cemented carbide cutting tool for stainless steel at constant $S=0.2$ mm/rev, $t=0.1$ mm $r=0$ and keeping fixed other angles ($\alpha=7^\circ$, $\alpha_1=7^\circ$, $\phi=50^\circ$, $\phi_1=25^\circ$, $\gamma=0^\circ$)	103
32. Figure-43 Relationship between intensity of tool flank wear, I_f and variable cutting angle, α keeping other angles fixed ($\alpha_1=6^\circ$, $\phi=45^\circ$, $\phi_1=20^\circ$, $\gamma=0^\circ$ & $\gamma_1=0^\circ$)	107

LIST OF FIGURES (Contd.)

	Page
33. Figure-44 Relationship between intensity of tool flank wear, I_h and variable cutting angle, α_1 keeping other angles fixed ($\alpha=7^\circ$, $\phi=45^\circ$, $\phi_1=20^\circ$, $\gamma=0^\circ$ & $\gamma_1=0^\circ$)	108
34. Figure-45 Relationship between intensity of tool flank wear, I_h and variable cutting angle, ϕ keeping other angles fixed ($\alpha=7^\circ$, $\alpha_1=7^\circ$, $\phi_1=20^\circ$, $\gamma=0^\circ$ & $\gamma_1=0^\circ$)	109
35. Figure-46 Relationship between intensity of tool flank wear, I_h and variable cutting angle, ϕ_1 keeping other angles fixed ($\alpha=7^\circ$, $\alpha_1=7^\circ$, $\phi=50^\circ$, $\gamma=0^\circ$ & $\gamma_1=0^\circ$)	110
36. Figure-47 Relationship between intensity of tool flank wear, I_h and variable cutting angle, γ keeping other angles fixed ($\alpha=7^\circ$, $\alpha_1=7^\circ$, $\phi=50^\circ$, $\phi_1=25^\circ$ & $\gamma_1=0^\circ$)	111
37. Figure-48 Relationship between intensity of tool flank wear, I_h and variable cutting angle, γ_1 keeping other angles fixed ($\alpha=7^\circ$, $\alpha_1=7^\circ$, $\phi=50^\circ$, $\phi_1=25^\circ$, $\gamma=0^\circ$).	112

LIST OF TABLES & DATA SHEETS

	Page
Data Sheet # 1 For turning operation at $S=0.2$ mm/rev., $t=0.1$, $r=0$, $\alpha=5^\circ$, $\alpha_1=6^\circ$, $\phi=45^\circ$, $\phi_1=20^\circ$, $\gamma=0^\circ$, $\gamma_1=0^\circ$ and different cutting speeds, V_c to determined co-efficient of chip shrinkage k .	56
Data sheet # 2 Observation of chip nature, quality and physical microscopic study to determine critical and optimum cutting speed.	58
Table - 1 Determined values of K at $S=0.2$ mm/rev., $t=0.1$ mm, $r=0$, $\alpha=5^\circ$, $\alpha_1=6^\circ$, $\phi=45^\circ$, $\phi_1=20^\circ$, $\gamma=0^\circ$, $\gamma_1=0^\circ$ at different cutting speeds in turning stainless steel	61
Sample Data sheet # 3 For turning stainless steel at $S=0.2$ mm/rev., $t=0.1$, $r=0$, $\alpha=5^\circ$, $\alpha_1=6^\circ$, $\phi=45^\circ$, $\phi_1=20^\circ$, $\gamma=0^\circ$, $\gamma_1=0^\circ$ with cemented carbide cutting tool.	67
Table-2 Determined values of I_p for various tool geometry and cutting speeds in turning stainless steel with cemented carbide cutting tool	68
Table - 3 Determined values of minimum intensity of tool flank wear for different tool geometry	97
Data sheet # 4 : Study data from fig. 37-42	104
Table - 4 Determined values of minimum intensity of tool flank wear for particular cutting speed at different tool geometry	113
Table - 5 Determined values of optimum tool geometry and related cutting speed in turning stainless steel with cemented carbide cutting tool	114
Table - 6 Determined values of optimum tool geometry and related cutting speed in turning stainless steel with cemented carbide cutting tool	115
Table - 7 Optimum values of tool geometry	115

CHAPTER ONE
INTRODUCTION AND AIMS
& OBJECTIVES



1.1 Introduction

In the age of Market Economy, it is essential that the production list of any part has to be minimum so that the part is competitive in the global market. To make a product competitive, its production cost has to be low. From this point of view tool geometry plays an important role in manufacturing economy of products. It is also important that the processes involved be efficient and capable of producing parts of acceptable quality at low cost. The choice of the proper tools, speed and feeds in cutting is a compromise since the faster a machine is operated, the higher the efficiency of both the operator and the machine.

It is well recognized that successful transfer of technical knowledge is essential in order to utilize modern technology properly. Otherwise the local engineering products will not be comparable to competing incoming forcing products. Thus, experiments have been performed with a view to enriching the technical knowledge in the field of metal cutting.

The country launched a programme of intensive industrialization including manufacturing of machine tools, cutting tool spare parts, agricultural and general purpose machines which involves huge amount of metal cutting and processing. The government, semi-government and private sectors have made a good head-way in developing the industrial capabilities. Although faced with numerous problems, the industrial sector is at present capable of meeting a major portion of the country's demand. One of the major problems which is faced by the machine building industry is shortage of technical knowledge for proper and economic operation of the existing machine tools. This is a hindrance to rapid industrial growth in the country. In factories a small number of engineers and almost no worker are aware of optimum conditions of machining, without which achievement of economy in industrial production is almost impossible. In the factory the scientific methods the whole metal cutting operation is based on thumb-rules, due to lack of proper technical knowledge. Thus devevelopment of new economical and scientific process of metal cutting variables are chosen either from experience as usually done by machine tool operators or selected from the available engineering tables. None of these methods take the process constraints into consideration and merely depend on the personal experience of the employed personnel and hence lead to values which are too far from the economic values. It results in low production rate and high machining cost which

is undesirable for the factory. Therefore, any means of improving this situation is of direct concern to all.

To avoid and to improve upon this condition, it is necessary to study the underlying principles of metal cutting and tool wear and to employ more effective methods of metal cutting with appropriate tool configuration. This will enable to raise productivity, to increase machining accuracy and to machine most economically. The primary purpose of machining economically, is to determine the machining parameters, corresponding to optimum conditions of tool geometry. The optimization is performed with respect to an objective function which may (a) The machining cost, (b) The Production rate, (c) Profit rate, or a suitable combination of these three functions. So, optimum results from metal cutting operations with proper tool geometry - in terms of piece cost, productivity and profit rate is of major importance to the factory.

Cemented carbide tools are suitable in machining operation of steel at a reasonable cutting speed with respect to economy and surface finish. The selection of cutting tool geometry has long been recognized as a major factor governing the economics of metal cutting. Experiences gained over the years have led to the determination of certain empirical rules or guiding principles for choosing the optimum tool geometry for a given

machining operation. With a view to using the optimum geometry and the principles of metal cutting in the factory, this experimental study has been made. A turning operation has been chosen to develop the proper geometry which needs no special or costly equipments and adequate technical know how of the workers to reach the above mentioned goals.

On the basis of the fundamentals of chip formation, cutting tool wear and the trends toward higher output in the metal cutting process, it is possible to establish well-ground optimum values for the geometric elements of the tool point the optimum tool geometry in any concrete case depends upon the material of the blank work material to be machined, material of the tool point or cutting component (tool material), type of cutting tool used and other actual condition of machining.

1.2 Aims and Objectives

Following objectives were set before the present work:

- i. To determine the critical cutting speed V_c for selection of experimental cutting speed range of metal.
- ii. To determine the relation between tool wear and cutting speed for various tool geometry values in the selected cutting speeds range.
- iii. To determine the optimum tool geometry from the relationship between intensity of tool flank wear and cutting speed.
- iv. To determine the optimum tool geometry of cemented carbide cutting tool for turning stainless steel in the optimum cutting speed range.

CHAPTER TWO BACKGROUND SYUDY AND GENERAL THEORY

2.1 BACKGROUND STUDY

Metal cutting has played a vital role in the advent of modern civilization. Most of the consumable goods are made by metal cutting processes. Metal cutting process is accompanied by a great deal of friction and heat generation. It is governed by definite laws which must be studied to make the process more productive and economical.

The first research on mechanics of machining started in nineteenth century. Research in metal cutting had already been carried out by the French scientist Tresca¹¹ as far back as 1873, although fundamental theories have been developed only during the past three or four decades. Beginning with Mallock¹² in 1881, and through 1900, several contributions were made toward understanding the metal cutting process by determining cutting forces and the effects of tool geometry and cutting environments. The first to make fundamental theoretical and experimental studies of the main problems in metal cutting were the Russian scientists I. Thime (1868-69), K. Zvorykin (1892), A. Briks (1896) and Usachev (1912-14). They can rightfully be called the founders of the theory of metal cutting.

Hermann and Zvorjkin made an analysis on metal machining and developed a relationship at the end of eighteenth century comprising shear angle, rake angle and friction angle at the chip-tool interface. This relationship, with slight modifications, has remained unchanged to the present time.

In 1907, Taylor¹³ developed a relationship between cutting speed and tool life. His works emphasized the role of temperature of the tool on its life. However, from that time until 1925 the developments led more toward producing empirical data than contributing to theoretical analysis.

In around 1920, Herbert and Rosenhain and Sturtevant established the term machinability which referred specially to the speed-life relationship and not to criteria like surface finish, chip disposal etc. But the presence of the tool-chip interface temperature was considered at this period.

In 1924, Milton C. drew the relationship between emf and temperature, between temperature and cutting speed, between tool and cutting speed in machining steel with cemented carbide tools. Eckersley and Trent³⁶ illustrated manufacture, nature, properties and application of cemented carbide. They observed that the melting point of tungsten carbide is over 2500°C. They also tested the hardness of the cemented carbide and showed the relationship between hardness and temperature. Trend studied the main type of wear, factors affecting wear,

including flank wear, the built-up-edge, plastic deformation, mechanical Chipping and thermal cracking. He studied first four of these factors separately and their occurrence over a wide range of conditions on a member of ferrous materials by a series of short time cutting tests. He also studied the flank wear occurring in short time cutting tests. The results suggest that the rate of wear is greatly influenced by the pattern of temperature distribution and flow of work material around the cutting edge.

In 1938 Ernst and Marellott¹⁴ confirmed the role of built-up-edge in metal cutting and presented their theories on the mechanics of its formation and breaking off and its effect on tool temperature and on the surface finish of the machine parts. Considerable stimulus was given to theory of metal cutting by Ernest and Martellott¹⁴ in 1938; Ernst¹⁵ in 1938, and Ernst and marchant in 1940. This group explained the mechanics of metal cutting and the interrelated effect of tool geometry, tool temperature, chip formation, cutting fluid and surface finish.

It was realized that the customary methods of solving machining problems in the period of 1950, which used the thumb rule, must give way to a scientific method. The requirements of metal cutting are changing and the results in continuing changing interrelated compromises which involve new materials, better surface finish and higher rate of production. Thus, it

is necessary that objectives be achieved in the very near future. This requirement has led to extensive developments in metal cutting since the year 1950.

In 1952, Merchant⁹, Ernst and Krabacher presented a scientific method of tool life testing, specially, for cemented carbide tool, the mechanical aspect of metal cutting was investigated by Zorev¹⁷ in 1952. In the same year, Laladzee³⁰, a leading scientist in USSR, presented a well recognized theory of chip formation during metal cutting process.

After 1950 the considerable effort has been expended on developing the optimum machining variables.

In 1955, Ernst and Gilbert optimized the cutting conditions with respect to minimum production cost. In this objective function, cost of production is a function of tool cost and machining cost.

In 1956, Rozenberg and Eremin³¹ carried out experiments on the basis of metal cutting principles and established a relationship between machining variables and metal cutting theory. Rozenberg also developed the relation between cutting forces co-efficient of chip strinkage.

In 1958, Laladzee¹⁸ presented the role of tool wear in optimization of metal cutting process. This was confirmed by

clushin³² in the same year after investigating the metal cutting process. Brewer⁸ also worked on the basic turning operation to optimize the cutting variables for maximum production rate. According to this objective function, production time depends on machining time, idle time, etc.

In 1966, Makarov¹⁹ performed various tests on tool wear optimization of metal cutting process. In the same year, Armerego and Russel² used maximum profit rate as an objective function for optimizing machining variable and proved that maximum profit depends on both tool cost and idle time.

In 1967, Zorev, Gronovsky, Larina and Tritiakov³³ explained the mechanics of metal cutting. In this years Bekes⁴ identified the restrictive conditions of optimization and presented a method for calculating the optimum cutting condition with in these conditions. In this method production rate was only the objective criterion. In the same year Basu⁵ modified this method by developing a new approach for chosing optimum cutting variable. Boothroyed, Engle and chisholm³⁴ determined the effect of tool flank wear on metal cutting process.

In 1968, Bjorke³ developed a methamatical model for calculating the cutting condition during turining operation.

In 1969, Talantov⁶ established that tool wear is a function of chip-tool contact process and minimum tool wear is observed in a definite range of cutting speed which is just below the

critical speed for a single carbide tool. The same authors determined experimentally the dependence of tool wear on cutting speeds. Considerable support was given to this theory by Roznikov in 1969.

In 1970, Time²² explained the resistance of metal during cutting operations. And in 1975, Babrov³⁵ presented the fundamental theory of optimization of the metal cutting process.

In 1978, Talantov, Chriomeshnikov¹⁰ and Kurchenko presented the relationship between cutting speed, metal cutting process, and tool life.

Rafiqu³⁷ Islam showed that the intensity of tool wear is directly proportional to the emf developed during turning with different types of carbide tips.

In 1984 Sankar²³ experimentally determined the optimum cutting conditions for low alloyed steel. In determining the critical cutting speed the co-efficient of chip shrinkage of nickel-chromium steel of known composition was measured. The optimum speed was found to correspond to the maximum value of the co-efficient of the chip shrinkage.

Abu Hanifa²⁶ has investigated of the effect of cutting speed on chip tool contact process and tool wear for steel of unknown composition.

Gullur Rahman²⁵, carried out study on the existing manufacturing process and quality of locally manufactured cemented carbide tool.

Khalilur Rahman²⁴ investigated the wear characteristics during cutting 'V' threads.

A considerable contribution also has been made to the solution of the principal problems of the cutting process and of tool design and production by research minded production engineers, technicians and operators. Present day development of metal cutting science and cutting tool design requires further research in the physics of cutting process, a search for new less expensive, stonger and wear resistant materials for the cutting elements of tool.

It is a surprising to note that a very few scientific investigations have been so far carried out on the influence of tool geometry, tool wear during turning operation of stainless steel as work material by cemented carbide tools. This work attempts to present an experimental method of selecting the optimum tool geometry during turning of

stainless steel work material by a cemented carbide tool material.

2.2 Theory

From the manufacturing point of view, production costs, production rates and profit have great importance during machining. But analysis of these three variables at a time is quite complex. So it was decided to use only one objective criterion, the production cost criterion. Therefore, minimum production time condition should be determined. For a given material and tool, the restrictions of feed, depth of cut, cutting speed, cutting forces (as function of power) and surface finish will be the restrictive criterion to determine the optimum cutting condition.

2.3 Tool Life

The life of a tool is an important factor in production work since considerable time is lost when ever a tool is ground and reset. The tool life, a measure of the length of time a tool will cut satisfactorily and like wise machinability, may be measured in a number of ways. Tool wear is observed in two places (Fig.9). One is on the flank of the tool where a small land, extending from the tip to some distance below, is abraded away. On high speed tools a failure is considered to have taken place if this land has worn 0.062 in and for

carbide tools when the wear land has reached 0.30 in. Wear also takes place on the face of the tool in the form of a small crater or depression behind the tip. Since tool life decreases as the cutting speed is increased.

It has been established that there is a definite relationship between the cutting speed and the life of a cutting tool. The higher the cutting speed, the shorter the tool life (curves 1 and 2 in Fig. 1). This is readily explained by the effect of cutting speed on heat generation and wear. In respect to carbide-tipped tools, this relationship is more complex. It follows from the relationship shown in Fig. 1 for certain conditions in machining unhardened steel that the life of a carbide-tipped tool is first reduced with an increase in cutting speed, then increased and finally reduced again.

In 1907, Frederick W. Taylor showed that a relationship exists between tool life and cutting speed, as follows:

$$VT^n = C$$

where

V = cutting speed, m/min.

T = tool life, min.

n = exponent depending upon cutting conditions

C = constant = the cutting speed for a tool-life of one minute

- 1. Carbon tool steel
- 2. High speed steel
- 3. Cemented carbide

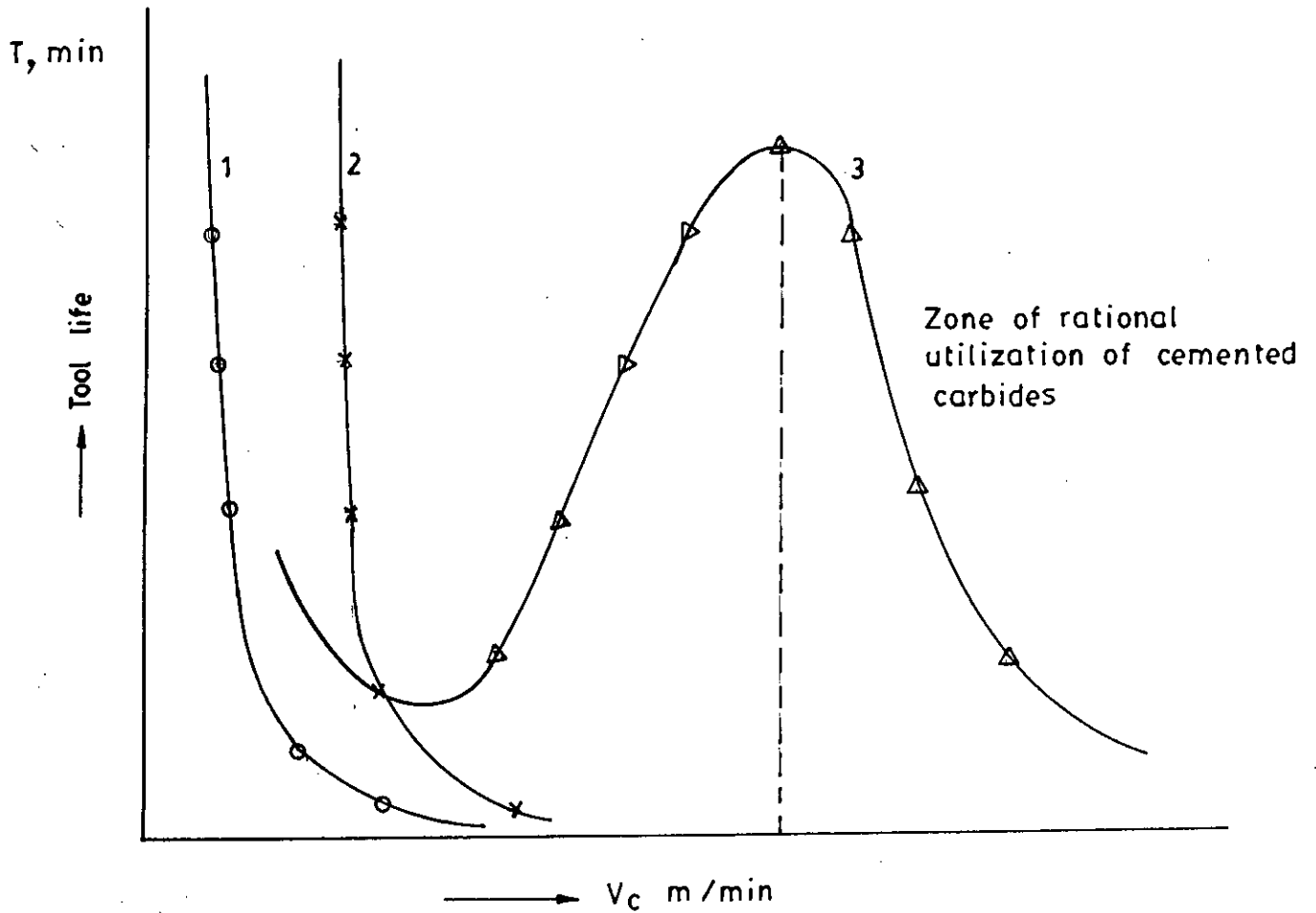


Fig.1 Relationship between cutting speed and tool life

2.4 Optimization

The optimization is performed with the feasible region defined by the relevant constraints, and with regard to the expected value of the objective function.

2.4.1 Conditions of Optimization :

There are several conditions for optimization, these are as follows:

1. Minimum cost (optimization of the cost condition)

$$C_p = C_i + C_c + C_{tc} + C_{tg} + C_{td}$$

2. Maximum production rate (condition of production time)

$$T_p = T_i + T_c + T_{tc} + T_{tc}/T_L$$

3. Maximum profit rate

$$P_R = \frac{I_p - C_p}{T_p}$$

2.4.2 Standard time and Machining Time during Cutting Operation :

The standard time (per piece) T_p required to machine a single work piece in a definite operation is made up of the following elements.

$$T_p = T_{pr} + T_h + T_s + T_f$$

where,

T_p = standard time (per piece), min.

T_{pr} = processing time, min.

T_h = handling time, min.

T_s = time required for servicing the work place, min.

T_f = fatigue allowance (time required for rest and personal needs), min.

The processing time is the time during which the chip is being cut from the work piece. In machine tool operation, processing time can be machining time or combined manual and machining time.

The machining time is the time during which the chip is being cut from the work piece without the direct participation of the operator (for example, the time is turning a shaft in a lathe when the power feed is engaged). In the following, this time will be denoted by T_m . In lathe work the machining time for one pass can be calculated by the formula

$$T_m = \frac{L_c}{ns} \quad \text{min}$$

where,

L_c = travels of the tool in the direction of the feed motion, mm.

n = speed of the work piece (spindle), rpm

s = rate of feed, mm per rev.

2.5 Effect of Cutting Speed

The effect of cutting speed on the cutting angle with BUE formation, chip contraction, cutting force F_2 and the coefficient of friction is shown in Fig.2. According to the curve, force F_2 is reduced beginning with a speed of 3 to 5 m per min. then begins to increase at a speed of $v = 20$ to 25 m per min, and finally drops again. Cutting force F_2 is first reduced because the formation of a built-up-edge leads to the increase of the rake angle, γ . The minimum value of F_2 corresponds to the zone of intensive BUE formation. With a further increase in the cutting speed, BUE formation decreases, and angle γ is decreased, approaching the rake angle of the tool obtained after sharpening. This leads to an increase in force F_2 . With a further increase in the cutting speed, built-up-edge disappears and force F_2 is reduced again because the co-efficient of friction decrease. The curve in Fig.2 show the effect of cutting speed on chip formation, the greater the deformation in the process of chip formation the greater the force will be.

At low speeds tool wear takes place largely by abrasion and interaction of surfaces under high pressure, and the formation and break-up of cold pressure welds. Temperature becomes an important cause of tool wear at high cutting speeds. As speed increases and temperature rises, the chip material next to the tool face becomes weaker and shears more easily in friction.

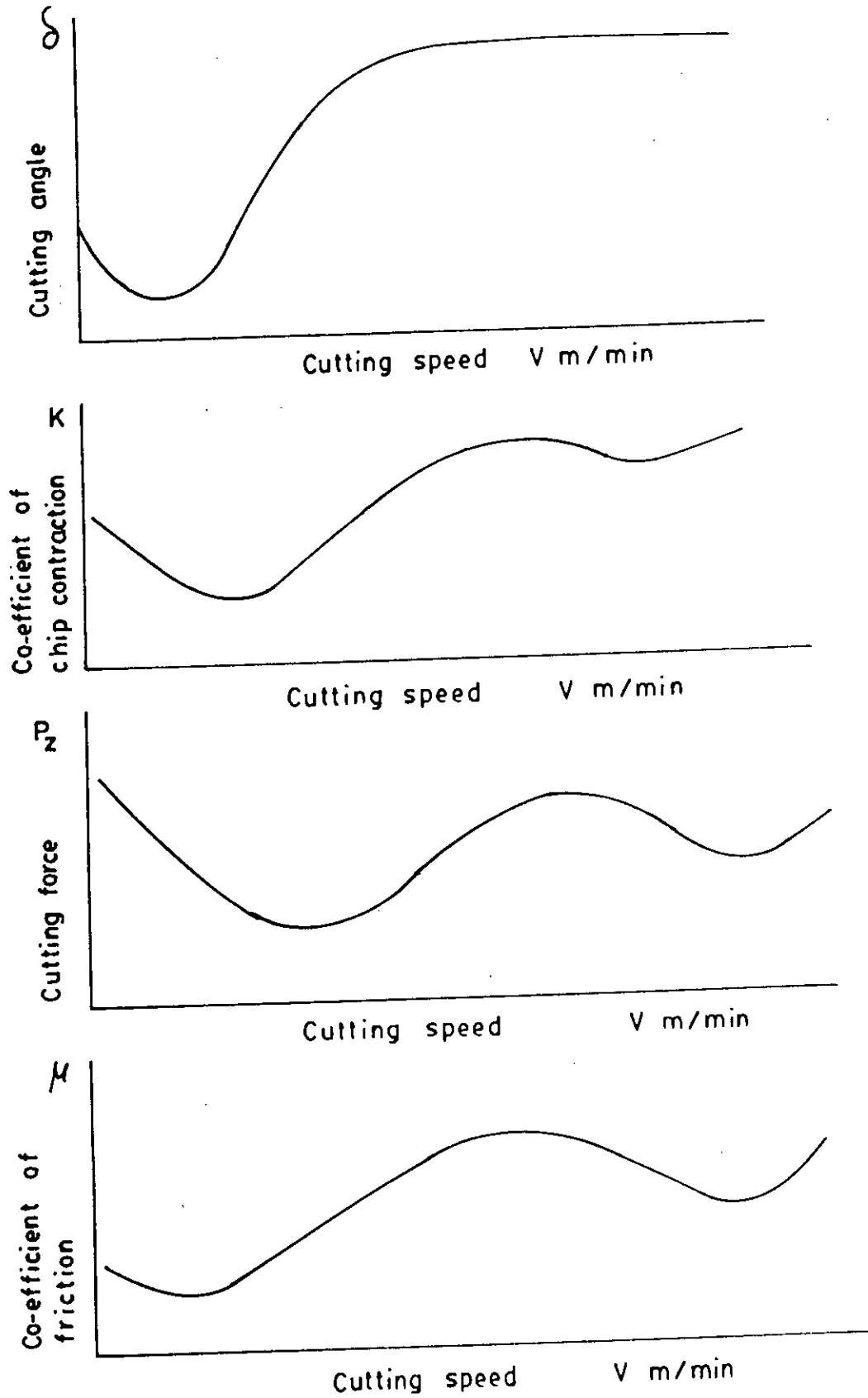


Fig.2 The effect of cutting speed on the cutting angles, chief contraction cutting force, co efficient of friction.

2.6 Effect of the Depth of Cut and Rate of Feed

The greater the depth of cut and feed, the larger the cross-sectional area of the uncut chip and the volume of deformed metal and consequently, the greater the resistance of the metal to chip formation and the larger the forces F_z , and F_y and F_x will be in the cutting process.

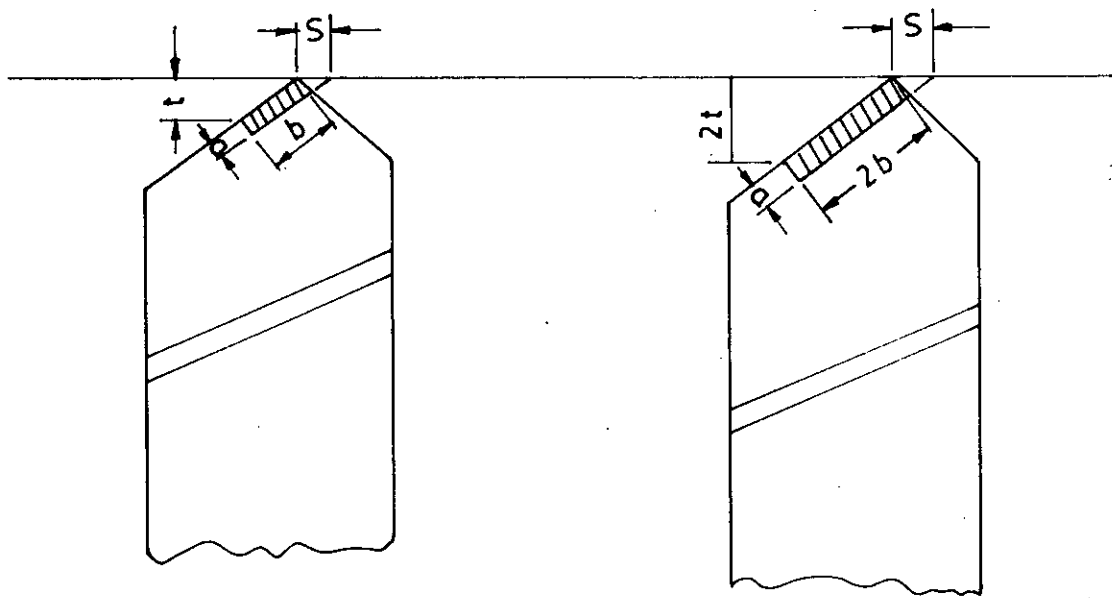
In longitudinal turning, the depth of cut has a greater effect on the cutting force than the rate of feed. If the depth of cut is increased, for example two fold, the width of the uncut chip is also increased two fold. Consequently, the load on the tool, caused by forces acting on its face and flanks will also increase two fold. Therefore,

$$F_z = C_1 t^x$$

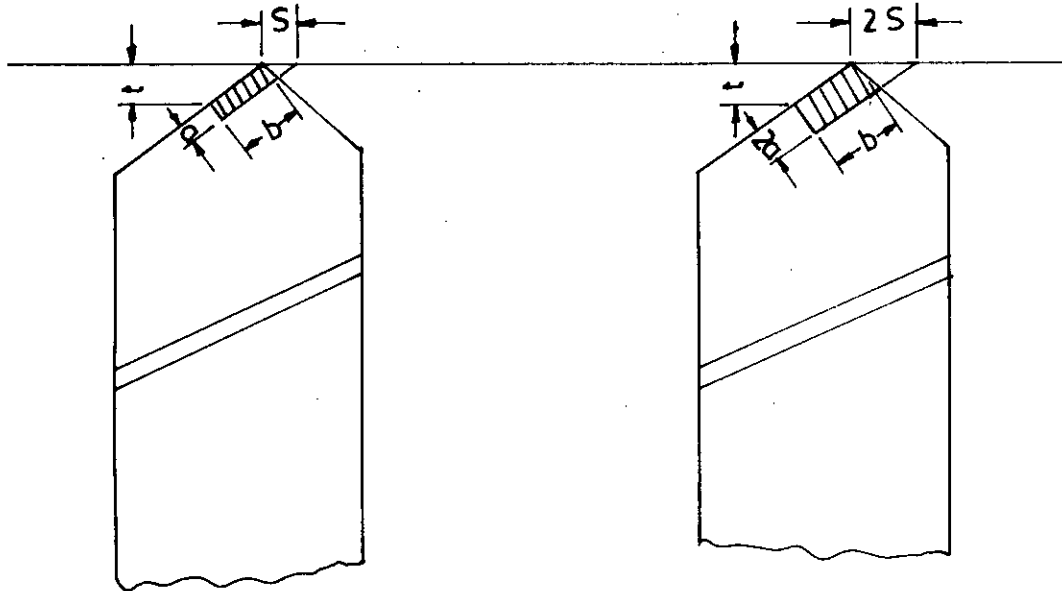
where,

$x = 1$ for any material being machined.

If, now, the feed is doubled, the cross-sectional area of the uncut chip is also doubled. With the width of the uncut chip remaining the same, its thickness will then be doubled. Also of importance is the maximum stress and deformation across the thickness of the layer being cut at the cutting edge, i.e. in layers near the plane of the cut. In layers further away from the plane of the cut, the stress and deformation are gradually reduced. This reduces the forces acting as the tool from the



(a)



(b)

Fig.3 Effect of depth of cut a) and rate of feed b) On the width and thickness of the uncut chip (at S Lt)

layer being cut. As a result, a two fold increase in feed leads to an increase in force F_z which is however less than two fold the previous value Fig. 3.

The dependence of force F_z on the rate of feed can be expressed by the following equation.

$$P_z = C_2 S^y$$

where,

$$y < 1 \text{ (at } s > 0.1 \text{ mm)}$$

2.7 Factors Affecting the Tool Geometry

It is customary to define the tool geometry i.e. tool angles in the static condition assuming that the plane of the cut is vertical. It is also assumed that the tool point is set at the same level of the work axis. Practically, in the cutting process, its position and consequently, the values of certain tool angles are affected by the position of the cutting edge, or certain of its points, in reference to the work axis i.e. higher or lower, the rate of feed and the work piece diameter.

It follows from the above discussion that three factors affect the tool angles in the cutting process. The factors are :

- 1) The position of the cutting edge of the tool in reference to the work axis.

- 2) The rate of feed and its direction which means the relative movement between tool and work piece with regard to both feed and direction.
- 3) The diameter of the work piece.

2.8 Effect of Cutting Tool Angles

Effect of Rake Angle :

The effect of the rake angle γ , on the tool life is shown in fig.4. A positive rake ($+\gamma$) is ground on a single-point cutting tool to promote chip formation. But the larger the rake angle γ , the smaller the wedge (tip) angle β this weakens the cutting edge. Therefore, in machining hard metals, when considerable forces act on the tool and in machining interrupted surfaces. When the tool is subject to impacts, as well as in machining brittle metals, when, due to the "loose" fractured chips are obtained, the load on the tool is concentrated on an area near the cutting edge. It becomes necessary to reduce the rake angle in order to increase the strength of the cutting edge. The softer the metal to be machined, the less the forces acting on the tool and consequently, the less the forces acting on the tool and consequently, the greater the positive rake angle $+\gamma$ may be. With a negative rake angle $-\gamma$, the tip is subjected almost exclusively to a compressive load readily withstood by cemented carbides. The application of negative rake not only changes the nature of the deformation undergone by the tip,

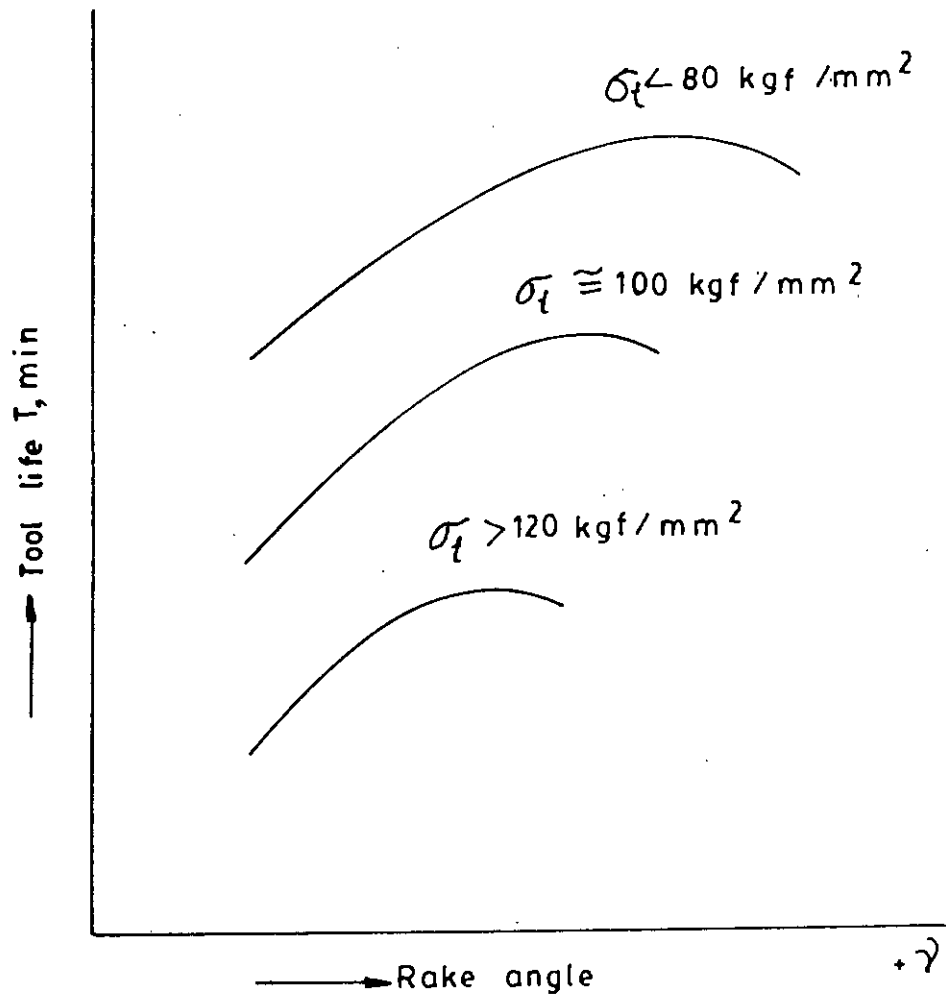


Fig.4 Relationship between tool life and the rake angle

but also helps to move the centre to pressure of the chip further from the cutting edge.

However, the use of an increased negative rake angle leads to an increase in forces acting in the cutting process. This, in turn causes vibration, reduces machining accuracy and raises the power expended in cutting. Hence, tool with negative rake should be used only when absolutely necessary.

Effect of Relief Angle

The friction between the tool flanks and the machined surface or the surface of the cut is reduced by grinding the side (main) flank to an angle α .

The effect of the relief angle α on the tool life is shown in Fig.5. The heavier the feed, smaller the optimum value of angle α will be (at which the life is maximum). The reason for this is that at heavy feeds, the cutting edge will be subject to the action of large forces, and a large wedge angle β will be required to prevent to failure the wedge angle is increased by reducing the relief angle α .

The interrelation between the optimum value of relief angle and the rate of feed is established by the following. The friction between the tool and work will be specially great, if the radius to which the cutting edge is rounded over is equal

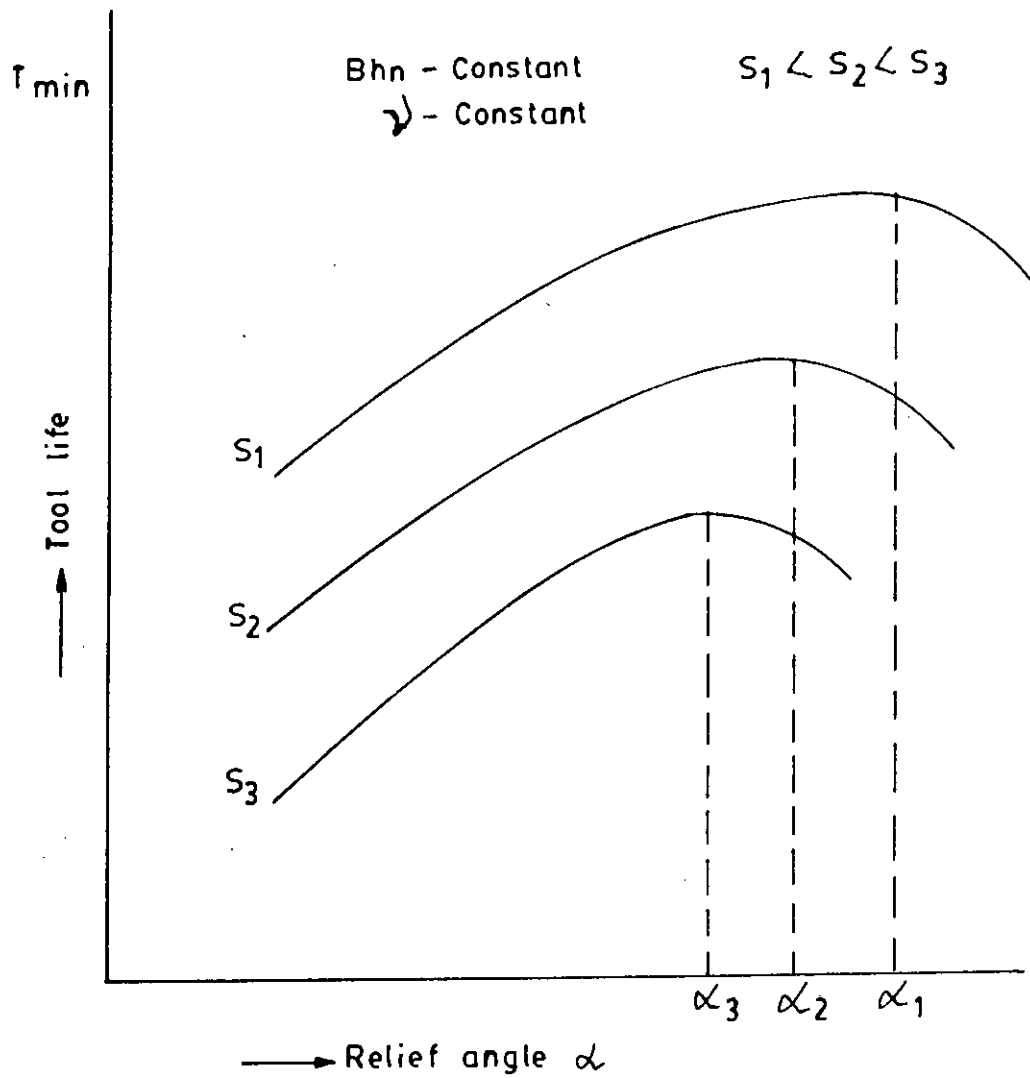


Fig 5 Relationship between the tool-life and the relief angle

to or more than the thickness of the layer being cut. The thinner the layer being cut, the smaller the radius ρ should be. Radius can be easily reduced by increasing relief angle α . Therefore the thinner the layer being cut, the larger angle α should be.

It is necessary to grind the tool flanks with two angles. The tip is ground to the relief angle α , and the shank below the chip, to the clearance, or secondary, angle $\alpha' = \alpha + (2^\circ \text{ or } 3^\circ)$. This is done to facilitate the grinding and lapping of the tip in sharpening and if it is a carbide tip, to reduce wear of the expensive diamond wheel or silicon carbide wheel used in sharpening since such a procedure avoids the loading or glazing of the grinding wheel with the shank material. First the clearance angle is ground on the shank using an ordinary aluminium oxide wheel.

Effect of End Relief Angle

To reduce the friction between the end flank and the work, this flank is ground to angle α_1 which is made equal to the side relief angle in all single point tools except cut off. The relief angle α is between the vertical line BB and the tool flank. Fig. 6(a) If the tool nose is set to a point higher than the work piece axis, the trace A'A' in Fig 6(b) of the plane of the cut normal to the radius passing through the tool nose, will be inclined at a certain angle τ to the line

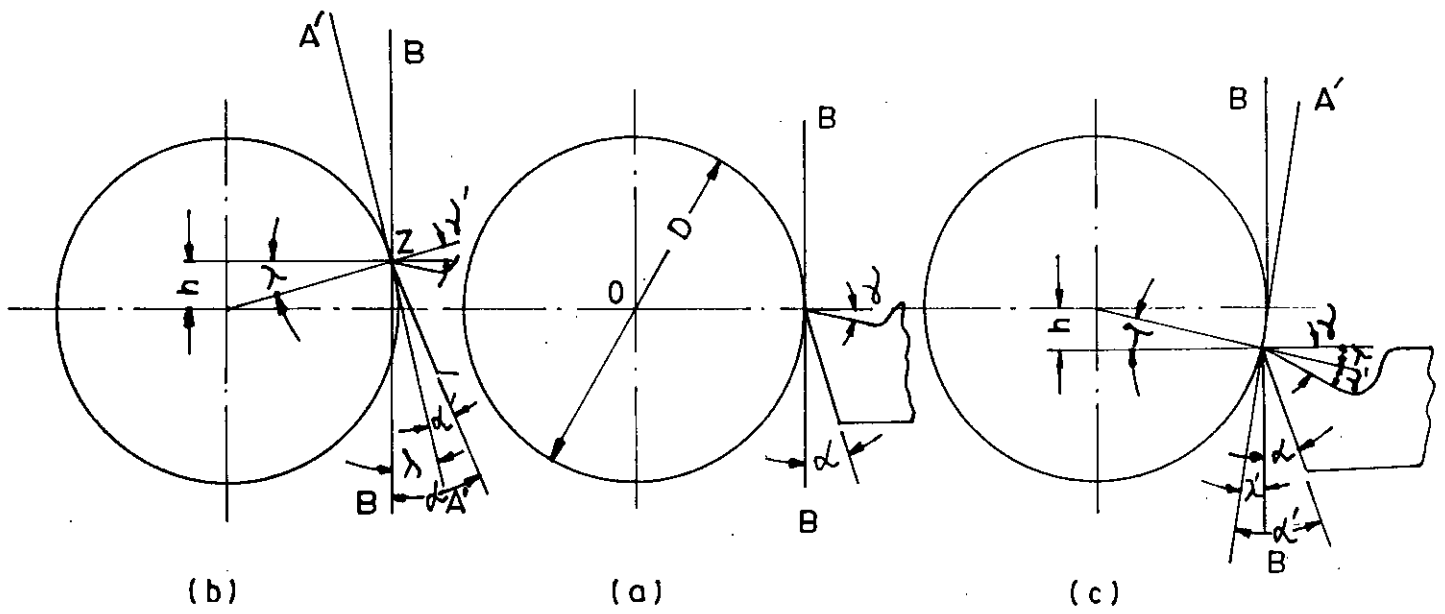


Fig.6 Effect on the tool angles of setting the tool nose above or below the work piece.

BB. Consequently, the actual relief angle α' will be reduced i.e. $\alpha' = \alpha - \tau$, the rake angle γ , on the contrary, will be increased $\gamma' = \gamma + \tau$.

If the tool is set with nose below the work piece axis Fig. 6(c) the opposite will be true, i.e. the rake angle will be reduced and the relief angle increased $\gamma'' = \gamma - \tau$ and $\alpha'' = \alpha + \tau$. The angle τ can be determined from triangle OKN in Fig. 6a. Thus,

$$\sin \tau = \frac{h}{ON} = \frac{2h}{D}$$

In boring operations, angle α and γ will change in the opposite directions i.e. the rake angle will increase and the relief angle will be reduced when the tool nose is set at a height lower than the workpiece axis.

Effect of Plan Approach Angle (Side cutting edge angle)

The effect of the plan approach angle on the cutting speed is shown in Fig. 7. The smaller the plan approach angle ϕ on a single point tool the greater the tool life and permissible cutting speed. In addition, the use of a tool with a small angle ϕ (and ϕ_1) enables a better surface finish, with less roughness, to be obtained.

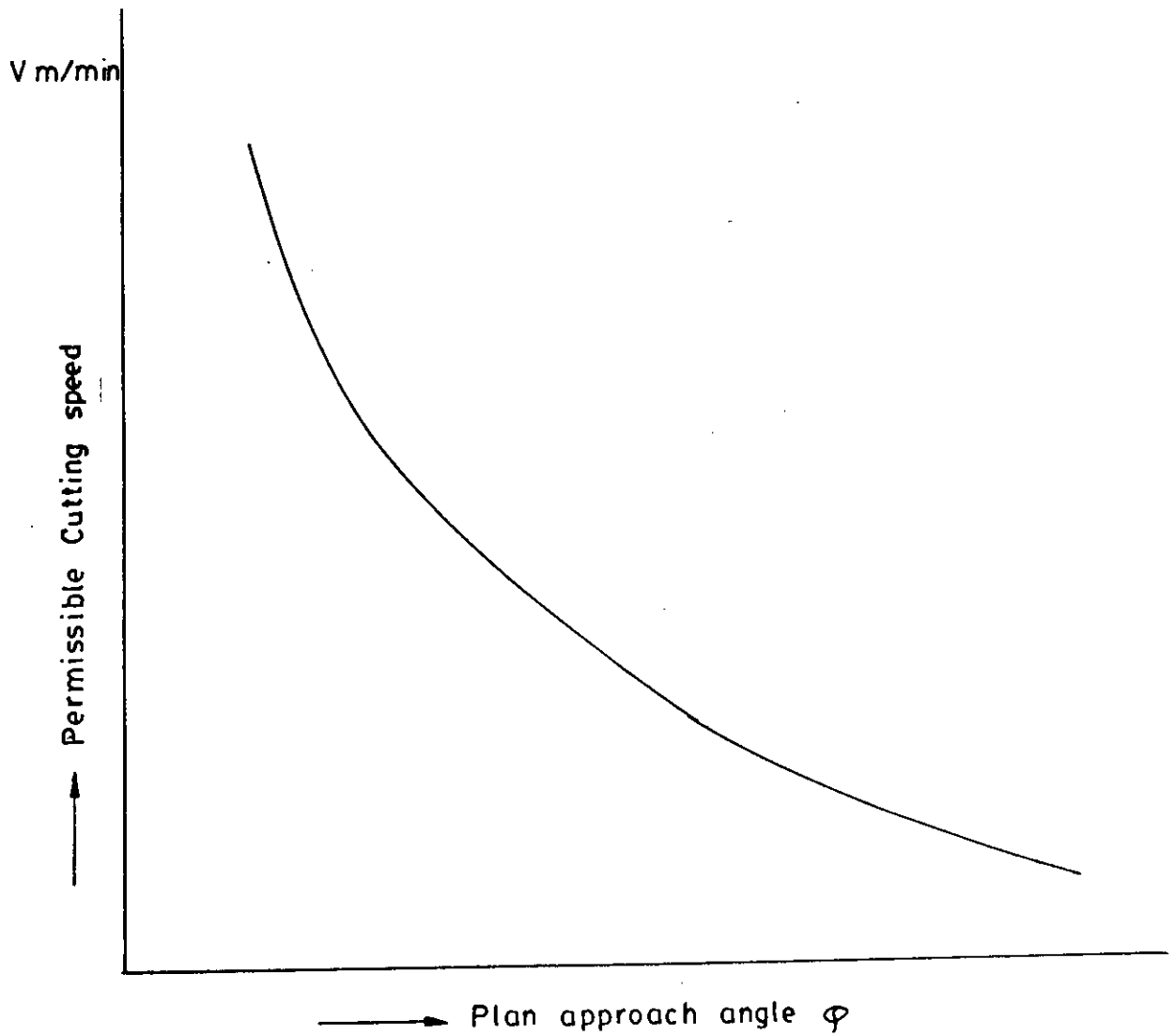


Fig.7 Relationship between the cutting speed and the plan approach angle

With a reduction in angle ϕ_1 however, the deflection of the tool away from the work will increase if, in this case, the machine fixture tool workpiece complex is sufficiently rigid, the machining accuracy may deteriorate and vibrations may be initiated that make further operation practically impossible, for this reason, under machining conditions which can not ensure sufficient rigidity of the complex, larger values of ϕ should be assigned.

The angle ϕ and ϕ_1 , obtained in sharpening, will not change in the cutting process if the tool shank is perpendicular to the work axis. If the tool is swivelled counterclockwise, looking from above, angle ϕ will increase and angle ϕ_1 will decrease.

2.9 Chip Contraction

As a result of plastic compression of the layer of metal being cut, the chip turns out to be shorter than the part of the work from which it has been cut i.e. $L < L_0$ in Fig. (8).

This shortening of the chip is called longitudinal chip contraction and its magnitude is characterized by the coefficient of contraction or cutting ratio or chip shrinkage.

The co-efficient of contraction, K is the ratio of the length of the section on the work from which the chip was not to the length of the chip removed, thus

$$K = \frac{L_0}{L}$$

Since $L < L_0$, the co-efficient of contraction $K > 1$ and may reach 5 or 6 depending upon the machining conditions.

The volume of the layer being cut is equal to the volume of the cut-off layer. Therefore, any contraction of the chip should be accompanied by an increase in its cross-sectional area. This is called transverse chip contraction and the increase in area is due mainly to the increase in chip thickness and only to a lesser extent to any increase in chip width.

The co-efficient of chip contraction, or cutting ratio, is a certain quantitative measure of the degree of plastic deformation in metal cutting. Thus, the smaller the chip contraction, the less the plastic deformation in the cutting process, and consequently, the more favourable the conditions of chip formation and the less the power consumed to machine the given blank.

The main factors affecting chip contraction are (1) geometric elements of the tool point (chiefly the cutting angle and the nose radius) (2) cutting variable (mainly the cutting speed and rate of feed) (3) cutting fluid and (4) metal being machined and its mechanical properties.

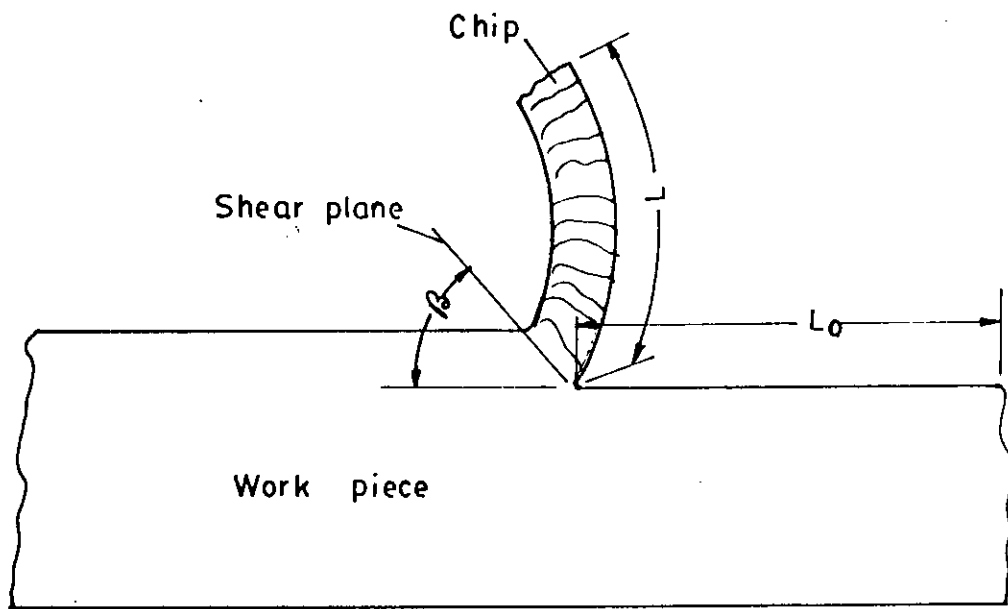


Fig. 8 Chip contraction

2.10 Causes of Tool Failure

Failure of the cutting tool is considered to have occurred when it is no longer capable of producing parts with in required specifications, the point of failure, together with the amount of wear that determines this failure. This is a function of machining, surface quality, dimensional stability, cutting forces, cutting horsepower, and production rates. It may, for instance, take very little wear to affect the stability of the built-up-edge, which in turn may affect surface quality, although the tool itself could continue to remove metal with little, if any loss of efficiency. In contrast only a few thousandths of an inch wear on a wide form tool might cause such a large increase in thrust or feeding forces that would result in a loss of dimensional stability, or required excessive power, in addition to a loss of surface quality.

Tool Wear

In the process of cutting metals, the tool is worn as a result of friction of the chip on the tool face and of the tool flanks on the workpiece tool wear involves abrasion and the removal of microparticles of the surface as well as microscoping chipping of the cutting edge.

Friction and the resulting wear in cutting metals differ somewhat from the general friction of the surfaces of machine parts, the physics of tool wear in metal cutting is extremely complicated. It involves abrasive, molecular and diffusive wear, there is no known tool material that can completely resist contact and rubbing.

The direct contact with the work material, there are three major regions on the tool where wear can take place, which are face, flanks and nose Fig. 9(a).

Face Wear

The face of the tool is the surface over which the chip passes during its formation. Wear takes the form of a cavity or crater which has its origin not along the cutting edge but at some distance away from it and within the chip contact area. As wear progresses with time, the crater gets wider, longer, and deeper and approaches the edges of the tool, tool face wear is shown in Fig. 9(b).

Flank Wear

Flank wear is always present regardless of work and tool material, or even of the cutting conditions, the flank is the clearance face of the cutting tool, along which the major cutting edge is located. It is the portion of the tool that is

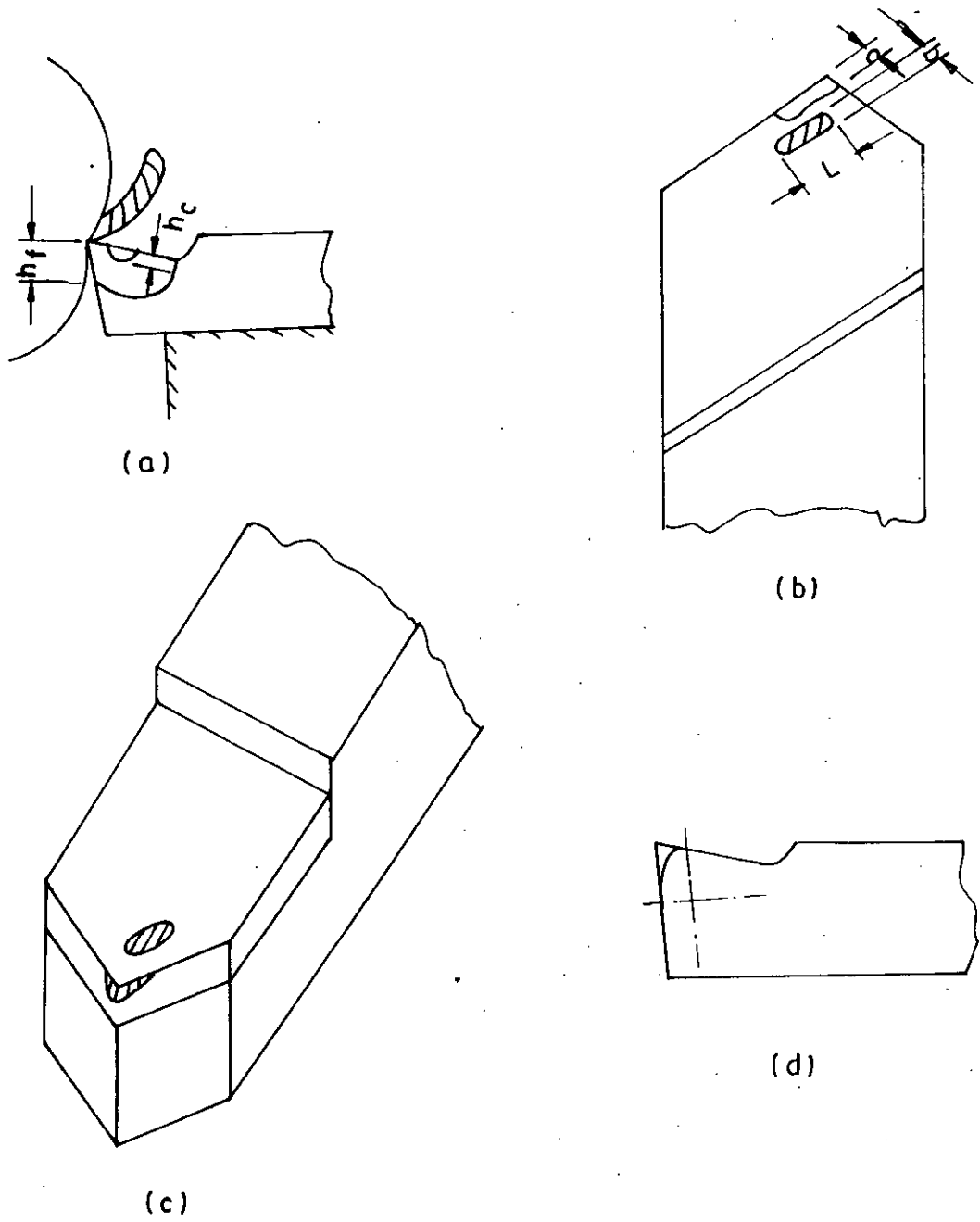


Fig. 9 Typical tool wear

in contact with the work at chip separation point and that resists the feeding forces. Because of the clearance, initial contact is made along the cutting edge. Flank wear begins at the cutting edge and develops into a wider and wider flat at increasing contact area called a wear land, tool flank wear shown in Fig. 9(c).

Nose Wear

Nose wear is similar to and often considered a part of flank wear. Nose wear sometimes proceeds at a faster rate than flank wear. Practically when one is working on rather abrasive material and using small nose radius. In finish turning operations, the nose is in direct contact with the workpiece, and excessive wear might affect dimensional stability as well as surface roughness. Where sharp corners are to be maintained, the rounding or flattening of the nose can cause failure long before flank wear itself becomes a factor. Tool nose wear shown in Fig. 9(d).

2.11 Optimum Wear Criterion

Optimum wear means wear for which the total service life of the tool will be the longest. The total service life M of a tool is determined by multiplying the number of sharpening (grinds) allowed by the tool tip for the given amount of wear by operating time during which such wear occurs, thus

$$M = K'T \text{ min}$$

where,

K' = number of sharpening allowed by the tip for the given amount of wear.

T = the machining time (tool life) corresponding to the given amount of wear.

The number of sharpenings allowed by a tool tip subject to face wear Fig. 10(a).

$$K_1' = \frac{\frac{2}{3}C'}{x'} = \frac{\frac{2}{3}C'}{h_c + \Delta}$$

where,

C' = height (thickness) of tip, mm

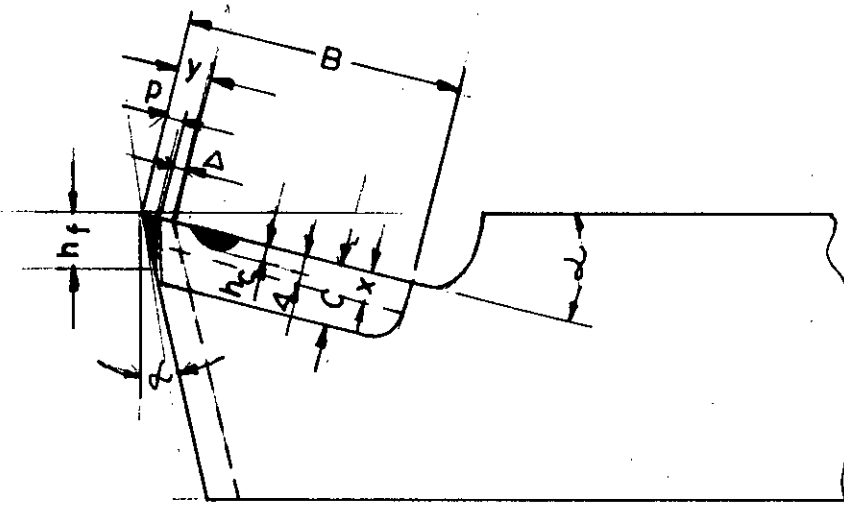
x' = layer removed in grinding the tool face in sharpening, mm

Δ = sharpening tolerance (for removing x' layer slightly thicker than the crater depth) $\Delta = 0.1$ to 0.2 mm.

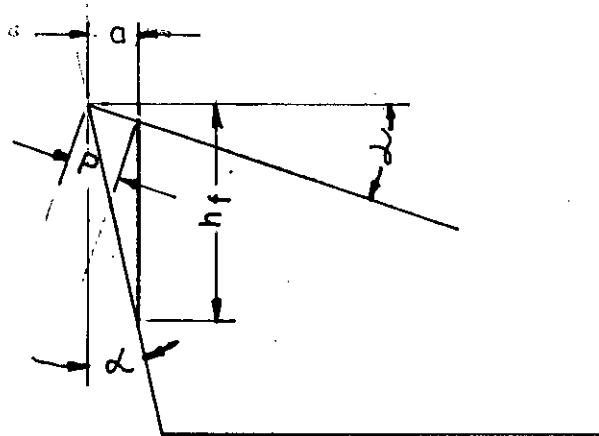
As a rule, the whole tip is not ground off to its base. This is taken care of in the formula by the factor $2/3$.

The number of sharpening allowed by the width of the chip when it is subject to flank wear is Fig.10(a).

$$K_2' = \frac{\frac{2}{3}B}{y'}$$



(a)



(b)

Fig.10 Elements of wear and tool sharpening

where,

B = width of the tip, mm; in a direction normal to the side (main) cutting edge

y' = layer removed in grinding the tool flank in sharpening, mm; it is measured along the width of the tip.

$$\text{But } y' = p + \Delta$$

From Fig. 10(b)

$$p = \frac{a}{\cos \gamma} \quad \text{and} \quad a = h_f \tan \alpha$$

$$\text{then } p = \frac{h_f \tan \alpha}{\cos \gamma}$$

$$y' = \frac{h_f \tan \alpha}{\cos \gamma} + \Delta$$

$$\text{and } K'_2 = \frac{\frac{2}{3}B}{\frac{h_f \tan \alpha}{\cos \gamma} + \Delta}$$

The average value of Δ is 0.15 mm.

CHAPTER THREE

METHODOLOGY AND CONDITIONS OF EXPERIMENTS

3.1 Methodology

The main factor influencing machining as well as the production costs is tool life. But it has some interpretations. It can either be the useful life of cutting tool expressed in minute between two grinds or the total time which a tool can withstand before complete destruction. This leads to frequent tool sharpening and consequently, to a loss of the labour of the workman sharpening the tool, a loss of time required to remove and set up the tool. Thus tool wear influences the output and the cost of machining operations.

For decreasing production cost and higher production rate, it is necessary to improve tool life. In order to form a basis for such improvement, much effort has been made to understand the nature of tool wear and other forms of tool failure, the life of a cutting tool can be brought to an end in many ways, these ways may be divided into two main groups.

- i) The gradual or progressive wear of certain regions of the face (crater wear) and flank (flank wear) of the tool.

ii) Failure of the tool-life at a premature stage.

In impractical operations, tool geometry plays an important role. In absence of definite cutting angle the greater the deformation, heat generation and forces acting on the tool, the more intensive tool wear will be, the surface will be rough and the shorter the tool life, but in certain cutting angle the deformation, heat generation and cutting forces are reduced and the tool life is increase. Therefore, an optimum value of the cutting edge exists for each work material, tool material and other machining variables at which the tool-life and consequently the permissible cutting speed will reach their maximum values. It is true that, under all circumstances the wear at the tool flank in the sole gage in prescribing the useful life of a cemented carbide tool.

It is also true that when tools are used in optimum tool geometry, the flank wear is minimum and the product is under economical control.

An increase in cutting speed leads of more productive machining by reducing machining time. But the cutting speed can not be assigned without taking into account the concrete machining conditions since the intensity of tool wear is sharply increased with the cutting speed.

So there should be a compromise between cutting speed and tool wear rate which leads to the term 'critical cutting speed'.

The critical cutting speed, V_c , is considered as the cutting speed at which few traces of unstable built-up-edge appear on or just disappear from the rake side of the chip, as it protects the tool from excessive wear. Co-efficient of chip shrinkage (k) is related with cutting speed, Rozenberg established an expression of cutting force P_z .

$$P_z = \frac{T_s \cdot S \cdot t \frac{\cos \gamma_o}{\sin \beta \cos(\beta - \gamma_o)}}{1 - \frac{\sin \eta}{K \cos(\eta - \gamma_o)}}$$

and shown in Fig. 11.

This indicates that P_z depends on the value of k , s and t . K , is the chip reduction co-efficient or chip shrinkage where

$$K = \frac{\cos(\beta - \gamma_o)}{\sin \beta} = \frac{L_o}{L_c} = \frac{\text{Length of uncut chip}}{\text{Actual length of the chip}}$$

The value of K is affect by -

- i. cutting variables i.e. v , s , t , etc.
- ii. cutting environment and auxiliary variables.

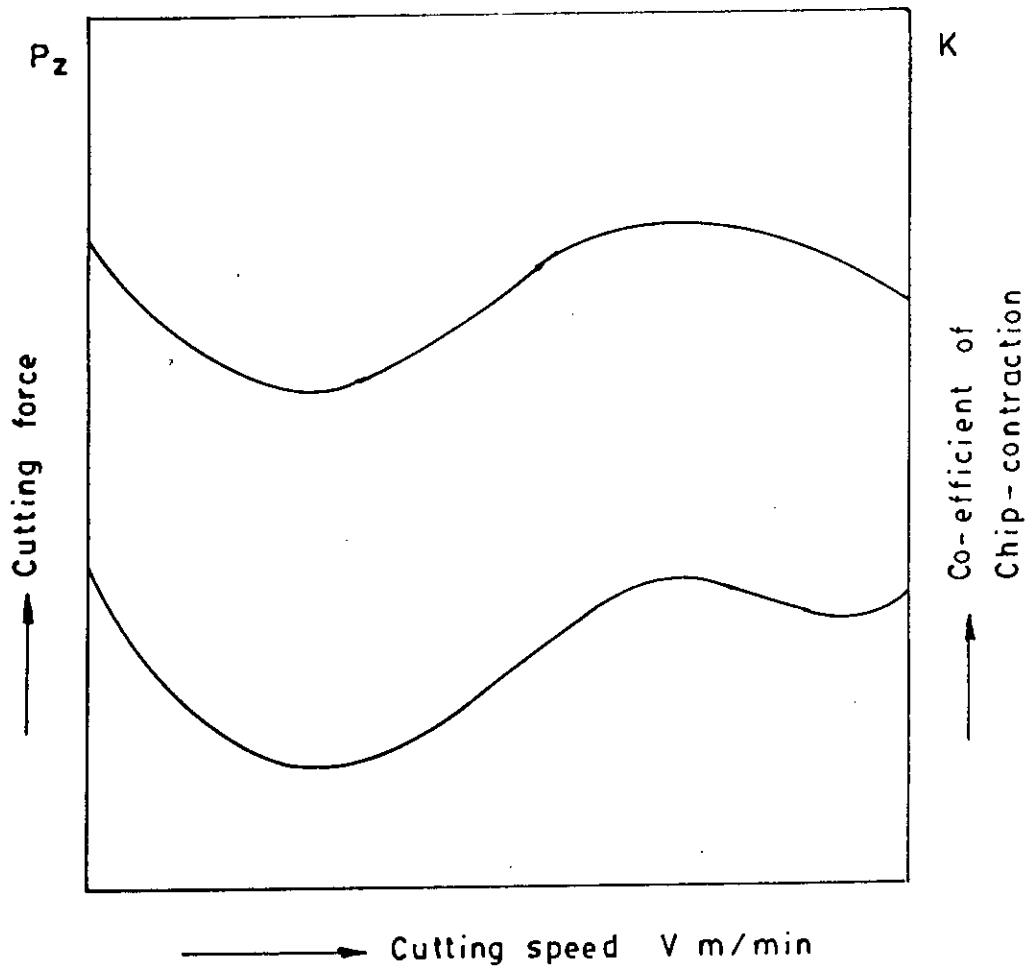


Fig.11. The behaviour of cutting force P_z and chip- shrinkage, K with respect to cutting speed, V

The behaviour of K as influenced by cutting variable fully depends on cutting force, P_z for determination of cutting force and to explain a cutting tool performance. The value of chip shrinkage K and its behaviour with respect to cutting variables is very important. Measurement of K is very easy and needs no costly and precise instrument where measurement of P_z is troublesome and costly. Rozenberg has demonstrated that the behaviour of cutting forces with respect to cutting speed is identical with chip shrinkage characteristics. That's why, in this present experiment to find critical cutting speed V_c , chip shrinkage K is used instead of cutting force P_z .

Critical cutting speed, V_c has been used to find a broad range of cutting broad speed known as experimental cutting speed.

The work materials stainless steel, have been turned with cemented carbide tool at these experimental cutting speeds for different tool angles. After turning a specific length of work material, corresponding tool wear has been measured with instrumental microscope. Flank wear, h_f vs. Cutting length, L curves shows the intensity of tool wear. Again, intensity of tool wear I_h vs. cutting speed, V_c for different values of same tool angles curves have been plotted. From these curves, the angles for which intensity of tool wear is minimum has been considered as 'Optimum tool angle'. This experiment has been performed for six tool angles - Back rake angle γ , side rake angle γ_1 , end relief angle, α_1 side relief angle, α End cutting

edge angle, ϕ_1 side cutting edge angle, ϕ from which a optimum tool geometry is obtained.

Thus, to find a optimum tool geometry, the experiments performed under this work are as follows:

- i. Determination of chip shrinkage
- ii. Determination of critical cutting speed
- iii. Determination of intensity of tool wear
- iv. Determination of optimum tool angle.

The optimization of each angle were done by varying it considering other angles fixed to determine the optimum tool geometry.

3.2 Description of Work and Tool Material

Experiments have been conducted with cemented carbide tool and stainless steel work material. Stainless steel possesses high resistance to corrosion. They are produced to cover a wide range of mechanical and physical properties and for particular applications at atmospheric, elevated and cryogenic temperature. Common applications of stainless steel include air-craft, railway, trucks, food processing equipment, cooking utensils, cutlery, flatware, jet engine parts, etc. Stainless steel materials are generally selected first on the basis of corrosion resistance and 2nd on the basis of strength or other

mechanical properties. More force is required faced by the tools and to bend, draw and cut, and slower cutting speeds and difficult tool geometrics are required for machining.

Cemented carbides have a high first cost but can be run relatively faster and they can produced much more than cheaper tool materials. They are most popular for production operations. Carbides are made in many grades to suit many purposes by varying the size and proportions of the carbide particles and the amount of binder. Cemented carbides are made and sold under a number of trade names such as Kennametal and carboloy. Cemented carbide have a high density, hardness and wear resistance at high temperature. In the production of metal cutting tools use is made of (1) straight tungsten cemented carbides which are grains of tungsten carbide held in a matrix of cobalt (grades BK2, BK3M, BK4, BK6, BK6M, BK8 and BK8B) (2) titanium tungsten cemented carbides consisting of grains of a solid solution of tungsten carbide in carbide of titanium and surplus grains of tungsten carbide, all bonded by the cobalt, or just the solid solution with out the surplus grains in the cobalt matrix (grades T5K10, T14K6, T30K4 and T5K12B and (3) titanium-tantalum-tungsten cemented carbides consisting of grains of a solid solution made up of the carbides of titanium, tantalum and tungsten and surplus grains of tungsten cemented carbide together by cobalt, (grade TT7K12 and TT7K15).

The following figure, the letter K in second group indicates the cobalt content, as before, while the figure after the T is the titanium carbide content in percent. Thus grade T5K10 contains 10 percent cobalt, 5 per cent titanium carbide and rest 85 per cent tungsten carbide-titanium-tungsten cemented carbide are also used efficiently for turning heat-resistant steels and super alloys, distinguished for their high toughness and low heat conductivity. The titanium tungsten group of cemented carbides is divided into (a) the strongest but least wear-resistant grade T5K10 (b) less strong but more wear resistant grades (T14K8 and T15K6) and (c) the most brittle grade but having the highest wear resistance (T30K4). Grade T5K10 is used in roughing steel for interrupted cuts. In the present experiments T5K10 type cemented carbide tools are used.

3.3 Selection of Grinding Wheel

To grind work of high quality at a high rate of output, the grinding wheel specifications must be properly selected to suit the concrete conditions of the job.

The kind of abrasive material is determined by the nature and properties of the work material. Thus, aluminium oxide abrasive is best for grinding steel, malleable iron and soft bronzes. Black silicon carbide abrasive is most efficient in grinding cast iron, bronze and aluminium castings and cemented

carbides. Green silicon carbide abrasive is used in sharpening carbide tipped cutting tools.

The grain size of the wheel is selected in accordance with the required surface finish, the work material and the size of the area of contact between the wheel and the work. In rough grinding, wheels of coarser grain size are used than in finish grinding. Coarser wheels are used in grinding ductile and soft metals to avoid rapid loading of the wheel, fine grained wheels are used for brittle and hard metals, the larger the area of contact with the work, the coarser the grain of the wheel should be. A grain size of 40 to 25 is suitable for wheels used in high velocity grinding.

The selection of the wheel grade is based on the observance of conditions favourable for self sharpening of the wheel in the grinding process. Consequently, the harder the metal being ground, the softer the wheel should be and vic-versa, since a grinding a hard metal the grains will wear more intensively and be broken out of the wheel more readily to expose new sharp grains.

To avoid breaking down, harder wheels should be more coarse grained, since other conditions being equal, the grain of a coarse-grained wheel is subject to a higher load than that of a fine-grained wheel.

The structure of the wheel is selected to suit the grinding conditions, wheels of dense structure which retain their shape well are used for finish and form grinding, wheels of medium dense structure are employed for grinding hardened steel parts, for sharpening cutting tools, wheels of open structure are used in grinding ductile and soft metals.

3.4 Considering Cutting Angles Ranges

The side cutting edge angle should be established first. It should be large enough to ease the tool into the work piece without endangering a breakdown of the nose, and while it must be 90° when machining in a lathe upto a square shoulder, it should average around 50° with values upto 30° for roughing cuts on ragged surfaces. The end cutting angle is necessary to avoid rubbing action between the tool and workpiece at points other than the cutting edge. It should be as small as possible to avoid weakening the nose and should range from 15° to 45° , with large angles introduced reluctantly in case where other means to reduce chatter have not met with success.

The rake and clearance are determined from -8° to $+15^{\circ}$ and make the side and end clearance angles from 5° to 15° . The smaller the relief angle, the stronger the cutting edge, but if the angle is too small, rubbing action will take place.

The nose radius should be selected next. If it is too large, it may cause chatter, and in cases where firm rigidity is hard to obtain, it should be made as small as possible. The nose radius has a distinct bearing on the chip formation and surface finish. Its dimension should not be too rigidly specified by the tool designer.

3.5 Assumptions and Conditions of Experiment

The aim of the experimental setup were to findout the critical values of the factors influencing the optimum cutting condition from the earlier theoretical investigation. It was proved that the influencing factors were cutting force, speed, feed, depth of cut, tool-life etc. Cutting fluid has considerable influence on cutting conditions, yet it was not used, since coolant quickly shatters cutting edge and forms crack for repeated quenching. To investigate the above mentioned factors carefully and systematically, experiment was conducted in several steps and the assumptions were state below:

- i) Tool geometry considered conventional and it is constant
- ii) The properties of the work material do not vary during and after the operations.
- iii) Instantaneous conditions of temperature, pressure and chip formation in the region of cutting corresponding to the appropriate steady-state conditions.

- iv) Feed, depth of cut remain unchange only cutting speed varying.
- v) Only the turning operation considered for the experiment.

3.6 Experimental Setup

The experiment has been done to obtain the result according to the methods mentioned in the methodology. The critical cutting speed was determined to get the range of experimental cutting speed by measuring chip shrinkage co-efficient.

There are several other ways to find out critical cutting speed (V_c), such as by studying chip tool contact process and intensity of tool wear with respect to cutting speed. Conventional method was applied to determine the critical cutting speed. In this experiment, a round solid bar of stainless steel was turned with cemented carbide cutting tool.

The bar initially was rough turned to make ready for the experiment, because chip lengths would be measured and recorded according to the uncut chip length also longer chips are usually unhandy while shorter chips do not permit sufficient accuracy. So to determine the value of chip shrinkage, K from turning operations, it is feasible and recognized to interrupt the cut by a groove in order to have a measure of the uncut length of the material which later is removed as a chip. A small groove parallel to the centre line

of the work piece leaves marks at the edge of the chip at a distance equal to one revolution of the work. The chip shrinkage, K was found out by measuring the distance of the mark on chip and dividing the circumference of the work piece by the measured length. The length of the chip is measured preferably on the smooth surface, chip-tool contact processes were estimated by viewing the scratch patterns on the rake face of the chip and by studying the photomicrographs of the chip.

There are many processes to determine the intensity of tool wear, one of them is radio-active method. In this method, radio-active equipment is required in operation and counting the wear particles which travel with chip as the cutting fluid. Geiger counter are used for counting the wear particle. It is complicated and expensive process. On the other hand, there are some conventional methods. One of them, is of machining with a cutting tool to a predetermined cutting length of certain amount of metal removed and measuring respective wear with a metallurgical microscope. Though this conventional method is simple and economical, so it was used in this experiment.

The lathe machine used to find out experimental cutting speed was also used to continue the experiment for the work and tool material. The intensity of wear of a single point cemented carbide cutting tool, depend upon various cutting conditions.

In this experiment to determine the rate of tool flank wear feed, depth of cut, nose radius, considered constant. Cutting fluid was not used during operations and temperature did not influence on cutting operation. Experiment was done with in a cutting speed range from 11m/min to 35m/min. Only the variable was tool geometry. The intensity of tool flank wear. It was found by measuring of tool flank wear with respect to cutting speed and tool geometry and dividing the respective cutting length.

There are several methods to determine optimum tool geometry such as radio active method and conventional method. In radio active method, a radio active tool in used for the rapid measurement of tool-life. This method measure wear on the cutting face as well as on the clearance face i.e. tool flank. And the other process is conventional method, which consists of machining with a cutting tool, either until its complete failure or to a predetermined amount of wear from cutting operation in time or length, as wear measured an instrumental microscope. The experiment had been done on the rate of tool-wear with respect to cutting length. Instrumental microscope was used to measure the tool wear.

To determine the optimum tool geometry, the following conventional process may be considered i.e. power consumption vs. tool angle, vibration vs. tool angle, co-efficient of friction vs. tool angle, temperature vs. tool angle, cutting

speed vs. tool angle, tool life vs. tool angle, BUE vs. tool angle, cutting force vs. tool angle. Co-efficient of chip shrinkage vs. tool angle, and intensity of tool flank wear vs. tool angle with respect to variables, under consideration such as, feed, depth of cut, speed, nose radius etc.

This experiment has been performed to compare the intensity of flank tool wear with respect to different tool angles. The intensity of tool flank wear was calculated. Graphs of intensity of tool flank wear vs. cutting angle and also cutting speed were then drawn. Optimum values of cutting tool angles have been selected by studying the above curves.

3.7 Experimental Details

3.7.1 Determination of Critical Cutting Speed

To determine the critical cutting speed, considering the above parameters, in chapter-2, a solid stainless steel bar of 85 mm diameter and 53 cm length were set on the said lathe. Turning operations were carried out for obtaining uniform diameter of 84 mm. Considering feed. $S=0.2$ mm/rev. and depth of cut, $t = 1$ mm for each turning operation.

To determine the value of chip shrinkage from turning operations, a slot was made on the work material along the horizontal axis by the hacksaw, the depth of slot was not more than depth of cut, cutting operations were performed at

Sl. No.	Dia. of workpiece D mm	RPM N	Speed of m/c. V m/min	Actual cutting speed V_c m/min.	Length of uncut chip, L_c m	Length of chip, L m
1.	84	38	10.028	11.0	263.894	129.6
2.	58	60	10.933	12.1	182.212	90.4
3.	64	60	12.064	13.3	201.062	101.5
4.	58	72	13.119	14.0	182.212	95.0
5.	62	72	14.024	15.0	194.779	107.5
6.	80	60	15.080	16.1	251.327	146.0
7.	54	95	16.116	17.2	169.646	103.4
8.	76	72	17.191	18.6	238.761	152.2
9.	80	72	18.076	19.2	251.327	155.0
10.	84	70	19.000	20.2	263.894	159.0
11.	54	118	20.018	21.4	169.646	101.0
12.	70	95	20.892	22.1	219.912	133.3
13.	74	95	22.085	23.3	232.478	144.4
14.	62	118	22.984	24.2	194.779	124.0
15.	80	95	23.876	25.1	251.327	166.5
16.	84	95	25.070	26.5	263.894	189.0
17.	64	130	26.138	27.6	201.062	135.8
18.	66	130	26.955	28.4	207.345	133.6
19.	76	118	28.174	29.6	238.761	150.0
20.	50	185	29.060	30.5	157.080	97.5
21.	74	130	30.222	31.4	232.478	142.6
22.	76	130	31.039	32.3	238.761	145.4

Data Sheet - 1 :

For turning operation at $S=0.2$ mm/rev., $t=0.1$, $r=0$, $\alpha=5^\circ$, $\alpha_1=6^\circ$, $\phi=45^\circ$, $\phi_1=20^\circ$, $\gamma=0^\circ$, $\gamma_1=0^\circ$ and different cutting speeds, V_c to determine co-efficient of chip shrinkage k .

Sl. No.	Dia. of workpiece D mm	RPM N	Speed of m/c. V m/min	Actual cutting speed V_c m/min.	Length of uncut chip, L_c m	Length of chip, L m
23.	78	130	31.856	33.9	245.044	146.8
24.	82	130	33.489	34.8	257.611	153.2
25.	84	130	34.306	35.7	263.894	154.0
26.	60	185	34.872	36.2	188.496	109.0
27.	62	185	36.034	37.1	194.779	110.6
28.	64	185	37.197	38.3	201.062	112.0

Data Sheet : (Continued)

For turning operation at $S=0.2$ mm/rev., $t=0.1$, $r=0$, $\alpha=5^\circ$, $\alpha_1=6^\circ$, $\phi=45^\circ$, $\phi_1=20^\circ$, $\gamma=0^\circ$, $\gamma_1=0^\circ$ and different cutting speeds, V_c to determined co-efficient of chip shrinkage k.

Sl.No.	Actual cutting speed V_c , m/min.	Observation of BUE	Types of chips	Workpiece surface finishing
1.	11	Fracture	Dis-continuous	Rough
2.	12.1	"	"	"
3.	13.3	"	"	"
4.	15.0	"	"	"
5.	16.1	Unstable BUE	"	Less rough
6.	17.2	"	"	"
7.	18.6	Without BUE	Ribbon	Good
8.	19.2	"	"	"
9.	20.2	"	"	Medium
10.	21.4	BUE	"	"
11.	22.1	"	"	Less Medium
12.	23.3	"	Continuous	"
13.	24.2	Unstable BUE	"	Medium
14.	25.1	"	"	"
15.	26.5	"	"	Good
16.	27.6	Without BUE	"	"
17.	28.4	"	"	"
18.	29.6	"	"	"
19.	30.5	Unstable, BUE	"	Medium

Data sheet # 2

Observation of chip nature, quality and physical microscopic study to determine critical and optimum cutting speed.

Sl.No.	Actual cutting speed V_c , m/min.	Observation of BUE ^r	Types of chips	Work material surface finishing
20.	30.5	Unstable BUE	Continuous	Medium
21.	31.4	"	"	"
22.	32.3	"	"	Less rough
23.	33.9	"	"	"
24.	34.8	BUE	"	"
25.	35.7	"	"	"
26.	36.2	"	"	Rough
27.	37.1	"	"	"
28.	38.3	"	"	"

Data sheet # 2 (Continued)

Observation of chip nature, quality and physical microscopic study to determine critical and optimum cutting speed.

various cutting speeds and respective chips were collected. The actual cutting speeds, were calculated from the reading of tachometer which was recorded during cutting operation and uncut chip length were calculated for the respective speed. The length of chip was measured by rolling the chip over a sheet of paper.

The chips were collected separately for each cutting speed at least three marked sections and chips lengths were measured carefully and accurately and average chip length was calculated. The value of chip shrinkage was found by dividing the uncut chip length by the respective measured chip length. During cutting operation observed chip tool contact type by the metallurgical microscope and noted for every case. With the values of chip shrinkage and the corresponding values of cutting speed, a curve, $k = f(v)$ was plotted Fig. 12, there were two peaks of chip shrinkage at two cutting speeds. It is known that the reduction of the chip shrinkage usually is associated with a reduction in cutting force and also with an increase in temperature and vice-versa. Thus, at maximum chip shrinkage force is also maximum and for minimum chip shrinkage force is minimum. The values of uncut chip lengths and respective chip lengths for each cutting speed are shown in data sheet-1. The values of co-efficient of chip shrinkage with respective cutting speed were calculated and recorded in the table-1. Data sheet-2 shows the observed of chip nature and quality as found by physical observations and also

Table - 1

Determined values of K at S=02 mm/rev., t=0.1 mm, r=0, $\alpha=5^{\circ}$, $\alpha_1=6^{\circ}$, $\phi=45^{\circ}$, $\phi_1=20^{\circ}$, $\gamma=0^{\circ}$, $\gamma_1=0^{\circ}$ at different cutting speeds in turning stainless steel.

Sl. No.	Actual cutting speeds V_c m/min.	Co-efficient of shrinkage $K = \frac{L_o}{L}$	Sl. No.	Actual cutting speeds V_c m/min.	Co-efficient of shrinkage $K = \frac{L_o}{L}$
1.	11.0	2.0362	15.	25.1	1.5095
2.	12.1	2.0156	16.	26.5	1.3963
3.	13.3	1.9809	17.	27.6	1.4806
4.	14.0	1.9180	18.	28.4	1.5520
5.	15.0	1.8119	19.	29.6	1.5918
6.	16.1	1.7214	20.	30.5	1.6111
7.	17.2	1.6407	21.	31.4	1.6303
8.	18.6	1.5687	22.	32.3	1.6421
9.	19.2	1.6215	23.	33.9	1.6692
10.	20.2	1.6597	24.	34.8	1.6815
11.	21.4	1.6797	25.	35.7	1.7136
12.	22.1	1.6498	26.	36.2	1.7293
13.	23.3	1.6100	27.	37.1	1.7611
14.	24.2	1.5708	28.	38.3	1.7952

microscopic studies during experiment. A curve was plotted with chip shrinkage vs. respective cutting speed using the data of table-1 Fig.12. There is no sharp point which may be considered as critical cutting speed, because the critical cutting speed is that speed where the co-efficient of chip shrinkage is maximum and built-up-edge, is absent. From the curve, $k=f(v)$ in Fig.12 it is clear that the critical cutting speed, V_c lies between the point -7 to -11 and point -15 to -19. The two values of critical cutting speeds were due to double carbide cutting tool material and the critical values of cutting speed are mentioned by a range, not by a particular value. The select optimum cutting speed for cutting operations, required a particular critical cutting speed, V_c . But it is not possible to say the accurate critical cutting speed value from the curve of Fig. 12 though critical cutting speed V_c lies within the cutting speed range.

By carefully studying the chip shrinkage vs cutting speed curve with the characteristics of chips and observed data of table -1, it was found that the values of critical cutting speeds $V_c = 18.6$ m/min and $V_c = 26.5$ m/min. Because at point 8 and point 16, the values of chip shrinkage is comparatively minimum and turn towards high and BUE is absent and also work material had a good finished surface.

91746

Determination of critical cutting speed V_c of stainless steel with cemented carbide cutting tool

63

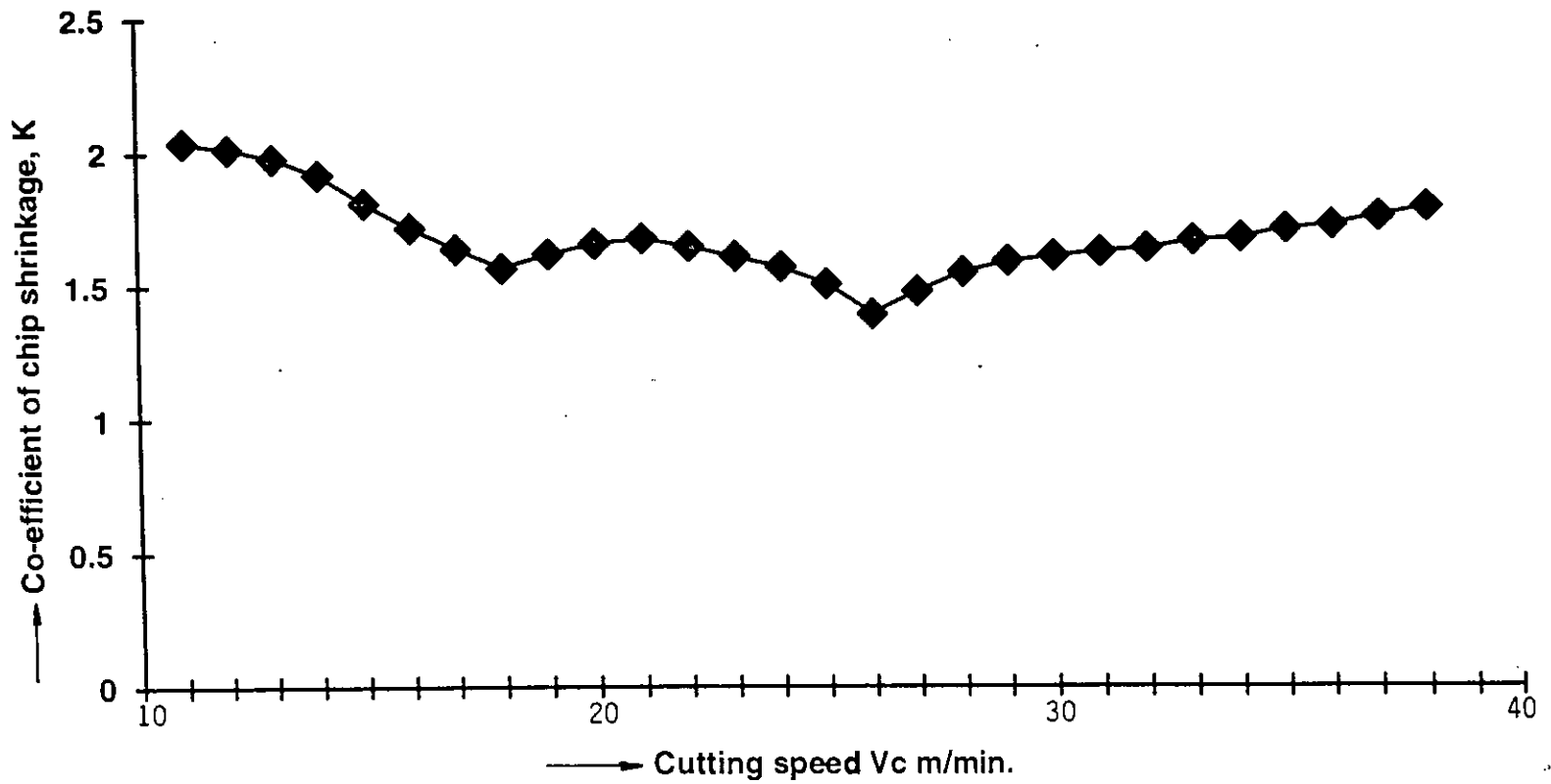


Fig. 12

3.7.2 Selection of experimental cutting speed to determine the optimum tool geometry

From Fig.12 and by observations of the cutting conditions, it was clear that there were two critical cutting speeds, i.e. double optimum cutting speed. That means turning operation could be selected in any one of the two optimum cutting speeds. Considering some other parameters such as chip characteristics, built-up-edge, tool wear, temperature, surface finish etc. metal cutting speed could be selected within a range. Therefore, the experimental cutting speeds, were selected at 15, 20, 25, 30, 35 m/min. by analyzing Fig. 12 and data sheet-2.

3.7.3 Determination of Intensity of Tool Flank Wear and Optimum Tool Geometry

Intensity of tool wear is defined as the wear per unit cutting length of the workpiece. In this experiment, intensity of tool flank wear was determined at a various conditions of tool geometry and cutting speeds. Cutting operation was carried out in the same lathe machine, which was used to determined critical cutting speed, using same work and tool materials of cutting conditions at $S=0.2$ mm/rev, $t=0.1$ mm, $r=0$ and different selected speeds for various tool geometry.

Solid shaft of stainless steel were turned at different speeds and cutting angles and turning was interrupted at a regular pre-determined traverse length, then measured

respective tool flank wear with an instrumental microscope by using chemical reagent aqua regia ($\text{HCl} : \text{HNO}_3 = 3:1$).

To measure the tool flank wear for each tool geometry and speed, cutting length of the workpieces were pre-determined and was divided into 3 to 5 divisions. Starting tool geometry was set at $\alpha=5^\circ$, $\alpha_1=6^\circ$, $\phi=45^\circ$, $\phi_1=20^\circ$, $\gamma=0^\circ$, & $\gamma_1=0^\circ$, which was used to determined critical cutting speed.

Tool flank wear was measured in this experiment by varying any one of the angles keeping the others fixed.

At first, side cutting relief angle α was varied and others angles were kept unchanged i.e. $\alpha_1=6^\circ$, $\phi=45^\circ$, $\phi_1=20^\circ$, $\gamma=0^\circ$, $\gamma_1=0^\circ$ was fixed and the values of α were 5° , 7° , 9° & 11° . First turning operation of the experiment was performed at side cutting relief angle $\alpha=5^\circ$, cutting speed was 16.1 m/min.

Stainless steel bar were cut five times each had predetermined traverse length (sample data sheet-3). Here after every turning operation the tool was carefully observed under the microscope and the tool flank wear was measured. The amount of wear was recorded each time (same data sheet-3). It was observed that the wear increased with the increase of traverse length is all cases.

A curve was plotted for these values of tool flank wear h_f and the corresponding values of length of cut L_c in Fig-13 for tool geometry $\alpha=5^\circ$, $\alpha_1=6^\circ$, $\phi=45^\circ$, $\phi_1=20^\circ$, $\gamma=0^\circ$, $\gamma_1=0^\circ$ and cutting speed 16.1 m/min. Straight line relationships were with different slope angles were obtain in different cases. From the slope of these curves intensity of tool flank wear I_h was calculated by using the relation, $I_h = \frac{h_f}{L_c}$. All of the values

of I_h were listed in table-2.

Similarly, in the same above tool geometry i.e. $\alpha=5^\circ$, $\alpha_1=6^\circ$, $\phi=45^\circ$, $\phi_1=20^\circ$, $\gamma=0^\circ$, $\gamma_1=0^\circ$; tool wear measured for cutting speeds in 21.7 m/min, 26.8 m/min, 30 and tool flank wear vs. cutting length L_c curves were drawn in Fig.13. Also intensity of tool flank wear I_h were calculated from the curves for respective cutting speed and were listed in table-2.

Similar cutting operations and calculations were performed for $\alpha=7^\circ$, $\alpha=9^\circ$ and $\alpha=11^\circ$ at different cutting speeds, where α_1 , ϕ , ϕ_1 , γ , γ_1 remain same as before and measured wear were recorded (sample data sheet-3). h_f vs. L_c curves were drawn in Fig. 14, 15 & 16 for $\alpha=7^\circ$, $\alpha=9^\circ$ and $\alpha=11^\circ$ respectively, and calculated intensity of tool flank wear were listed in table-2.

In the same proceses, similar experiment was done for end cutting relief angle α_1 , side cutting edge angle ϕ , end

Obn. No.	Machine rpm N	Work piece dia, d, mm	Actual cutting speed V_c , m/min	Time for each turning operation T. min	Length of cut, L_c m	Flank wear, h_f mm
1	60	80	16.1	5 min 5 sec	81.681	0.06
2				10 min 10 sec	163.363	0.083
3				15 min 16 sec	245.044	0.125
4				20 min 22 sec	326.726	0.16
5				25 min 28 sec	408.407	0.196
1	95	68	21.7	3 min 5 sec	85.451	0.067
2				7 min 54 sec	170.903	0.108
3				11 min 51 sec	256.354	0.16
4				15 min 49 sec	341.805	0.205
5				19 min 47 sec	427.257	0.252
1	118	68	26.8	2 min 48 sec	74.770	0.05
2				5 min 36 sec	149.540	0.081
3				9 min 36 sec	256.354	0.142
1	130	70	30.3	2 min 33 sec	76.969	0.073
2				5 min 7 sec	153.938	0.11
3				8 min 39 sec	260.752	0.17
1	130	78	33.9	2 min 22 sec	79.639	0.062
2				4 min 45 sec	159.779	0.11
3				7 min 8 sec	238.918	0.164
4				9 min 31 sec	318.558	0.213
5				11 min 54 sec	398.197	0.257

Sample Data sheet # 3

For turning stainless steel at $S=0.2$ mm/rev., $t=0.1$, $r=0$, $\alpha=5^\circ$, $\alpha_1=6^\circ$, $\phi=45^\circ$, $\phi_1=20^\circ$, $\gamma=0^\circ$, $\gamma_1=0^\circ$ with cemented carbide.

Table-2

Determined values of I_h for various tool geometry and cutting speeds in turning stainless steel with cemented carbide cutting tool

Tool geometry	Actual cutting speed, V_c m/min	Intensity of tool flank wear $I_h \times 10^{-4}$ mm/m	Tool geometry	Actual cutting speed, V_c m/min	Intensity of tool flank wear $I_h \times 10^{-4}$ mm/m
$\alpha=5^\circ$, $\alpha_1=6^\circ$, $\phi=45^\circ$, $\phi_1=20^\circ$, $\gamma=0^\circ$, $\gamma_1=0^\circ$	16.1	4.28494	$\alpha_1=5^\circ$, $\alpha=7^\circ$, $\phi=45^\circ$, $\phi_1=20^\circ$, $\gamma=0^\circ$, $\gamma_1=0^\circ$	16.3	2.93918
	21.7	5.50002		22.0	3.22270
	26.8	5.23174		25.8	2.84030
	30.3	5.44070		33.6	3.24300
	33.9	6.27836			
$\alpha=7^\circ$, $\alpha_1=6^\circ$, $\phi=45^\circ$, $\phi_1=20^\circ$, $\gamma=0^\circ$, $\gamma_1=0^\circ$	16.1	2.98400	$\alpha_1=7^\circ$, $\alpha=7^\circ$, $\phi=45^\circ$, $\phi_1=20^\circ$, $\gamma=0^\circ$, $\gamma_1=0^\circ$	14.4	3.01900
	20.2	3.50545		22.6	2.74470
	22.1	3.59204		25.9	2.43580
	25.8	2.79058		34.2	2.84360
	28.0	3.08815			
	30.6	3.57100			
$\alpha=9^\circ$, $\alpha_1=6^\circ$, $\phi=45^\circ$, $\phi_1=20^\circ$, $\gamma=0^\circ$, $\gamma_1=0^\circ$	17.3	2.93030	$\alpha_1=9^\circ$, $\alpha=7^\circ$, $\phi=45^\circ$, $\phi_1=20^\circ$, $\gamma=0^\circ$, $\gamma_1=0^\circ$	15.0	3.46500
	19.6	3.32517		19.6	3.59700
	23.3	3.81100		25.0	3.31500
	26.5	3.63170		28.4	3.56500
	28.5	3.99500			
	31.9	4.54346			
$\alpha=11^\circ$, $\alpha_1=6^\circ$, $\phi=45^\circ$, $\phi_1=20^\circ$, $\gamma=0^\circ$, $\gamma_1=0^\circ$	15.0	3.10850	$\alpha_1=11^\circ$, $\alpha=7^\circ$, $\phi=45^\circ$, $\phi_1=20^\circ$, $\gamma=0^\circ$, $\gamma_1=0^\circ$	15.2	3.64600
	18.6	3.62875		20.4	4.36500
	24.6	4.49380		26.9	3.74300
	28.4	4.27969		31.9	4.44000
	33.2	5.37086			

Tool geometry	Actual cutting speed, V_c , m/min	Intensity of tool flank wear $I_f \times 10^{-4}$ mm/m	Tool geometry	Actual cutting speed, V_c , m/min	Intensity of tool flank wear $I_f \times 10^{-4}$ mm/m
$\phi=30^0$, $\alpha=7^0$, $\alpha_1=7^0$, $\phi_1=20^0$, $\gamma=0^0$, $\gamma_1=0^0$	15.1	3.35986	$\phi_1=15^0$, $\alpha=7^0$, $\alpha_1=7^0$, $\phi=50^0$, $\gamma=0^0$, $\gamma_1=0^0$	13.2	2.54669
	21.9	3.86084		19.5	2.72845
	28.1	3.78403		23.8	2.45161
	33.9	3.42827		31.2	2.67402
$\phi=40^0$, $\alpha=7^0$, $\alpha_1=7^0$, $\phi_1=20^0$, $\gamma=0^0$, $\gamma_1=0^0$	16.3	3.02041	$\phi_1=25^0$, $\alpha=7^0$, $\alpha_1=7^0$, $\phi=50^0$, $\gamma=0^0$, $\gamma_1=0^0$	12.7	2.60831
	22.0	2.80409		19.3	2.64000
	26.0	3.22413		22.8	2.07780
	33.6	3.96857		30.7	2.59850
$\phi=50^0$, $\alpha=7^0$, $\alpha_1=7^0$, $\phi_1=20^0$, $\gamma=0^0$, $\gamma_1=0^0$	15.5	2.56410	$\phi_1=35^0$, $\alpha=7^0$, $\alpha_1=7^0$, $\phi=50^0$, $\gamma=0^0$, $\gamma_1=0^0$	12.5	3.43115
	22.2	2.65258		18.8	3.26797
	27.0	2.37043		22.1	2.96040
	32.0	2.61050		29.9	3.38601
$\phi=60^0$, $\alpha=7^0$, $\alpha_1=7^0$, $\phi_1=20^0$, $\gamma=0^0$, $\gamma_1=0^0$	15.1	3.09390	$\phi_1=45^0$, $\alpha=7^0$, $\alpha_1=7^0$, $\phi=50^0$, $\gamma=0^0$, $\gamma_1=0^0$	18.0	3.37918
	21.9	3.07690		21.8	3.61493
	26.9	2.68112		27.7	3.45659
	34.5	3.08756		34.2	3.93891

Tool geometry	Actual cutting speed, V_c , m/min	Intensity of tool flank wear $I_h \times 10^{-4}$ mm/m	Tool geometry	Actual cutting speed, V_c , m/min	Intensity of tool flank wear $I_h \times 10^{-4}$ mm/m
$\gamma = -8^\circ$, $\alpha = 7^\circ$, $\alpha_1 = 7^\circ$, $\phi = 50^\circ$, $\phi_1 = 25^\circ$, $\gamma_1 = 0^\circ$	16.5	3.66316	$\gamma_1 = -7^\circ$, $\alpha = 7^\circ$, $\alpha_1 = 7^\circ$, $\phi = 50^\circ$, $\phi_1 = 25^\circ$, $\gamma = 0^\circ$	15.7	3.33467
	20.8	3.12629		21.7	3.18345
	27.1	3.12252		26.8	3.90168
	33.4	4.25255		33.8	4.34020

$\gamma = 0^\circ$, $\alpha = 7^\circ$, $\alpha_1 = 7^\circ$, $\phi = 50^\circ$, $\phi_1 = 25^\circ$, $\gamma_1 = 0^\circ$	16.1	2.23506	$\gamma_1 = 0^\circ$, $\alpha = 7^\circ$, $\alpha_1 = 7^\circ$, $\phi = 50^\circ$, $\phi_1 = 25^\circ$, $\gamma = 0^\circ$	15.4	2.24291
	19.2	2.19780		20.4	2.11355
	25.8	1.92237		26.0	1.96834
	32.0	2.14418		32.0	2.25080

$\gamma = 5^\circ$, $\alpha = 7^\circ$, $\alpha_1 = 7^\circ$, $\phi = 50^\circ$, $\phi_1 = 25^\circ$, $\gamma_1 = 0^\circ$	17.4	2.48820	$\gamma_1 = 5^\circ$, $\alpha = 7^\circ$, $\alpha_1 = 7^\circ$, $\phi = 50^\circ$, $\phi_1 = 25^\circ$, $\gamma = 0^\circ$	14.0	2.05761
	22.6	2.44211		19.4	1.98915
	27.2	2.07882		25.9	1.67993
	31.9	2.23230		33.9	1.92898

$\gamma = 10^\circ$, $\alpha = 7^\circ$, $\alpha_1 = 7^\circ$, $\phi = 50^\circ$, $\phi_1 = 25^\circ$, $\gamma_1 = 0^\circ$	17.8	2.62187	$\gamma_1 = 10^\circ$, $\alpha = 7^\circ$, $\alpha_1 = 7^\circ$, $\phi = 50^\circ$, $\phi_1 = 25^\circ$, $\gamma = 0^\circ$	16.3	2.40816
	23.6	2.51290		22.0	2.50095
	30.0	2.83207		25.8	2.29674
	33.9	2.99262		33.6	3.14342

cutting edge angle ϕ_1 . Back rake angle γ and side rake angle, γ_1 measured data and calculated values of I_h were recorded in same sample data sheet and table and graphs were plotted as follows. h_f vs. L_c curves were drawn in fig. 17, 18, 19 & 20 for variable α_1 of 5° , 7° , 9° & 11° respectively, where other angles were fixed. Fig. 21, 22, 23 & 24 for variable ϕ of 30° , 40° , 50° & 60° respectively, where others angle were fixed, Fig. 25, 26, 27 & 28 for variable ϕ_1 of 15° , 25° , 35° & 45° respectively, where other angles were fixed. Fig. 29, 30, 31 & 32 for variable γ of -8° , 0° , 5° & 10° respectively and other angles fixed, Fig. 33, 34, 35 & 36 for variable γ_1 of -7° , 0° , 5° & 10° respectively where others angle fixed.

For every tool geometry, it should be noted here that after the turning operation for a particular speed. It was carefully grinded the tool flank wear to the original tool angle, which was created during cutting operation. Actual rpm and cutting times were also measured and recorded (sample data sheet 3) during turning operations. Chips were also collected for microscopic analysis and to determine optimum tool geometry.

There were five cutting speeds for tool geometry $\alpha=5^\circ$, $\alpha_1=6^\circ$, $\phi=45^\circ$, $\phi=20^\circ$, $\gamma=0^\circ$, $\gamma_1=0^\circ$ where α was variable and others were fixed. h_f vs. L_c curves were drawn in Fig. 13 for each cutting speed and intensity of tool flank were I_h was calculated from each curve for the respective cutting speed and was listed in

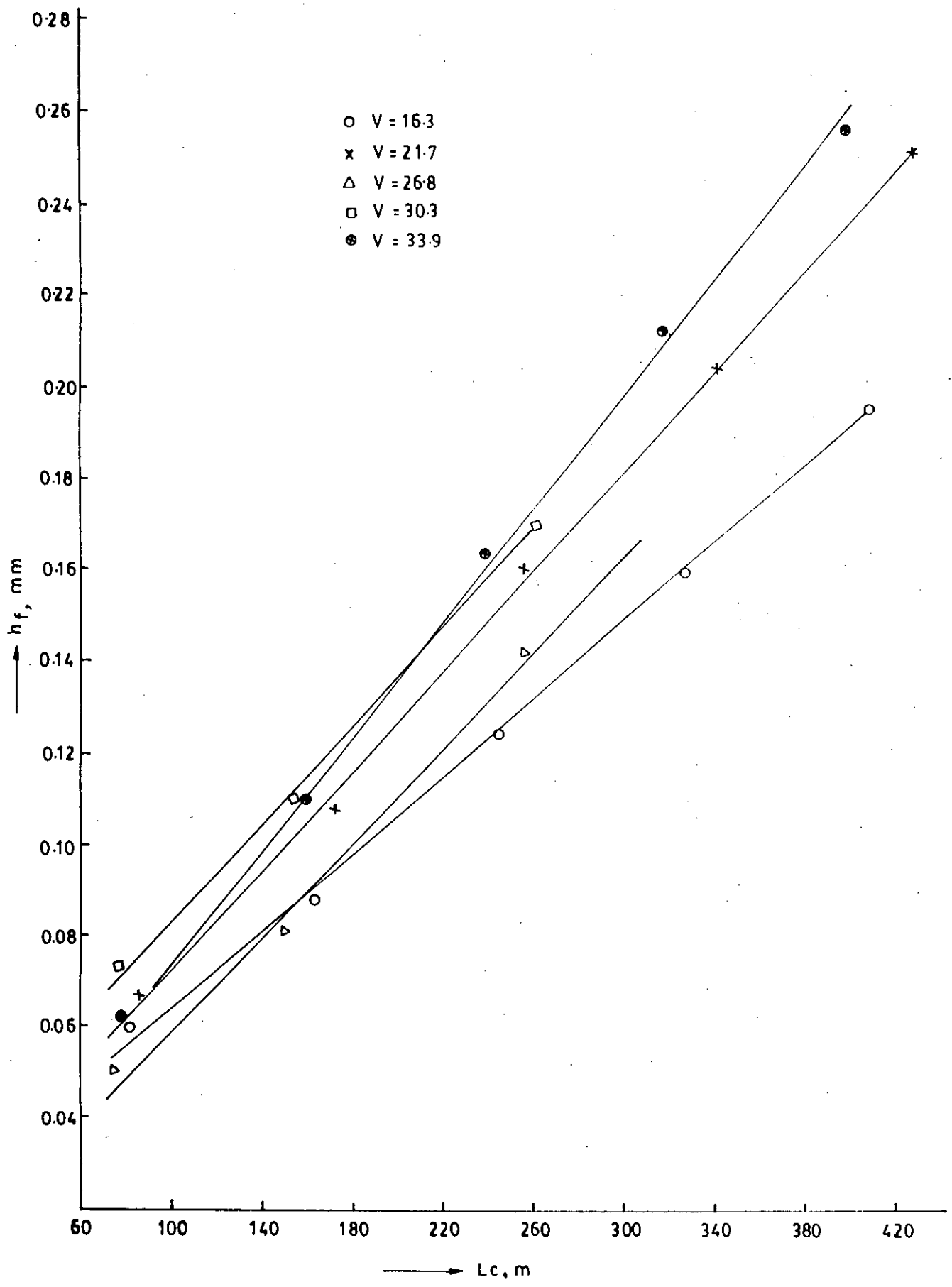


Figure-13 .
 Effect of cutting length on tool flank wear, h_f at
 constant $S=0.2$ mm/rev, $t=0.1$ mm $r=0$, $\alpha=5^\circ$, $\alpha_1=6^\circ$, $\phi=45^\circ$
 $\phi_1=20^\circ$, $\gamma=0^\circ$ & $\gamma_1=0^\circ$ in turning with stainless steel
 with cemented carbide cutting tool.

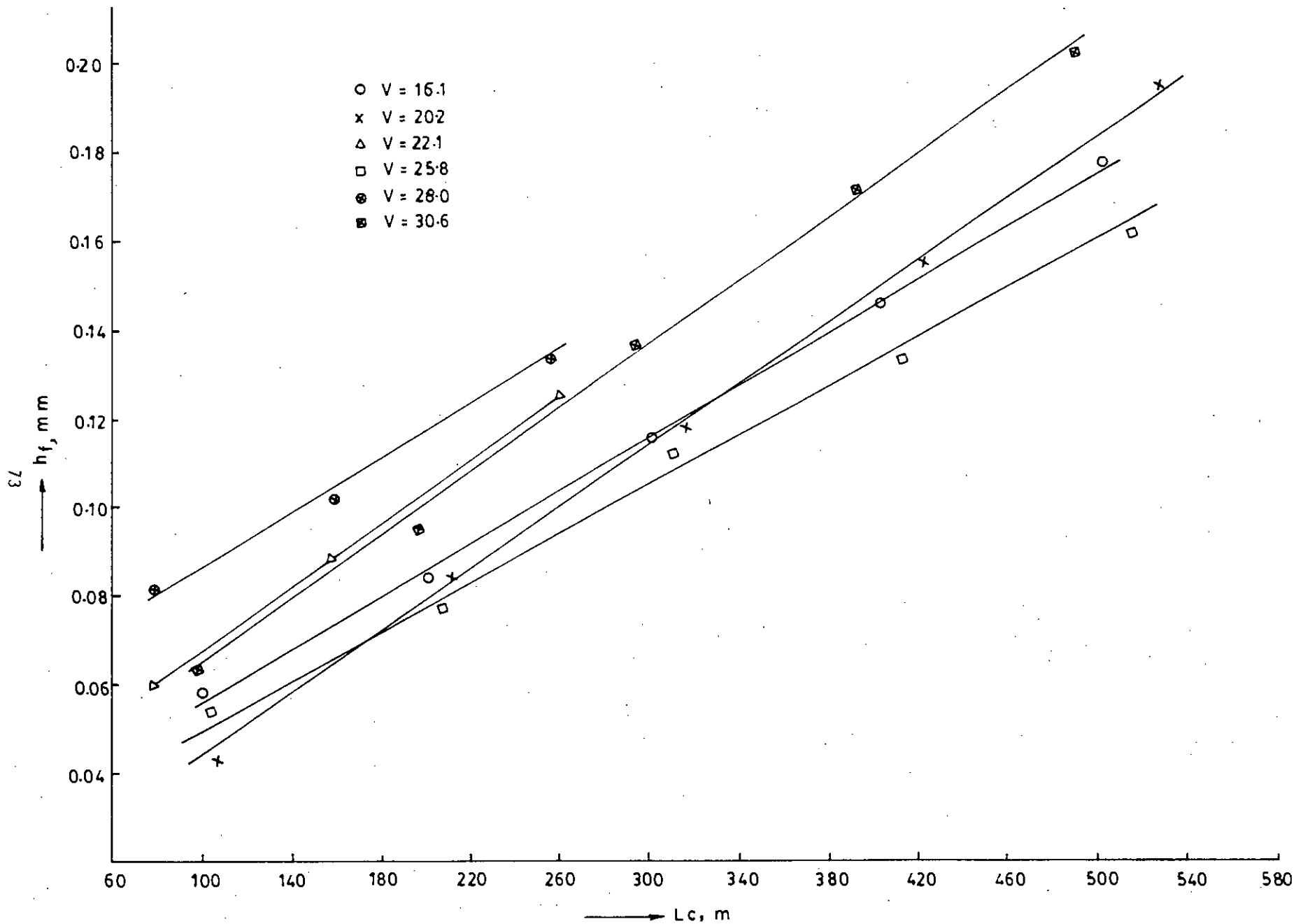


Figure-14
 Effect of cutting length on tool flank wear, h_f at
 constant $S=0.2 \text{ mm/rev}$, $t=0.1 \text{ mm}$, $r=0$, $\alpha=7^\circ$, $\alpha_1=6^\circ$, $\phi=45^\circ$
 $\phi_1=20^\circ$, $\gamma=0^\circ$ & $\gamma_1=0^\circ$ in turning with stainless steel
 with cemented carbide cutting tool.

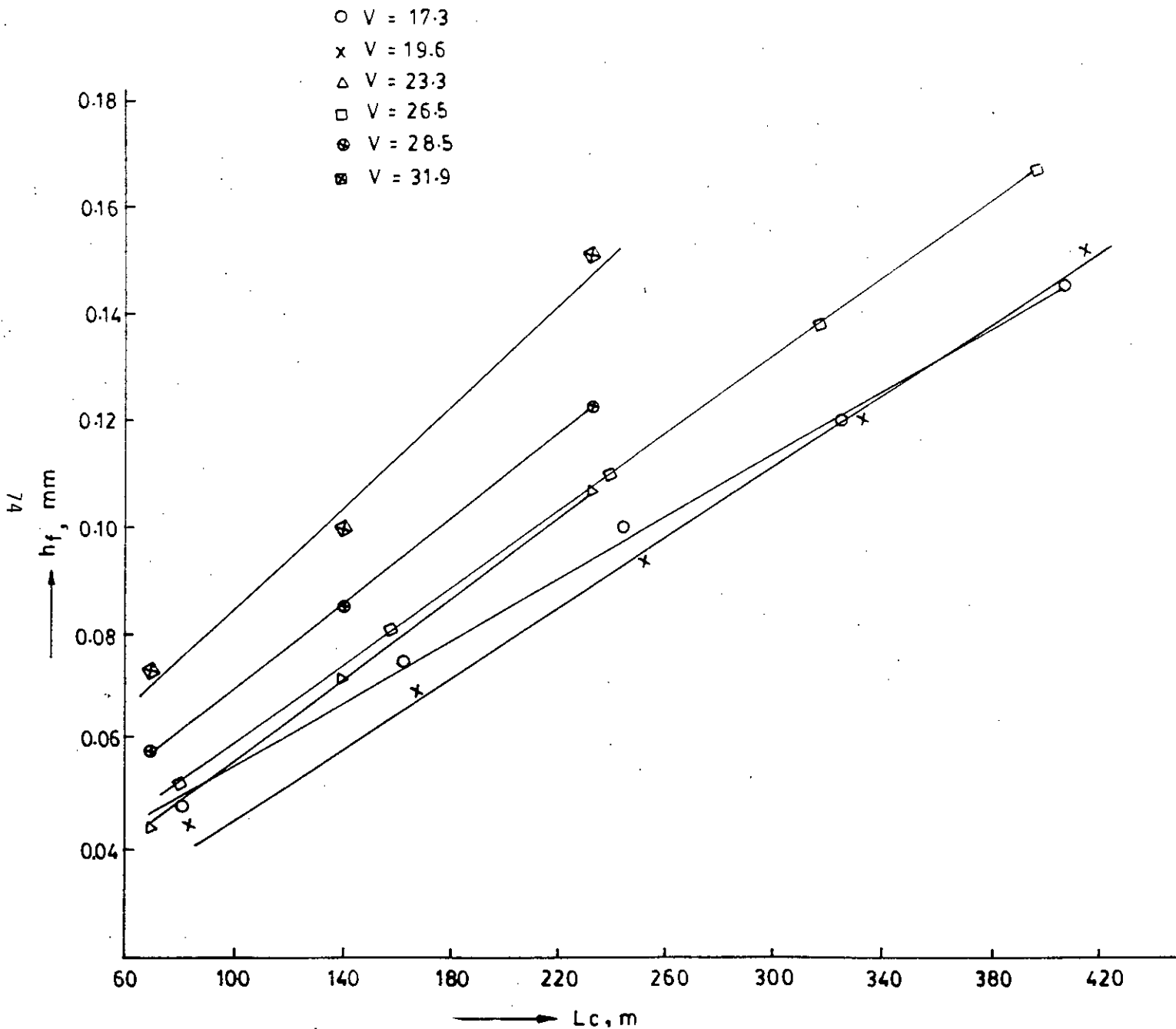


Figure-15
 Effect of cutting length on tool flank wear, h_f at
 constant $s=0.2$ mm/rev, $t=0.1$ mm $r=0$, $\alpha=9^\circ$, $\alpha_1=6^\circ$, $\phi=45^\circ$
 $\phi_1=20^\circ$, $\gamma=0^\circ$ & $\gamma_1=0^\circ$ in turning with stainless steel
 with cemented carbide cutting tool.

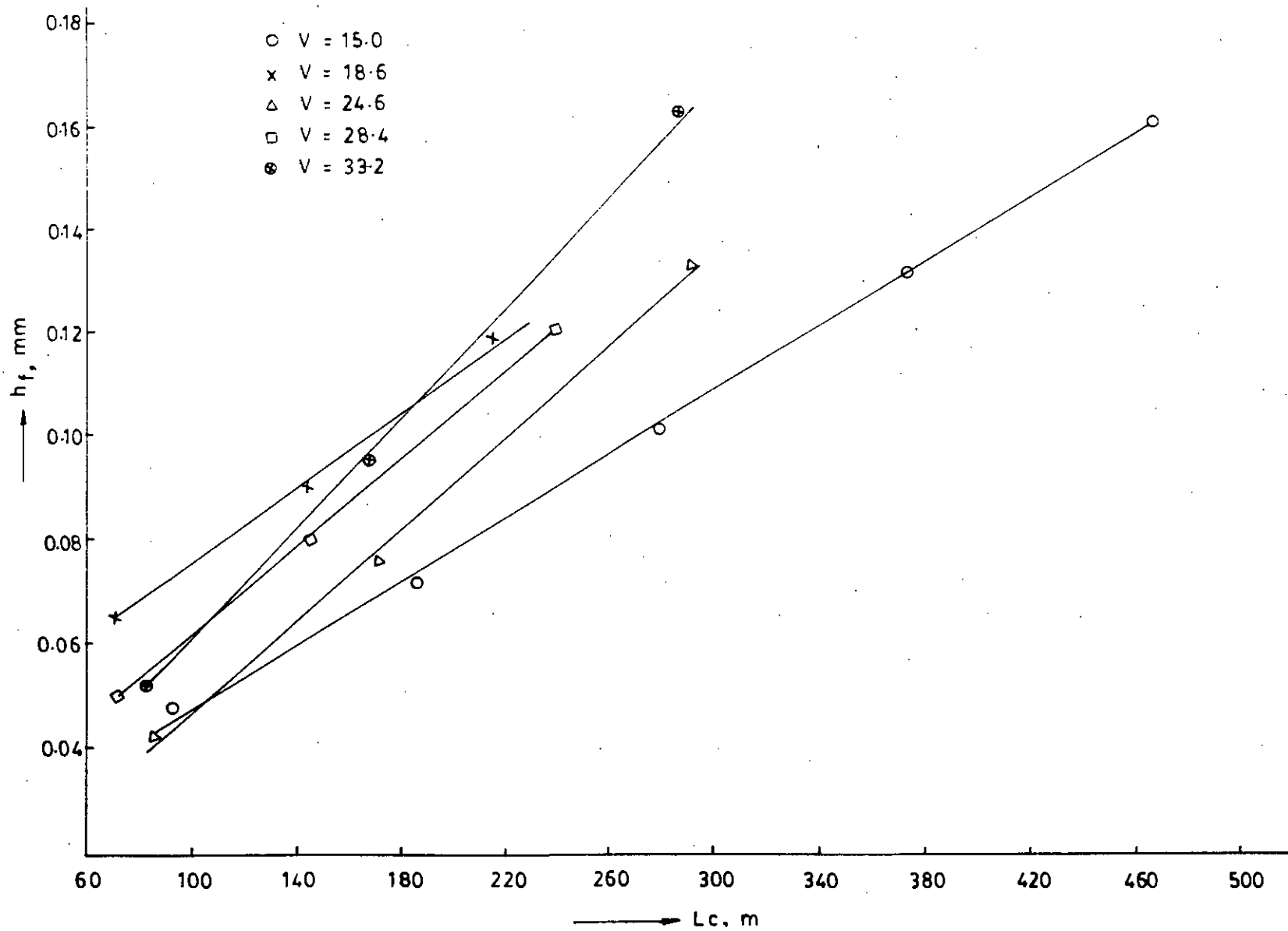


Figure-16
 Effect of cutting length on tool flank wear, h_f , at
 constant $S=0.2$ mm/rev, $t=0.1$ mm $r=0$, $\alpha=11^\circ$, $\alpha_1=6^\circ$, $\phi=45^\circ$
 $\phi_1=20^\circ$, $\gamma=0^\circ$ & $\gamma_1=0^\circ$ in turning with stainless steel
 with cemented carbide cutting tool.

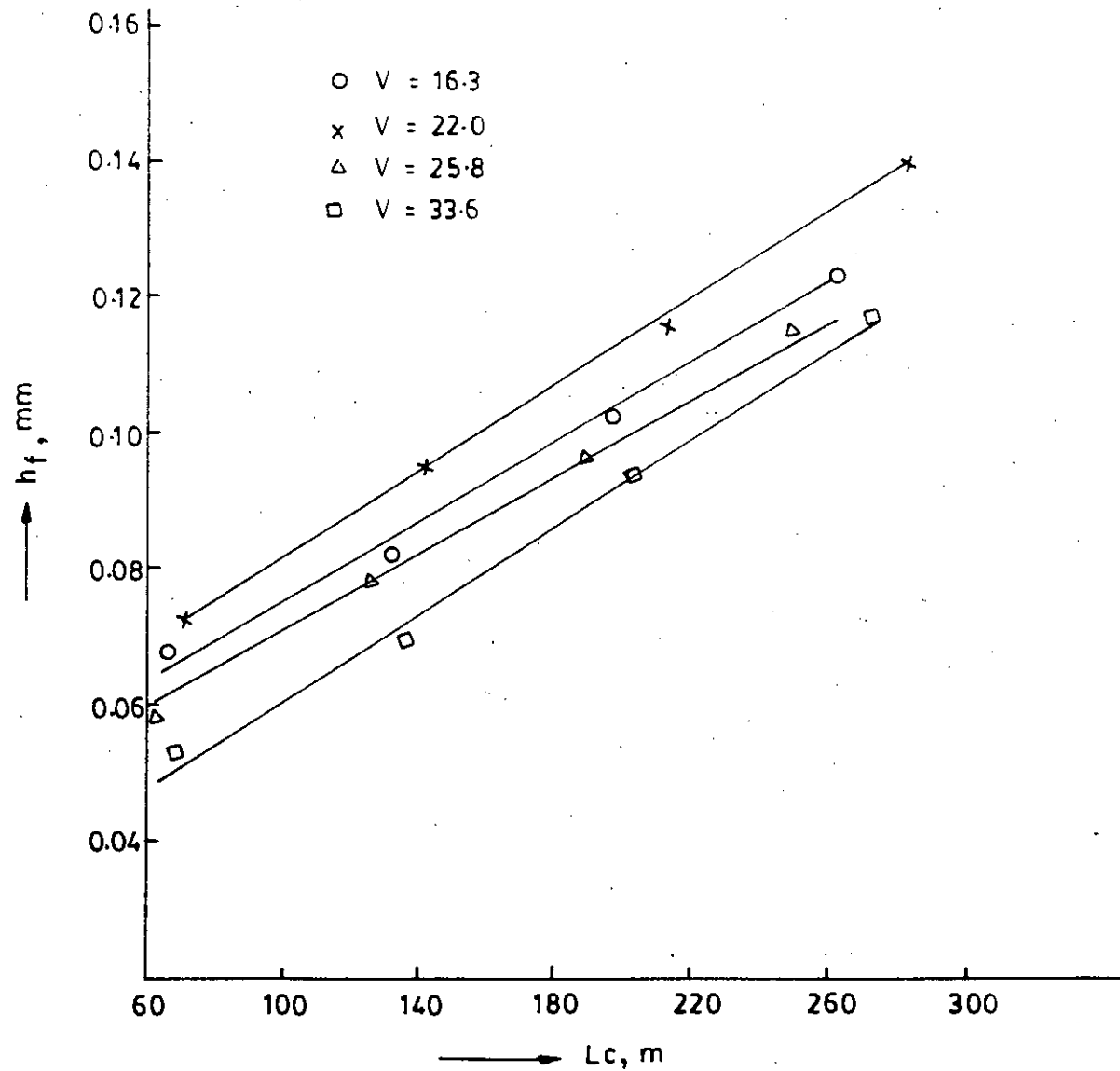


Figure-17
 Effect of cutting length on tool flank wear, h_f at constant $S=0.2$ mm/rev, $t=0.1$ mm $r=0$, $\alpha=7^\circ$, $\alpha_1=5^\circ$, $\phi=45^\circ$, $\phi_1=20^\circ$, $\gamma=0^\circ$ & $\gamma_1=0^\circ$ in turning with stainless steel with cemented carbide cutting tool.

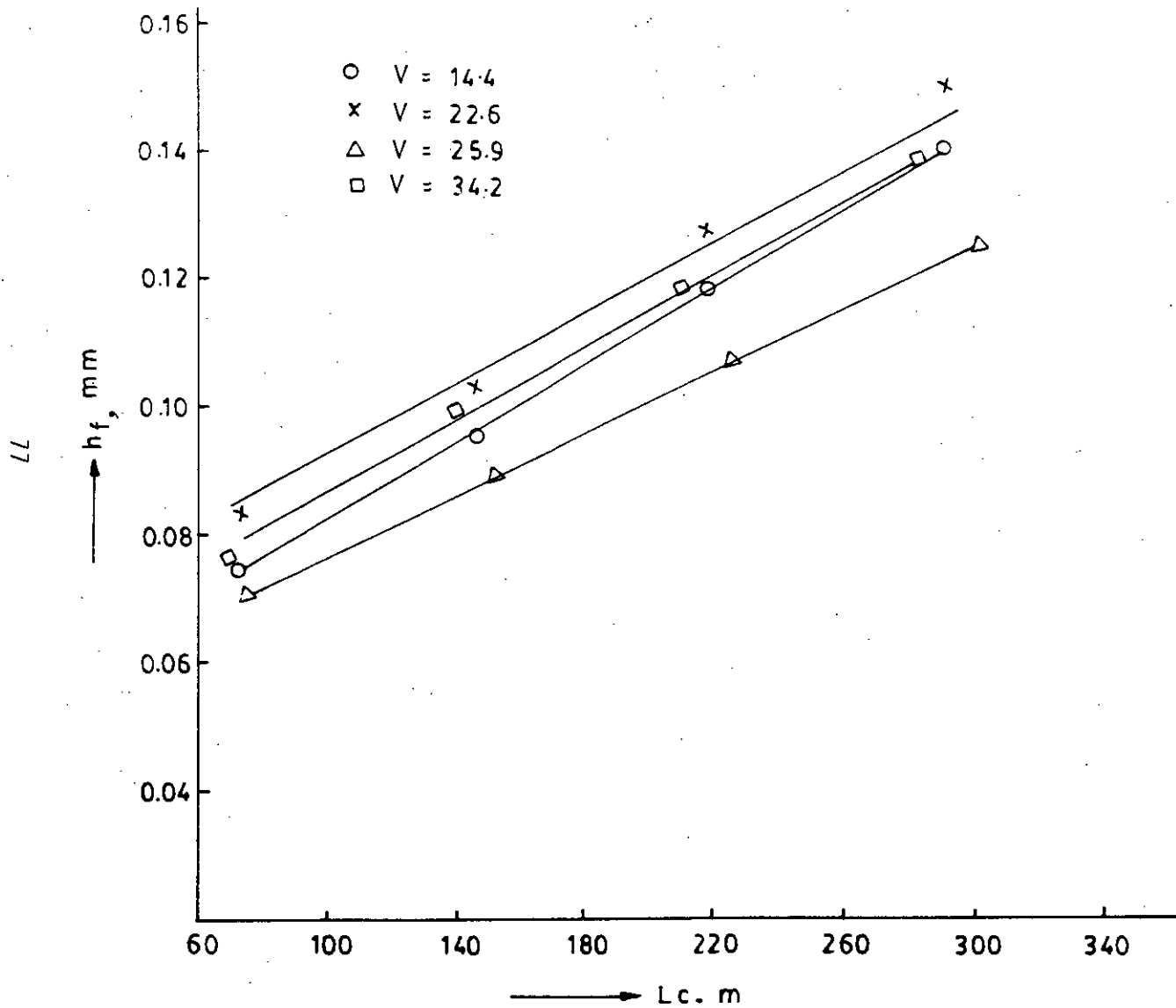


Figure-18
 Effect of cutting length on tool flank wear, h_f at constant $S=0.2$ mm/rev, $t=0.1$ mm $r=0$, $\alpha=7^\circ$, $\alpha_1=7^\circ$, $\phi=45^\circ$, $\phi_1=20^\circ$, $\gamma=0^\circ$ & $\gamma_1=0^\circ$ in turning with stainless steel with cemented carbide cutting tool.

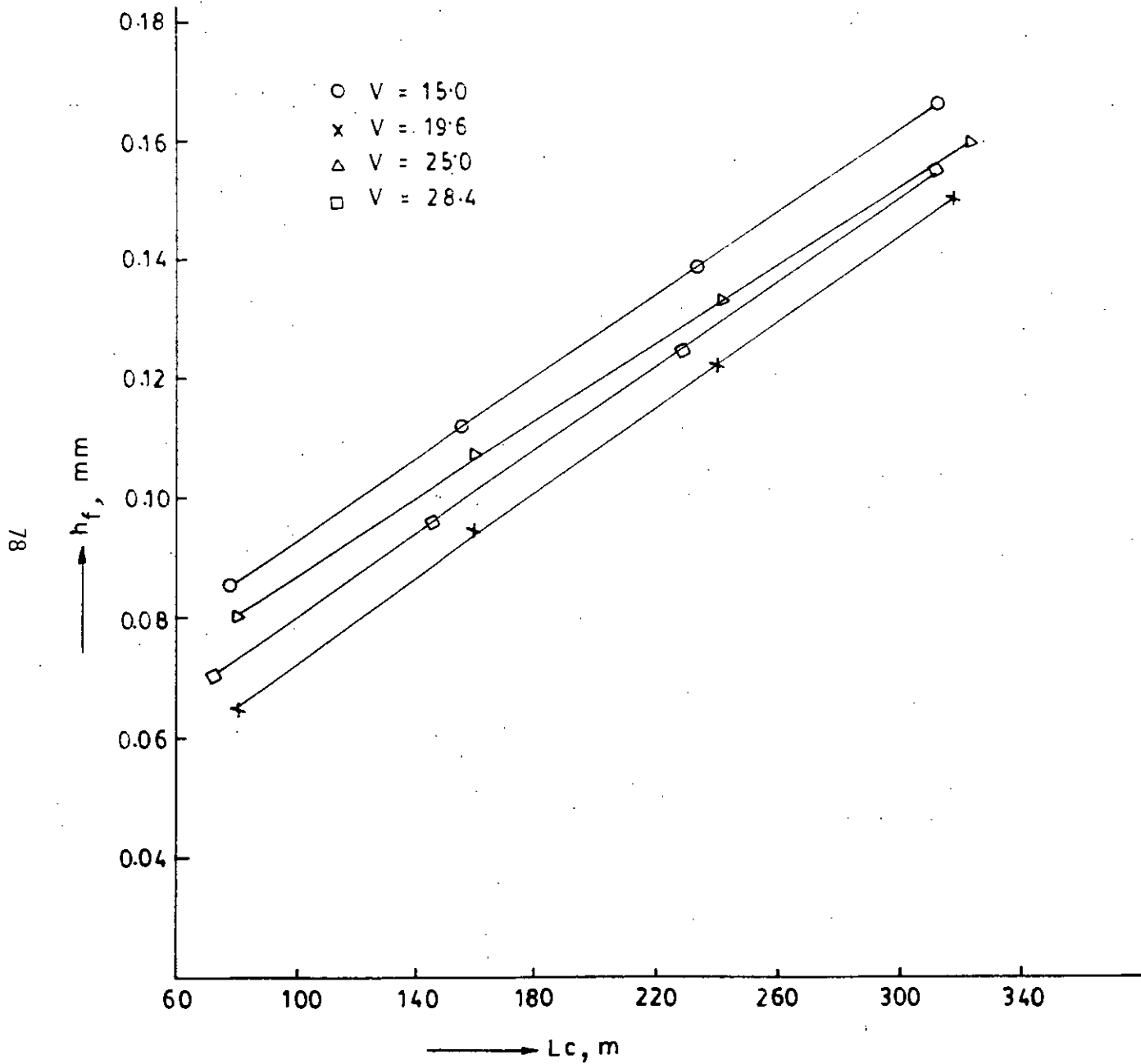


Figure-19

Effect of cutting length on tool flank wear, h_f at constant $S=0.2$ mm/rev, $t=0.1$ mm $r=0$, $\alpha=7^\circ$, $\alpha_1=9^\circ$, $\phi=45^\circ$, $\phi_1=20^\circ$, $\gamma=0^\circ$ & $\gamma_1=0^\circ$ in turning with stainless steel with cemented carbide cutting tool.

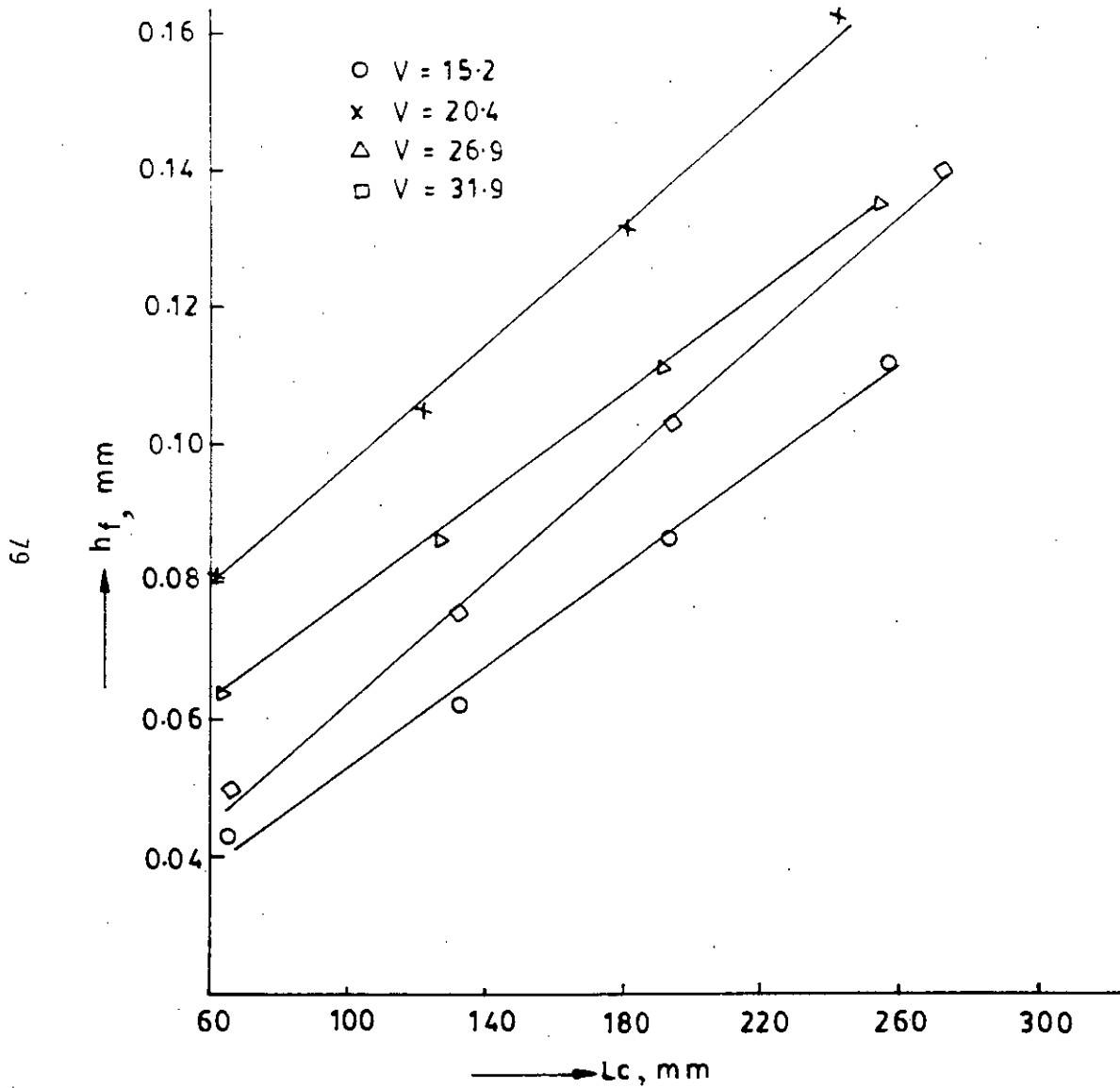


Figure-20
 Effect of cutting length on tool flank wear, h_f at constant $S=0.2$ mm/rev, $t=0.1$ mm $r=0$, $\alpha=7^\circ$, $\alpha_1=11^\circ$, $\phi=45^\circ$, $\phi_1=20^\circ$, $\gamma=0^\circ$ & $\gamma_1=0^\circ$ in turning with stainless steel with cemented carbide cutting tool.

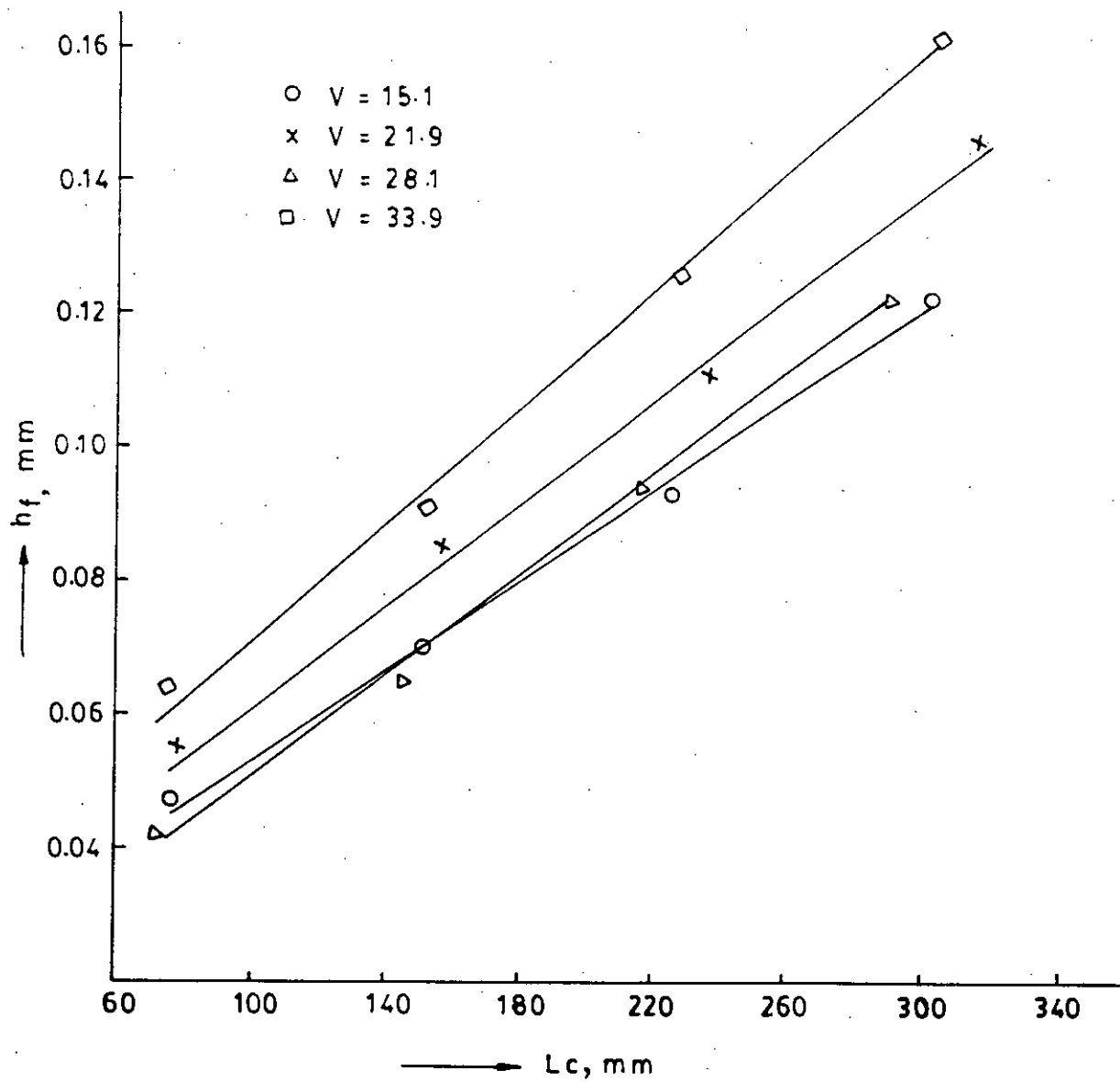


Figure-21
 Effect of cutting length on tool flank wear, h_f at constant $S=0.2$ mm/rev, $t=0.1$ mm $r=0$, $\alpha=7^\circ$, $\alpha_1=7^\circ$, $\phi=30^\circ$, $\phi_1=20^\circ$, $\gamma=0^\circ$ & $\gamma_1=0^\circ$ in turning with stainless steel with cemented carbide cutting tool.

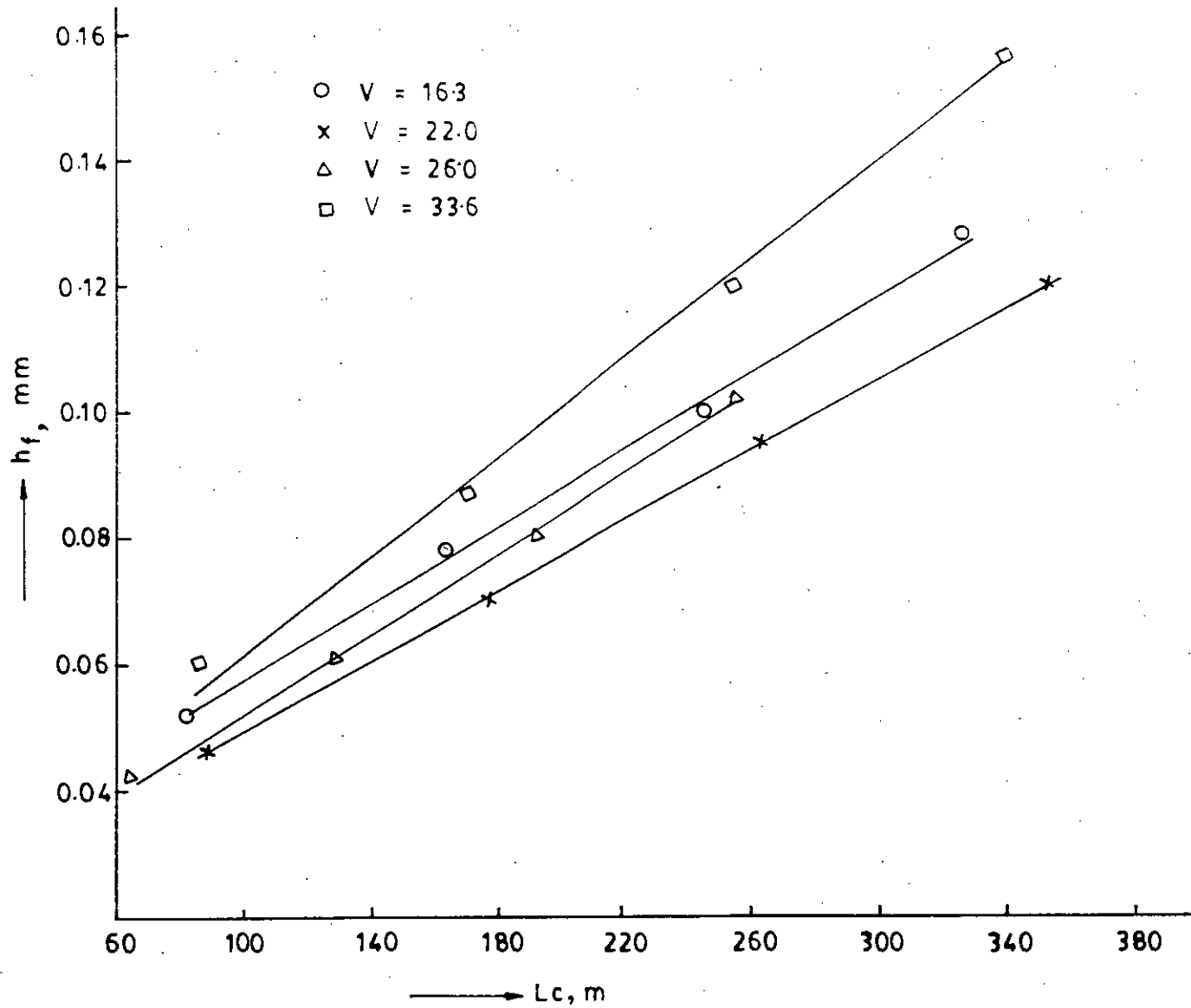


Figure-22

Effect of cutting-length on tool-flank wear, h_f , at constant $S=0.2$ mm/rev, $t=0.1$ mm $r=0$, $\alpha=7^\circ$, $\alpha_1=7^\circ$, $\phi=40^\circ$, $\phi_1=20^\circ$, $\gamma=0^\circ$ & $\gamma_1=0^\circ$ in turning with stainless steel with cemented carbide cutting tool.

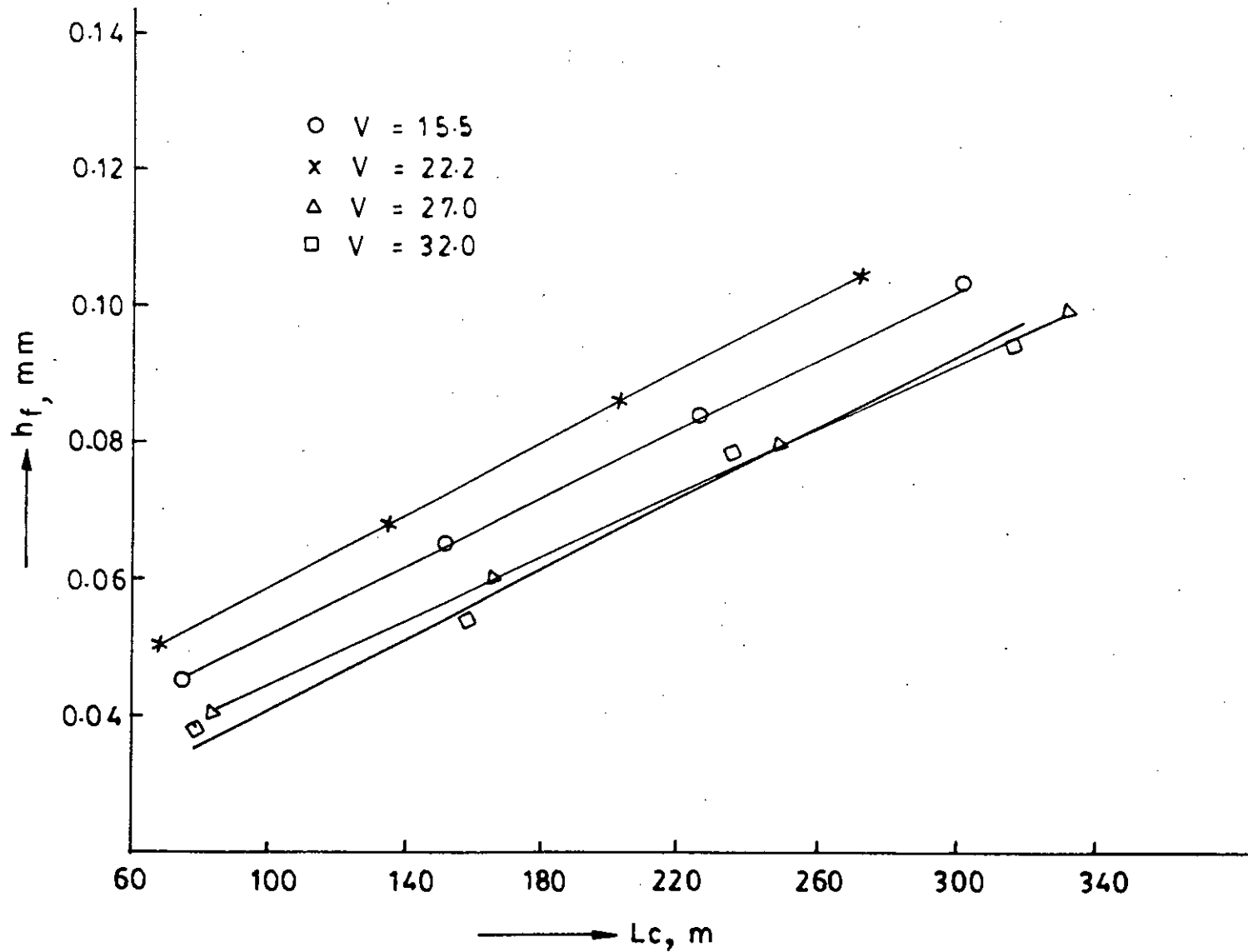


Figure-23

Effect of cutting length on tool flank wear, h_f at constant $S=0.2$ mm/rev, $t=0.1$ mm $r=0$, $\alpha=7^\circ$, $\alpha_1=7^\circ$, $\phi=50^\circ$, $\phi_1=20^\circ$, $\gamma=0^\circ$ & $\gamma_1=0^\circ$ in turning with stainless steel with cemented carbide cutting tool.

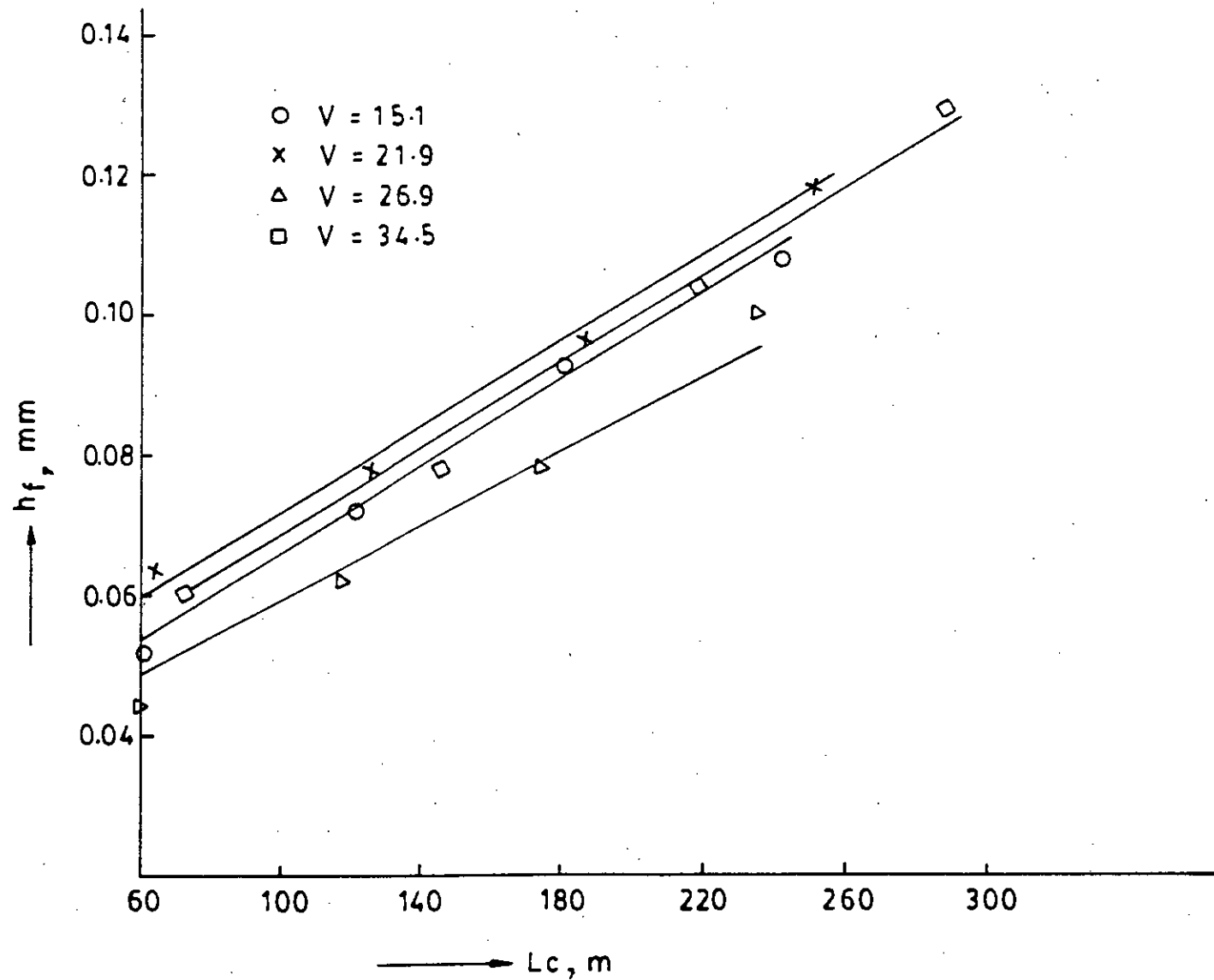


Figure-24

Effect of cutting length on tool flank wear, h_f at constant $S=0.2$ mm/rev, $t=0.1$ mm $r=0$, $\alpha=7^\circ$, $\alpha_1=7^\circ$, $\phi=60^\circ$, $\phi_1=20^\circ$, $\gamma=0^\circ$ & $\gamma_1=0^\circ$ in turning with stainless steel with cemented carbide cutting tool.

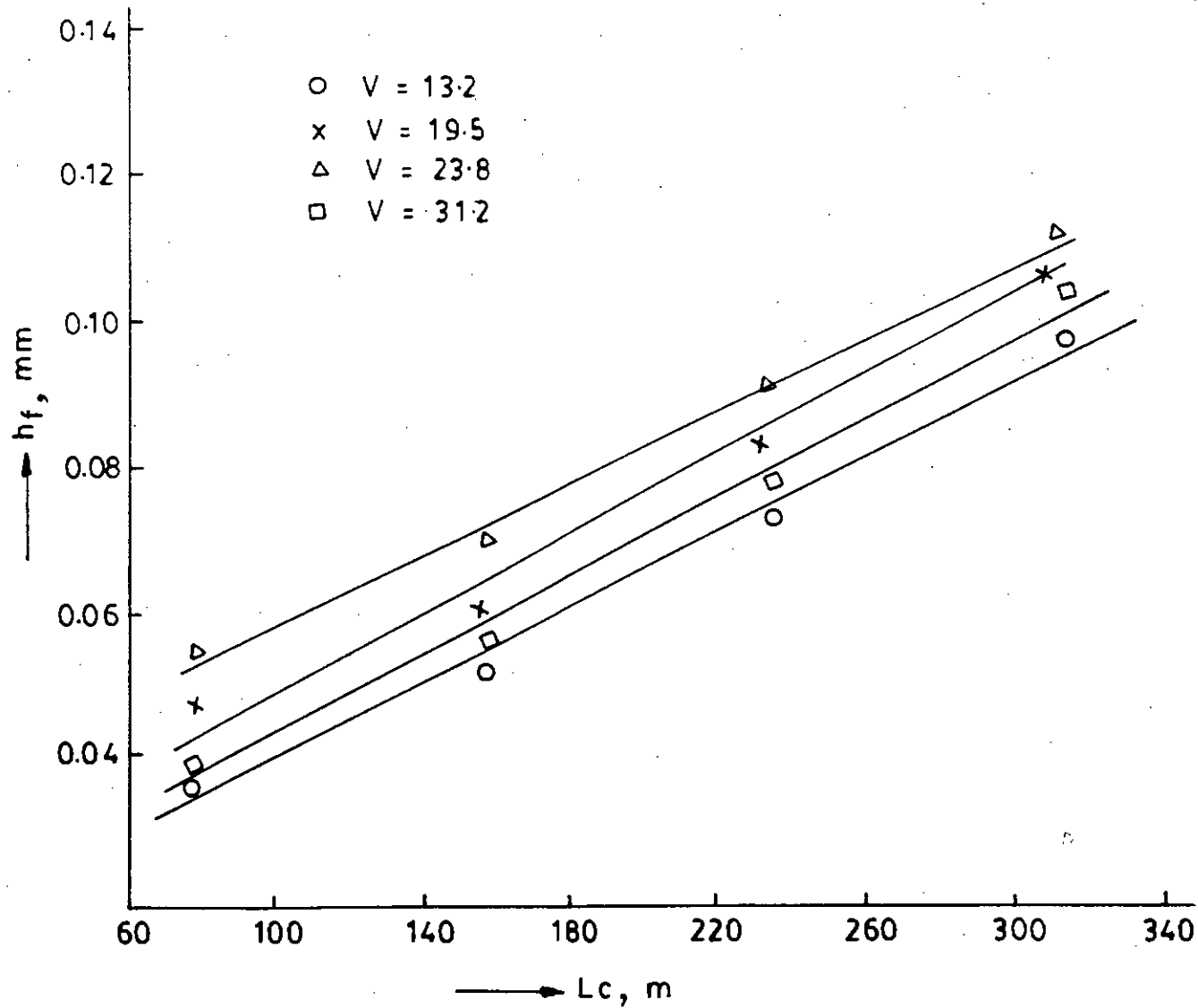


Figure-25
 Effect of cutting length on tool flank wear, h_f at constant $S=0.2$ mm/rev, $t=0.1$ mm $r=0$, $\alpha=7^\circ$, $\alpha_1=7^\circ$, $\phi=50^\circ$, $\phi=15^\circ$, $\gamma=0^\circ$ & $\gamma_1=0^\circ$ in turning with stainless steel with cemented carbide cutting tool.

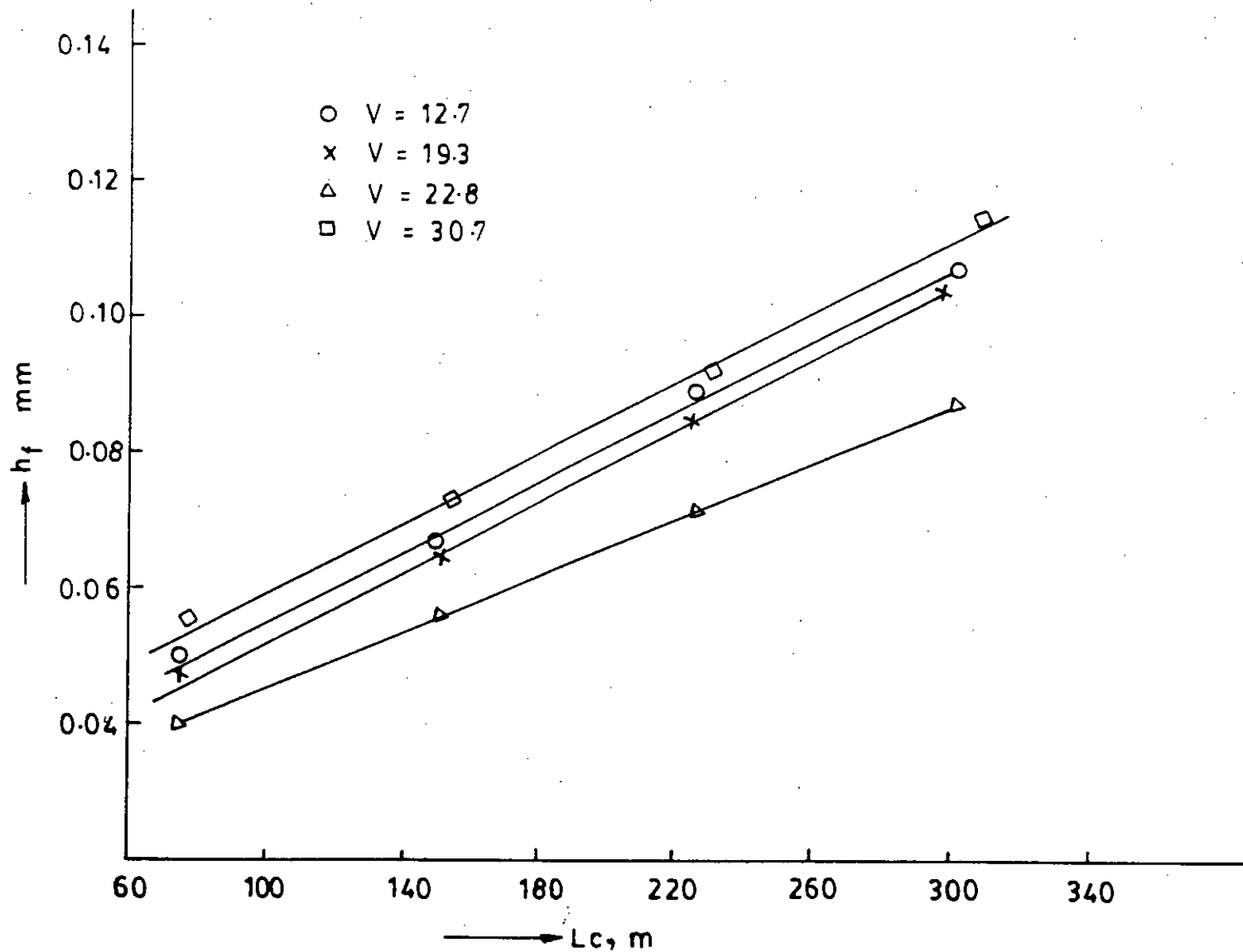


Figure-26
 Effect of cutting length on tool flank wear, h_f at constant $S=0.2$ mm/rev, $t=0.1$ mm $r=0$, $\alpha=7^\circ$, $\alpha_1=7^\circ$, $\phi=50^\circ$, $\phi_1=25^\circ$, $\gamma=0^\circ$ & $\gamma_1=0^\circ$ in turning with stainless steel with cemented carbide cutting tool.

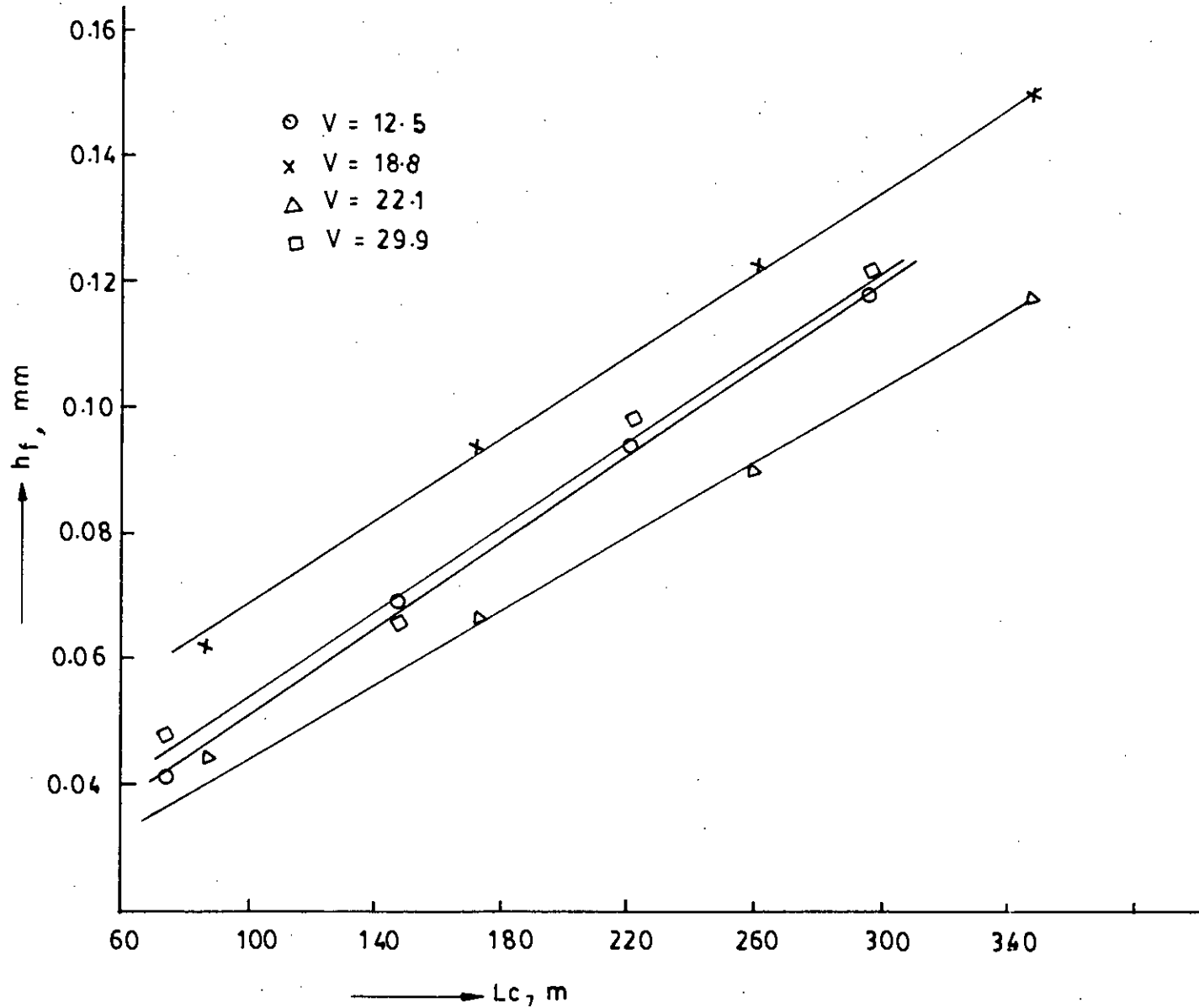


Figure-27

Effect of cutting length on tool flank wear, h_f at constant $S=0.2$ mm/rev, $t=0.1$ mm $r=0$, $\alpha=7^\circ$, $\alpha_1=7^\circ$, $\phi=50^\circ$, $\phi_1=35^\circ$, $\gamma=0^\circ$ & $\gamma_1=0^\circ$ in turning with stainless steel with cemented carbide cutting tool.

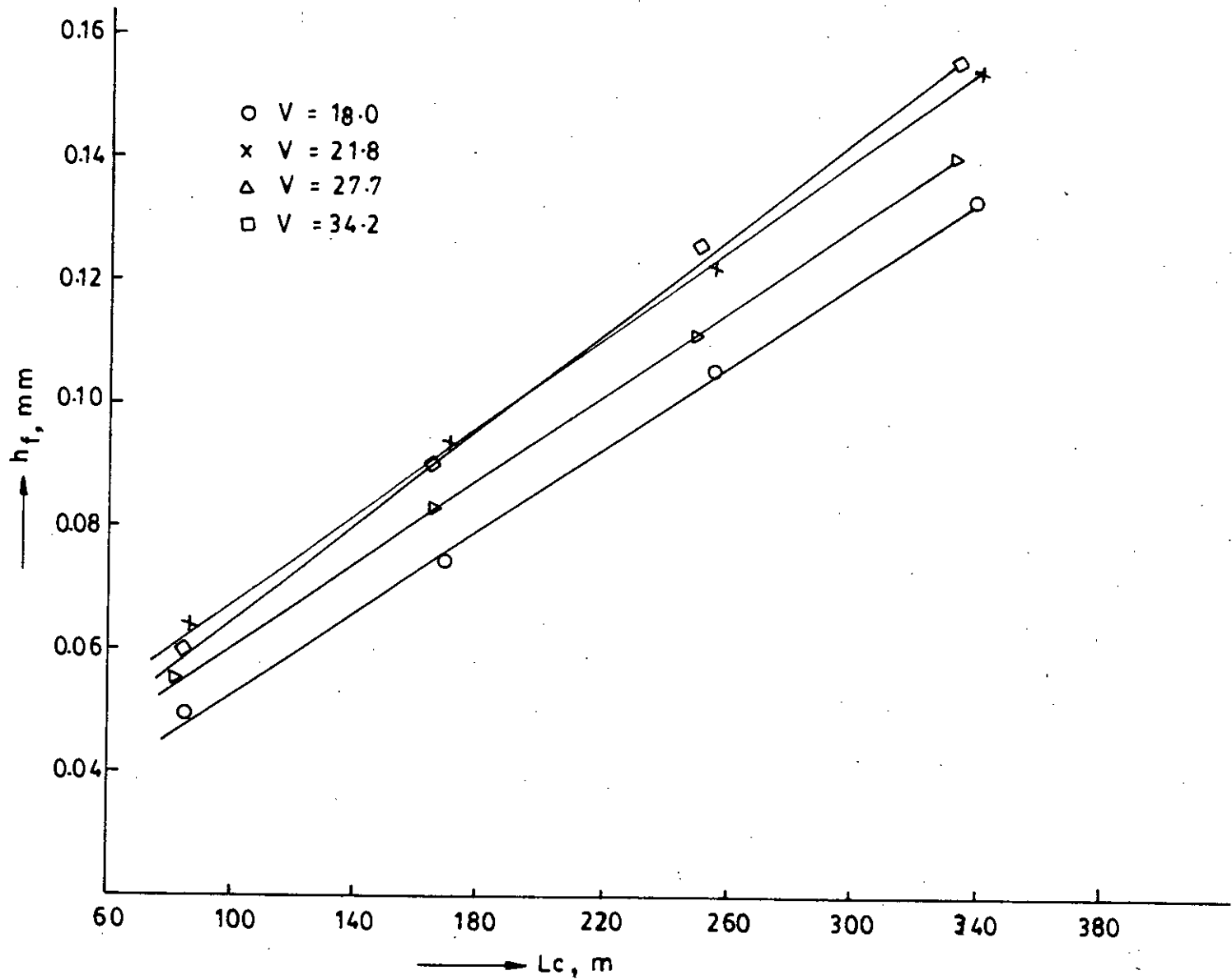


Figure-28

Effect of cutting length on tool flank wear, h_f at constant $S=0.2$ mm/rev, $t=0.1$ mm $r=0$, $\alpha=7^\circ$, $\alpha_1=7^\circ$, $\phi=50^\circ$, $\phi_1=45^\circ$, $\gamma=0^\circ$ & $\gamma_1=0^\circ$ in turning with stainless steel with cemented carbide cutting tool.

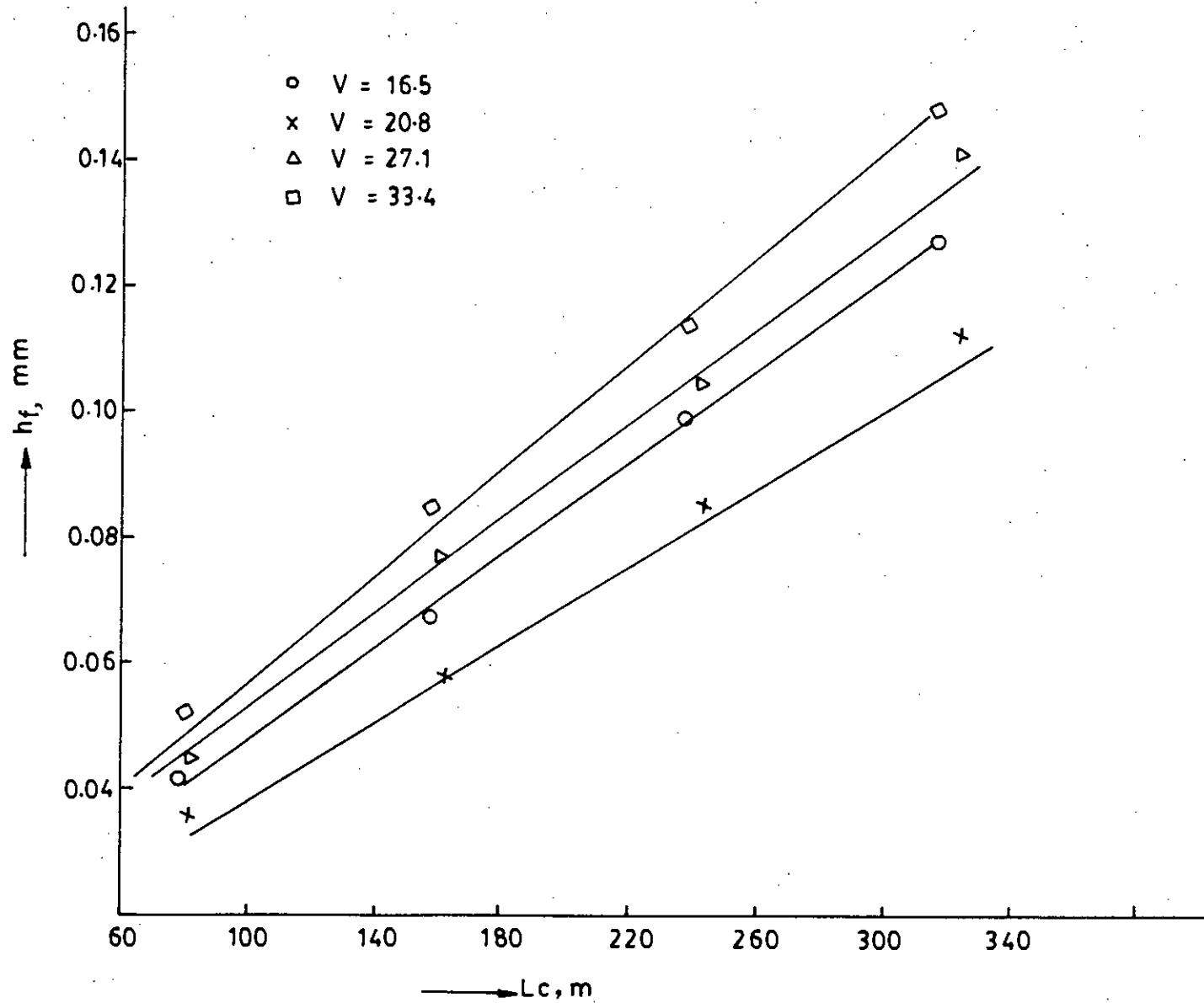


Figure-29
 Effect of cutting length on tool flank wear, h_f at constant $S=0.2$ mm/rev, $t=0.1$ mm $r=0$, $\alpha=7^\circ$, $\alpha_1=7^\circ$, $\phi=50^\circ$, $\phi_1=25^\circ$, $\gamma=-8^\circ$ & $\gamma_1=0^\circ$ in turning with stainless steel with cemented carbide cutting tool.

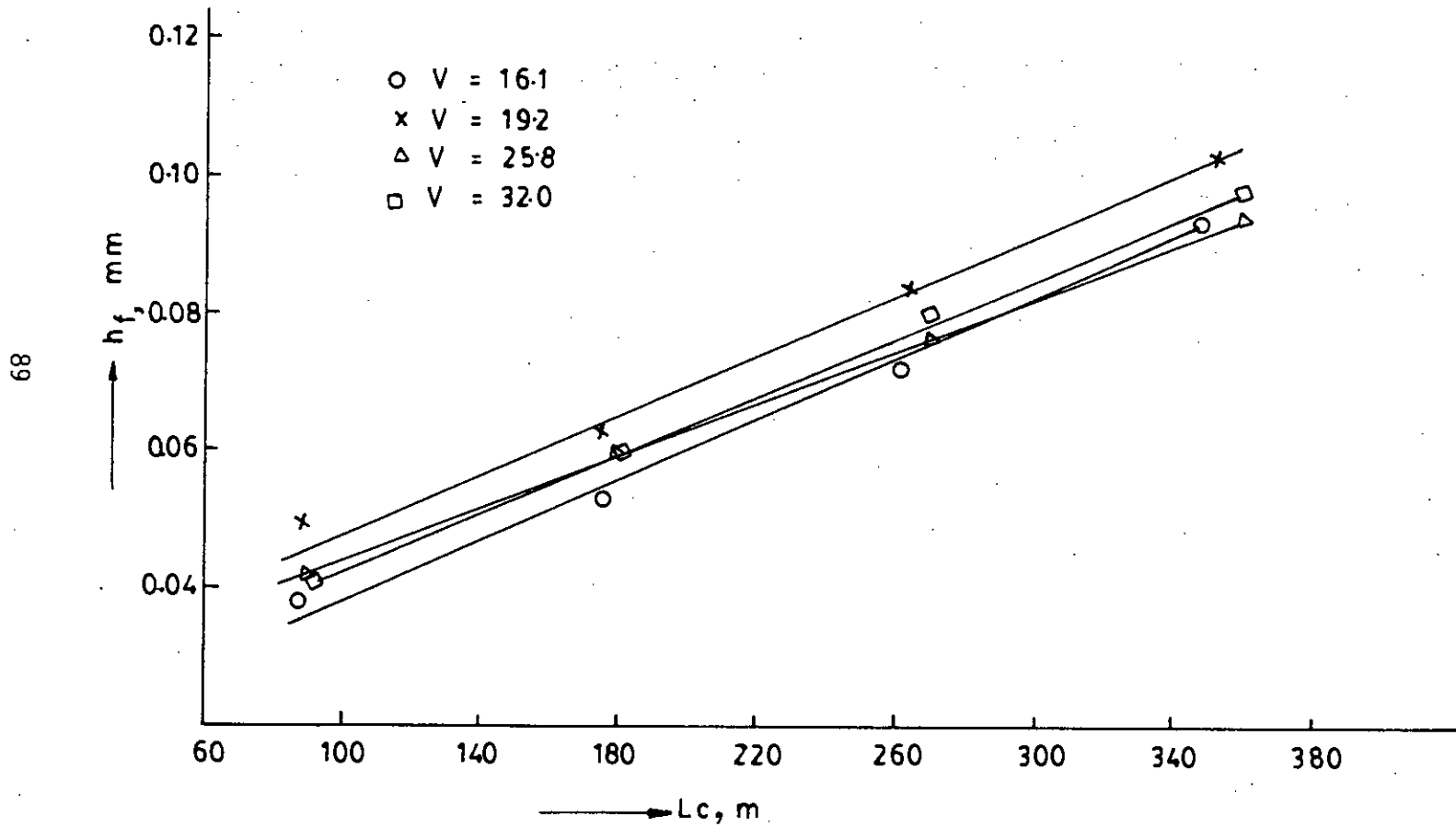


Figure-30
 Effect of cutting length on tool flank wear, h_f at
 constant $S=0.2$ mm/rev, $t=0.1$ mm $r=0$, $\alpha=7^\circ$, $\alpha_1=7^\circ$, $\phi=50^\circ$
 $\phi_1=25^\circ$, $\gamma=0^\circ$ & $\gamma_1=0^\circ$ in turning with stainless steel
 with cemented carbide cutting tool.

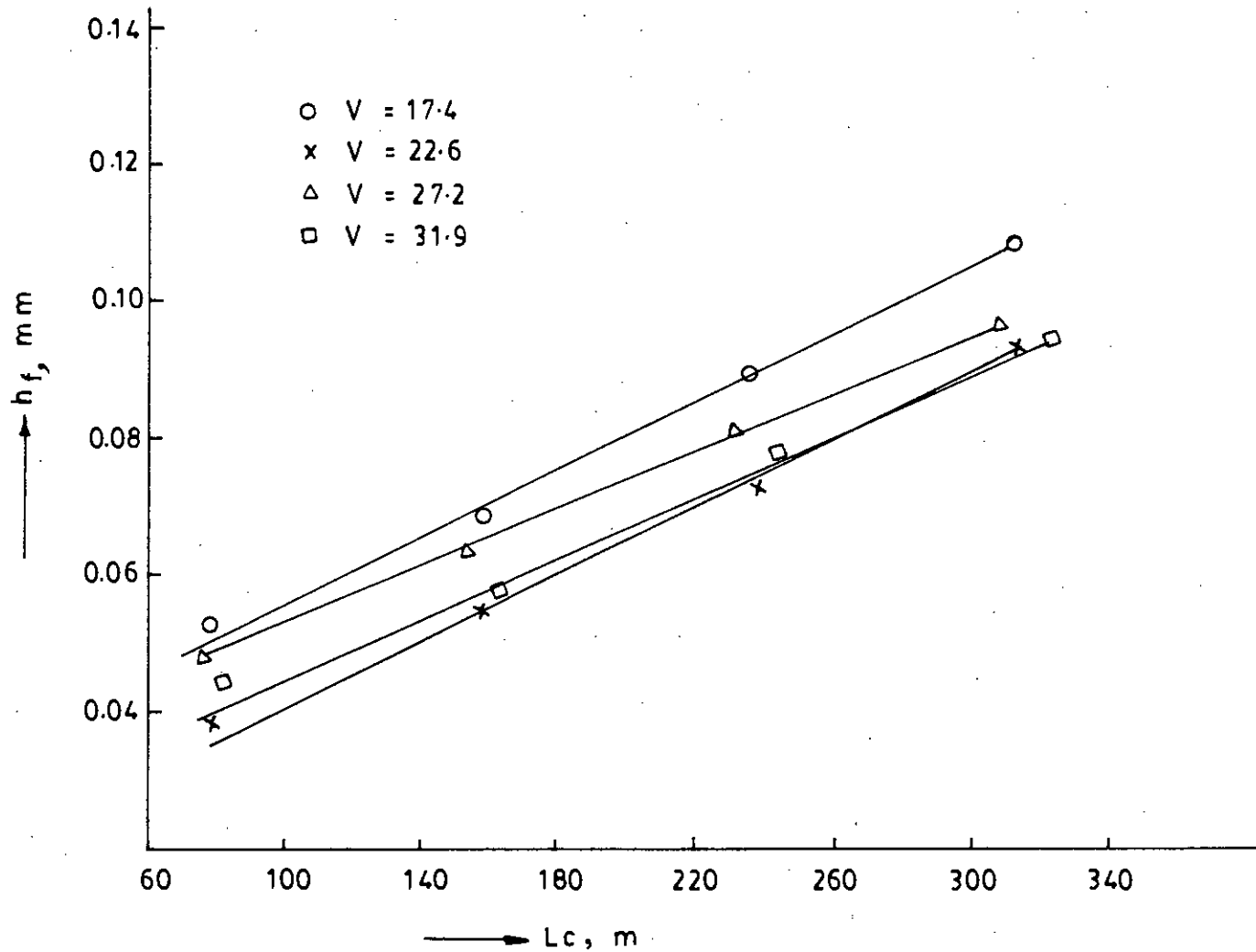


Figure-31

Effect of cutting length on tool flank wear, h_f at constant $S=0.2$ mm/rev, $t=0.1$ mm $r=0$, $\alpha=7^\circ$, $\alpha_1=7^\circ$, $\phi=50^\circ$, $\phi_1=25^\circ$, $\gamma=5^\circ$ & $\gamma_1=0^\circ$ in turning with stainless steel with cemented carbide cutting tool.

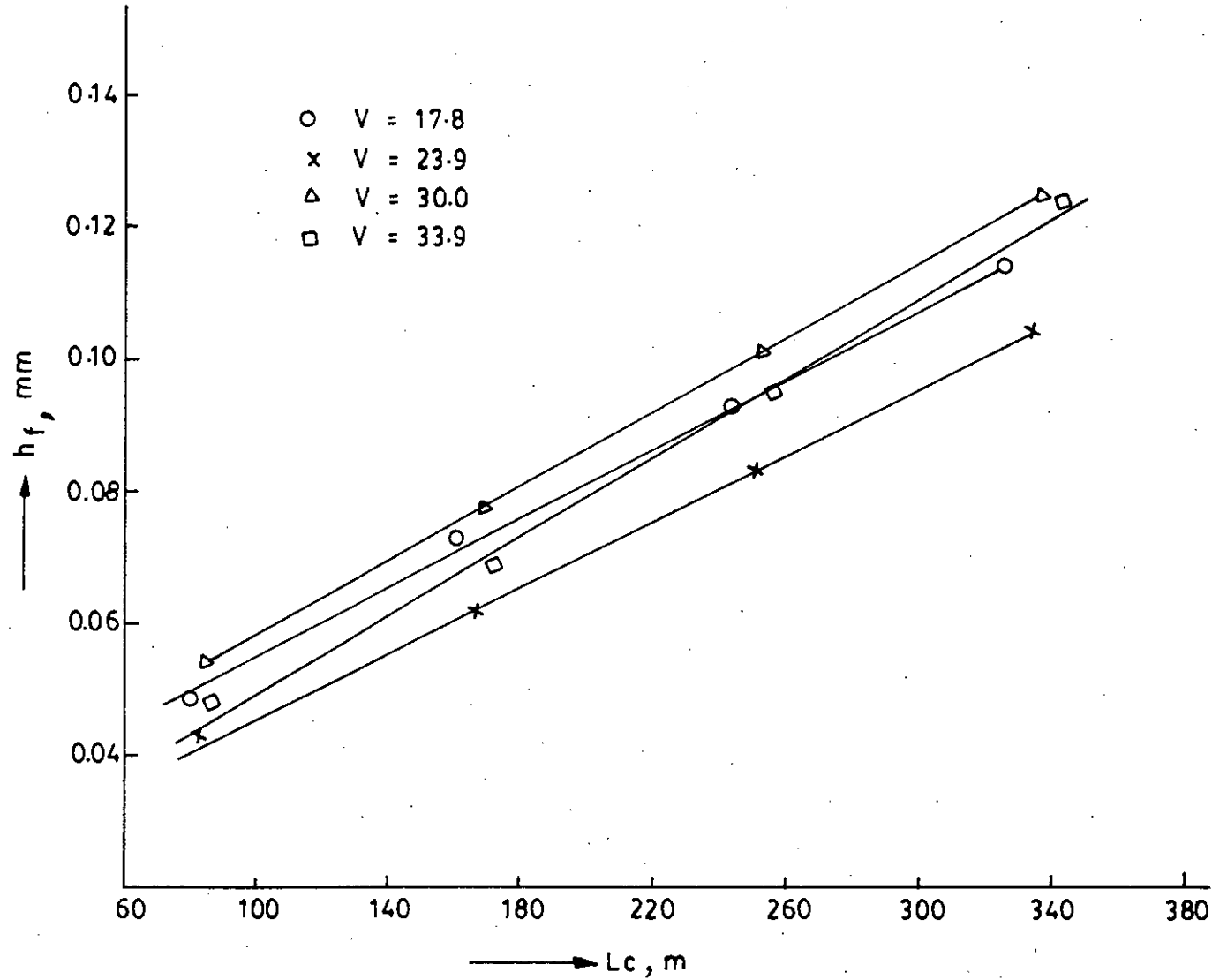


Figure-32

Effect of cutting length on tool flank wear, h_f at constant $S=0.2$ mm/rev, $t=0.1$ mm $r=0$, $\alpha=7^\circ$, $\alpha_1=7^\circ$, $\phi=50^\circ$, $\phi_1=25^\circ$, $\gamma=10^\circ$ & $\gamma_1=0^\circ$ in turning with stainless steel with cemented carbide cutting tool.

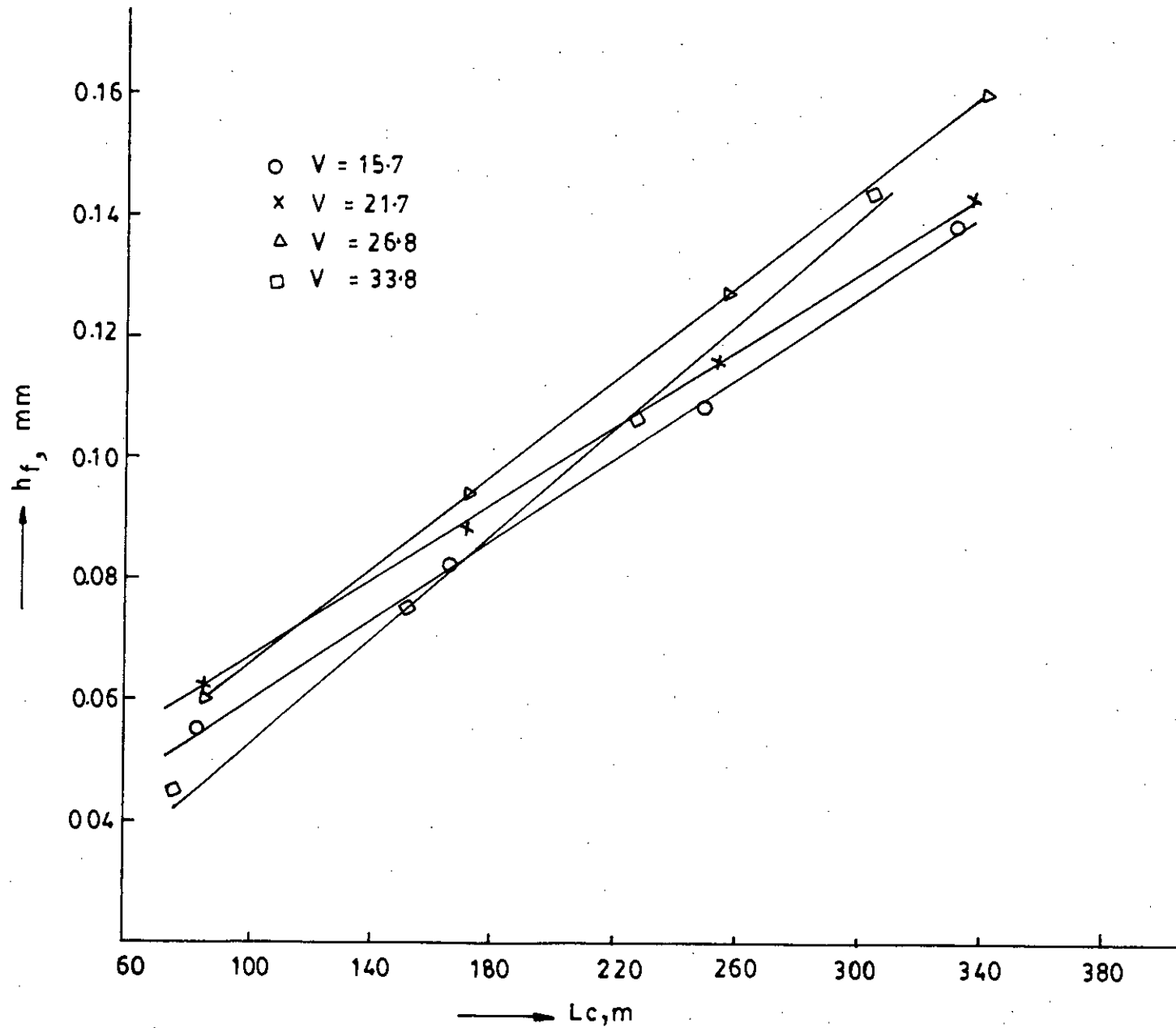


Figure-33
 Effect of cutting length on tool flank wear, h_f at
 constant $S=0.2$ mm/rev, $t=0.1$ mm $r=0$, $\alpha=7^\circ$, $\alpha_1=7^\circ$, $\phi=50^\circ$
 $\phi_1=25^\circ$, $\gamma=0^\circ$ & $\gamma_1=-7^\circ$ in turning with stainless steel
 with cemented carbide cutting tool.

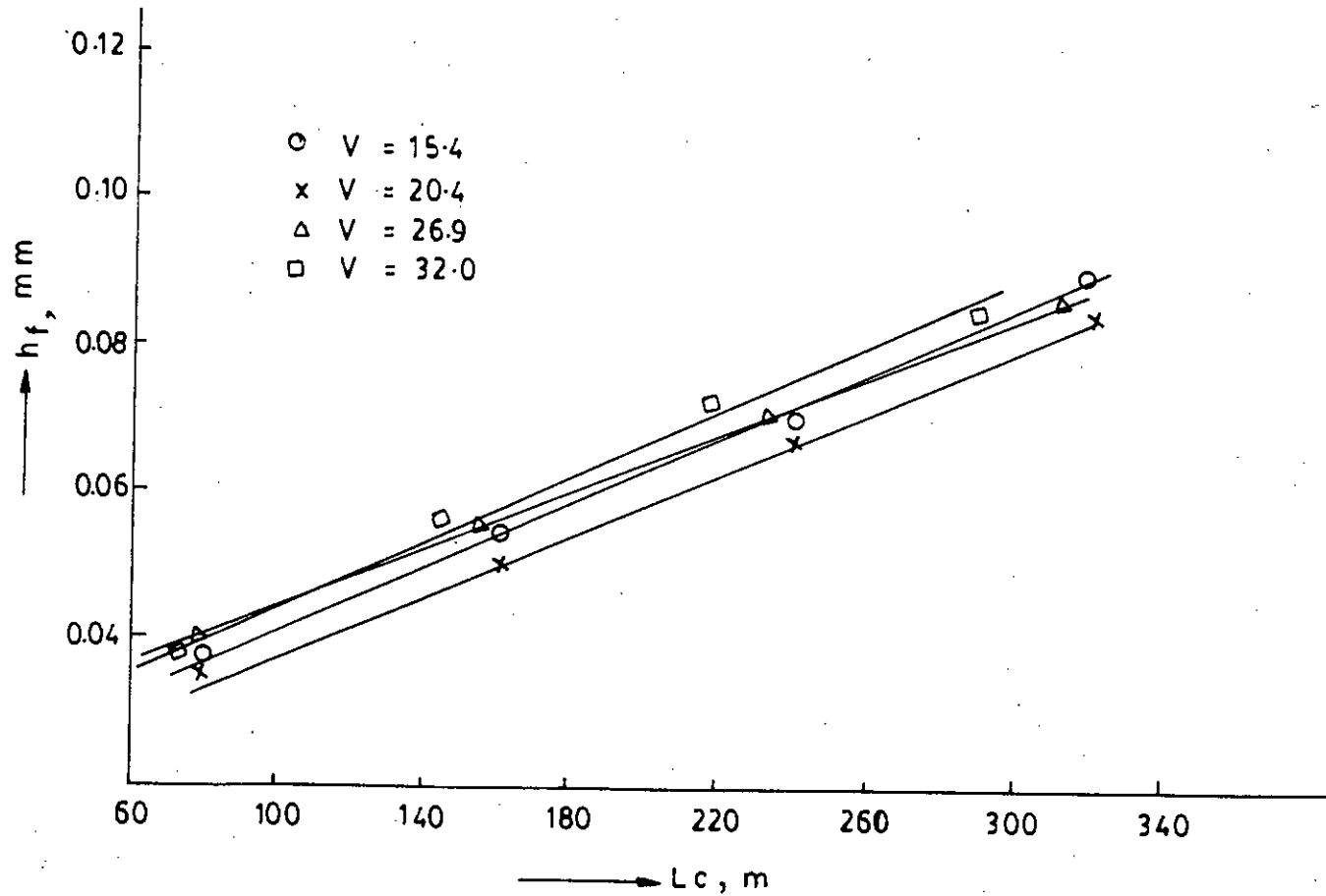


Figure-34
 Effect of cutting length on tool flank wear, h_f at
 constant $S=0.2$ mm/rev, $t=0.1$ mm $r=0$, $\alpha=7^\circ$, $\alpha_1=7^\circ$, $\phi=50^\circ$
 $\phi_1=25^\circ$, $\gamma=0^\circ$ & $\gamma_1=0^\circ$ in turning with stainless steel
 with cemented carbide cutting tool.

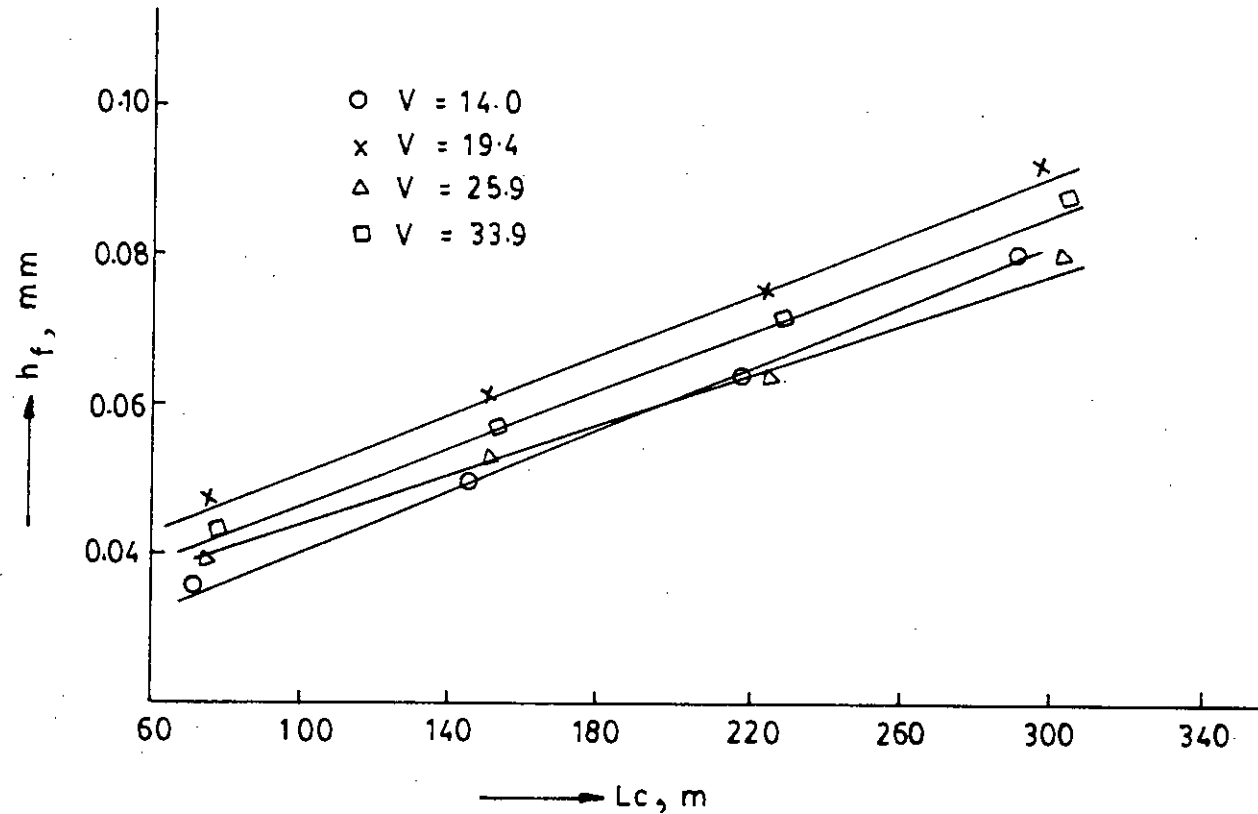


Figure-35
 Effect of cutting length on tool flank wear, h_f at
 constant $S=0.2$ mm/rev, $t=0.1$ mm $r=0$, $\alpha=7^\circ$, $\alpha_1=7^\circ$, $\phi=50^\circ$
 $\phi=25^\circ$, $\gamma=0^\circ$ & $\gamma_1=5^\circ$ in turning with stainless steel
 with cemented carbide cutting tool.

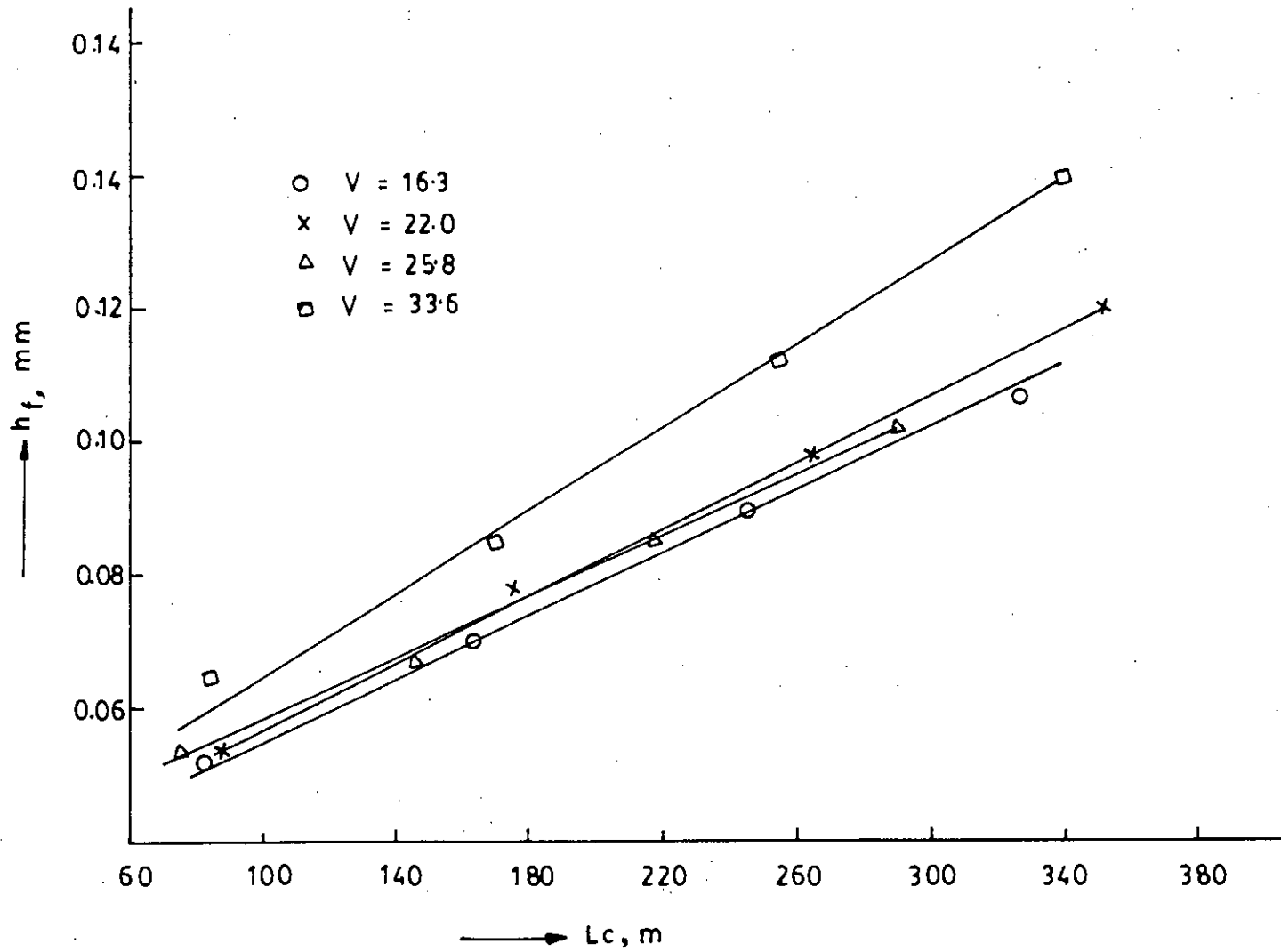


Figure-36

Effect of cutting length on tool flank wear, h_f at constant $S=0.2$ mm/rev, $t=0.1$ mm $r=0$, $\alpha=7^\circ$, $\alpha_1=7^\circ$, $\phi=50^\circ$, $\phi_1=25^\circ$, $\gamma=0^\circ$ & $\gamma_1=10^\circ$ in turning with stainless steel with cemented carbide cutting tool.

table-2. The curves of intensity of tool flank wears I_h vs. cutting speeds V_c were plotted in Fig. 37.

Similarly the curves were plotted in the same Fig. 37 for values of variable $\alpha=7^\circ, 9^\circ$ & 11° from Fig. 14, 15 & 16. It was seen that there were two lower values of each curve. i.e. intensity of tool flank were lower at two speeds, the minimum intensity of tool flank was 2.79058×10^{-4} mm/m for $\alpha=7^\circ$ at 25.8 m/min. Observation of chips, work piece surface finishing & vibration was in good conditions at the angle $\alpha=7^\circ$ and cutting speed 25.8 m/min. From this experiment, the optimum tool angle for side cutting relief angle α was determined equal to 7° .

In Fig. 38, 39, 40, 41 & 42 graphs were plotted for I_h vs. cutting speed, V_c for different sets of tool geometry. Influence of tool angles $\alpha_1, \phi, \phi_1, \gamma$ & γ_1 were showing on I_h . From these curves the optimum tool geometry were determined. Determined values of minimum intensity of tool flank wear for different tool geometry was listed in Table-3. In the optimum tool geometry, intensity of tool flank wear is minimum the values of minimum intensity of tool flank wear and optimum tool geometry are listed in table 5.

By studying the curves 37, 38, 39, 40, 41 & 42 data of intensity of tool flank wear were listed in data sheet-4 for some cutting speeds at different tool geometry and determined

Table - 3
Determined values of minimum intensity of tool flank wear
for different tool geometry

Tool geometry		Corresponding Cutting speed V_c m/min.	Minimum intensity of tool flank wear I_h mm/m
Fixed	Variable		
$a_1=6^0$, $\phi=45^0$ $\phi_1=20^0$, $\gamma=0^0$ $\gamma_1=0^0$	$a = 5^0$	16.1	4.2849
	$a = 7^0$	25.8	2.7906
	$a = 9^0$	17.3	2.9303
	$a = 11^0$	15.0	3.1085

$a=7^0$, $\phi=45^0$ $\phi_1=20^0$, $\gamma=0^0$ $\gamma_1=0^0$	$a_1 = 5^0$	25.8	2.8403
	$a_1 = 7^0$	25.9	2.4358
	$a_1 = 9^0$	25.0	3.3150
	$a_1 = 11^0$	15.2	3.6460

$a=7^0$, $a_1=7^0$ $\phi_1=20^0$, $\gamma=0^0$ $\gamma_1=0^0$	$\phi = 30^0$	15.1	3.3399
	$\phi = 40^0$	22.0	2.8041
	$\phi = 50^0$	27.0	2.3704
	$\phi = 60^0$	26.9	2.6811

$a=7^0$, $a_1=7^0$ $\phi=50^0$, $\gamma=0^0$ $\gamma_1=0^0$	$\phi_1 = 15^0$	23.8	2.4516
	$\phi_1 = 25^0$	22.8	2.0778
	$\phi_1 = 35^0$	22.1	2.9604
	$\phi_1 = 45^0$	18.1	3.3792

$a=7^0$, $a_1=7^0$ $\phi=50^0$, $\phi_1=25^0$, $\gamma_1=0^0$	$\gamma = -8^0$	27.1	3.1225
	$\gamma = 0^0$	25.8	1.9224
	$\gamma = 5^0$	27.2	2.0788
	$\gamma = 10^0$	23.6	2.5129

$a=7^0$, $a_1=7^0$ $\phi=50^0$, $\phi_1=25^0$, $\gamma=0^0$	$\gamma_1 = -7^0$	21.7	3.1835
	$\gamma_1 = 0^0$	26.0	1.9684
	$\gamma_1 = 5^0$	25.9	1.6799
	$\gamma_1 = 10^0$	25.8	2.2967

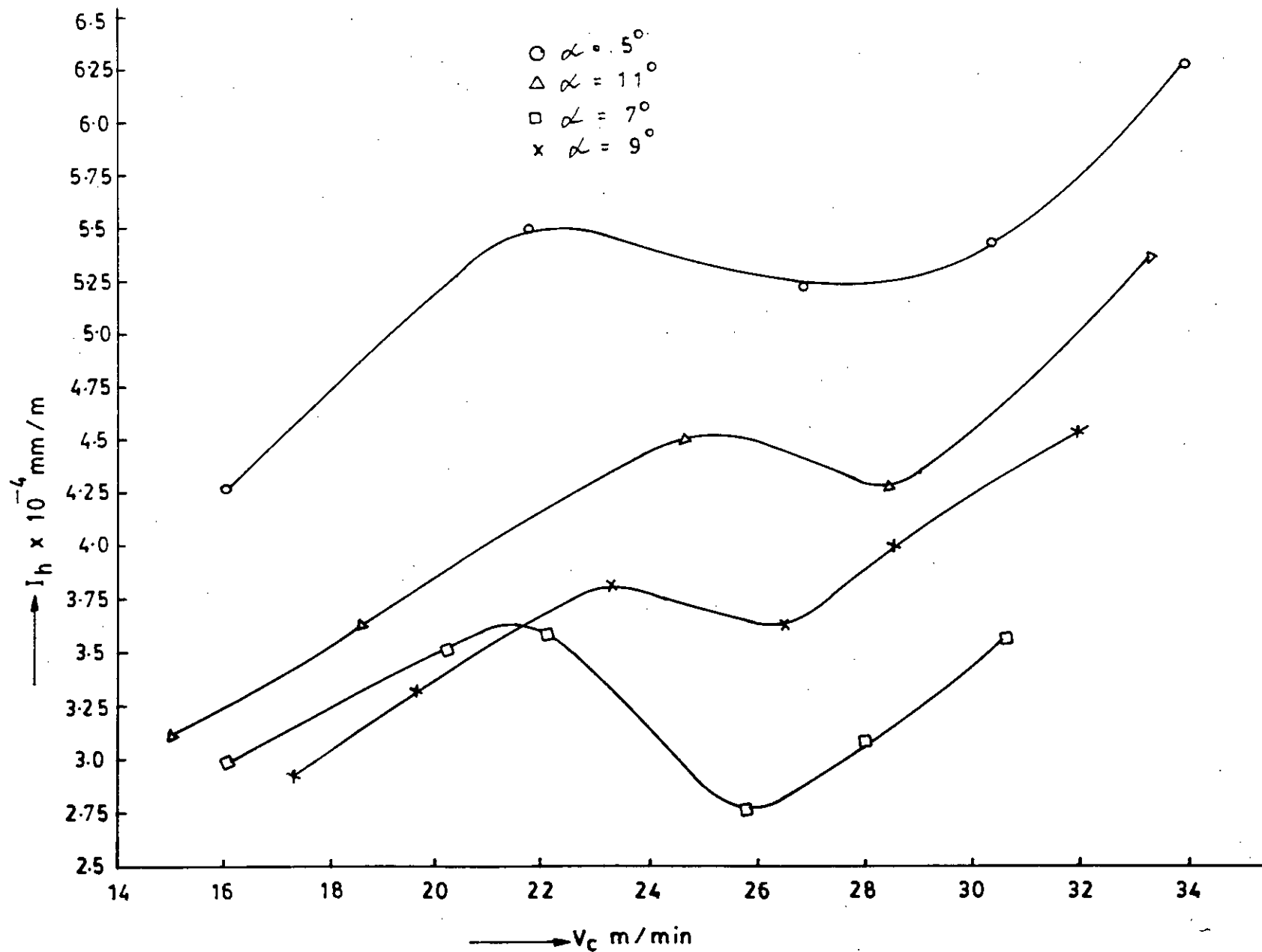


Figure-37

Determination of optimum tool angle α of cemented carbide cutting tool for stainless steel at constant $S=0.2$ mm/rev, $t=0.1$ mm $r=0$ and keeping fixed other angles ($\alpha_1=6^\circ$, $\phi=45^\circ$, $\phi_1=20^\circ$, $\gamma=0^\circ$ & $\gamma_1=0^\circ$)

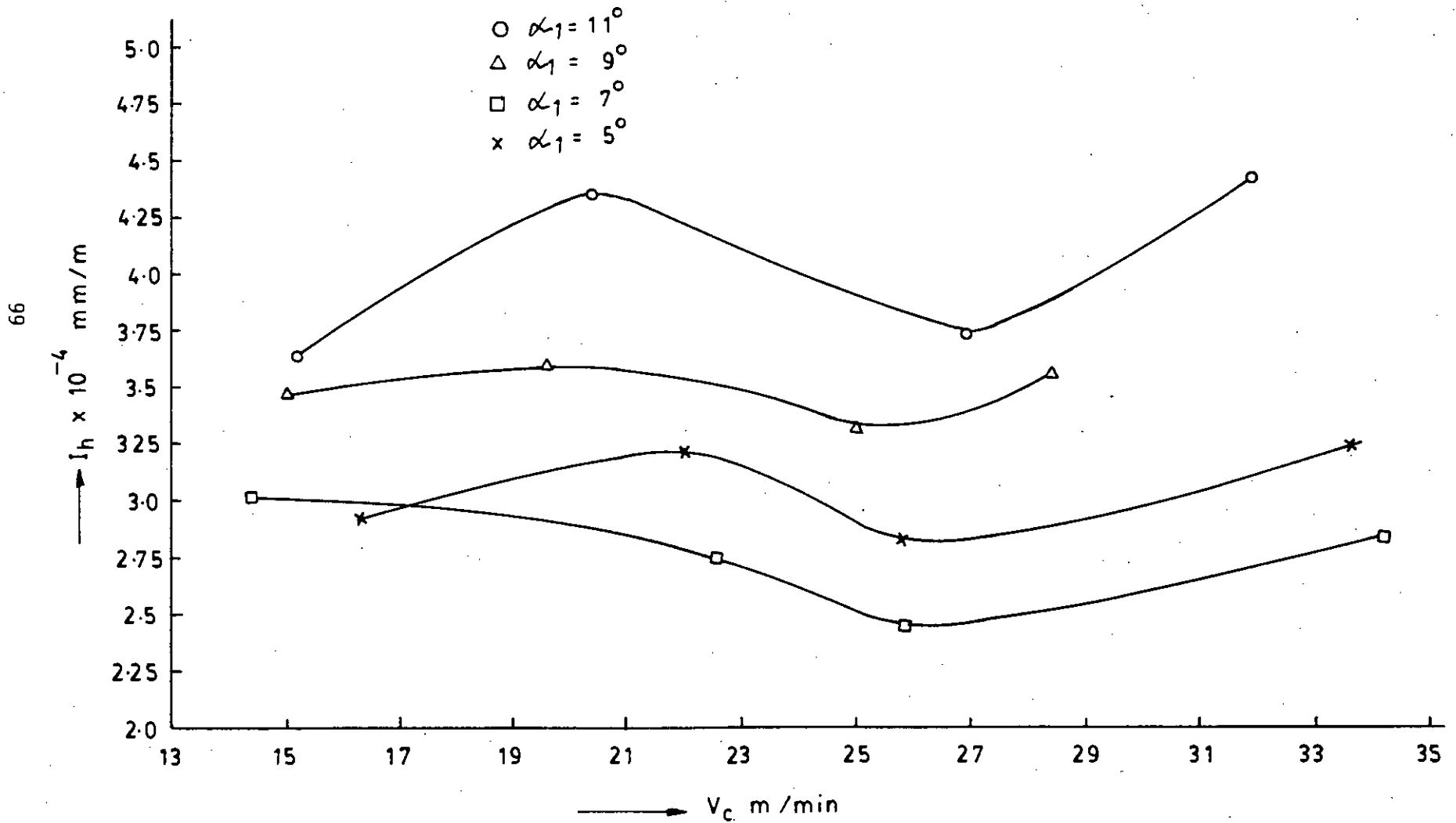


Figure-38
 Determination of optimum tool angle α_1 of cemented carbide cutting tool for stainless steel at constant $S=0.2$ mm/rev, $t=0.1$ mm $r=0$ and keeping fixed other angles ($\alpha=7^\circ$, $\phi=45^\circ$, $\phi_1=20^\circ$, $\gamma=0^\circ$ & $\gamma_1=0^\circ$)

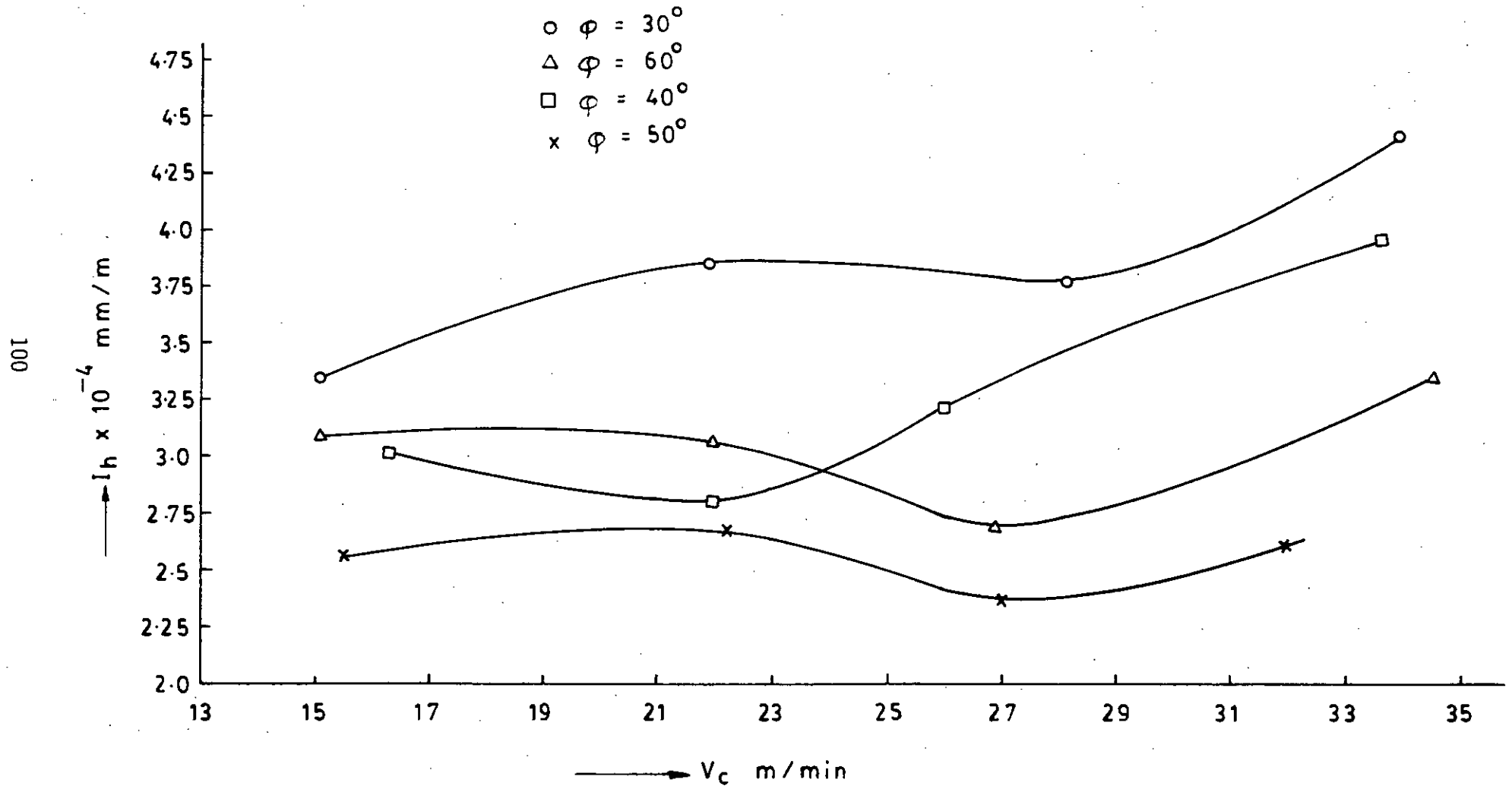


Figure-39

Determination of optimum tool angle ϕ of cemented carbide cutting tool for stainless steel at constant $S=0.2$ mm/rev, $t=0.1$ mm $r=0$ and keeping fixed other angles ($\alpha=7^\circ$, $\alpha_1=7^\circ$, $\phi_1=20^\circ$, $\gamma=0^\circ$ & $\gamma_1=0^\circ$)

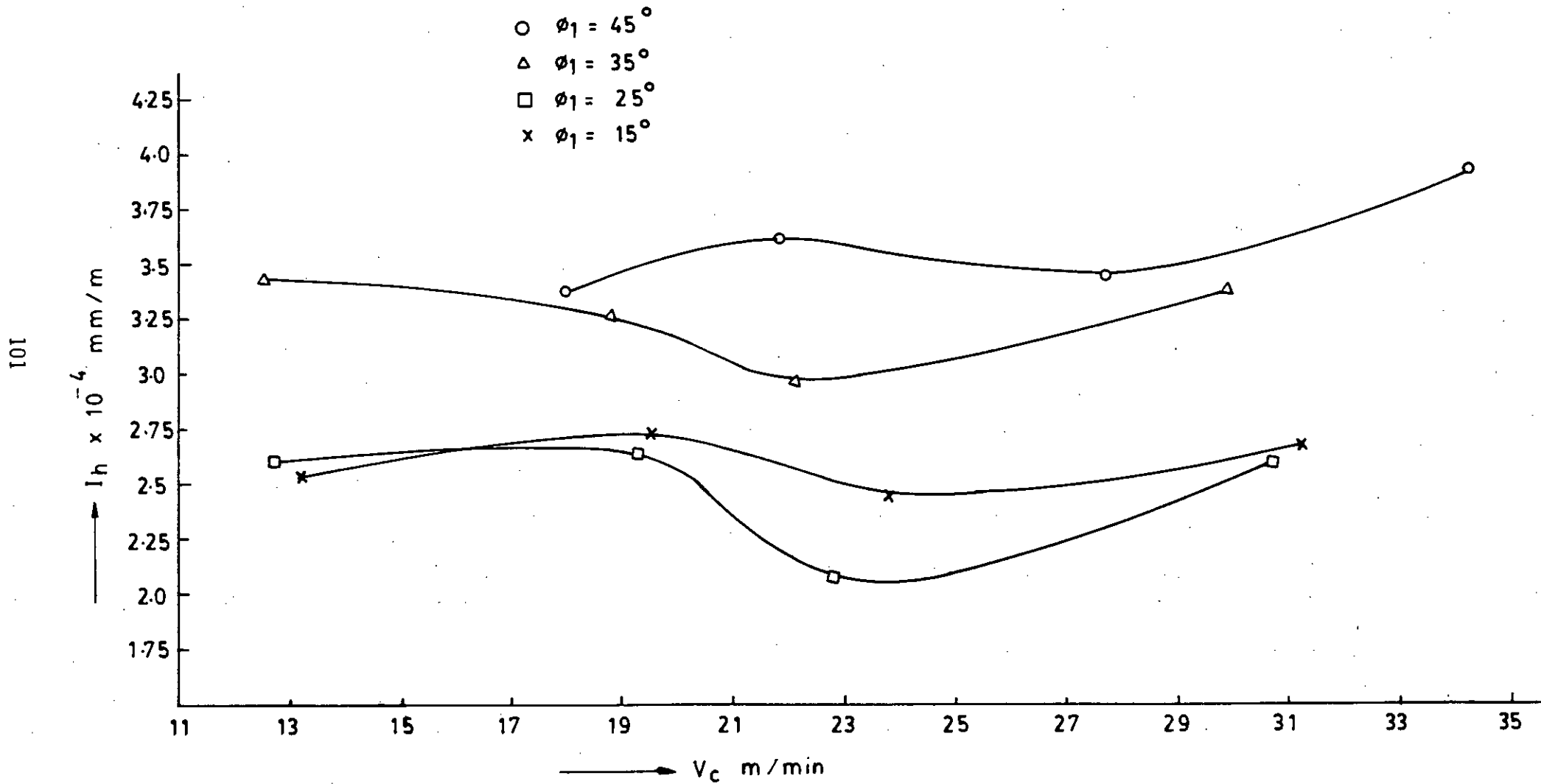


Figure-40
 Determination of optimum tool angle ϕ_1 of cemented carbide cutting tool for stainless steel at constant $S=0.2$ mm/rev, $t=0.1$ mm $r=0$ and keeping fixed other angles ($\alpha=7^\circ$, $\alpha_1=7^\circ$, $\phi=50^\circ$, $\gamma=0^\circ$ & $\gamma_1=0^\circ$)

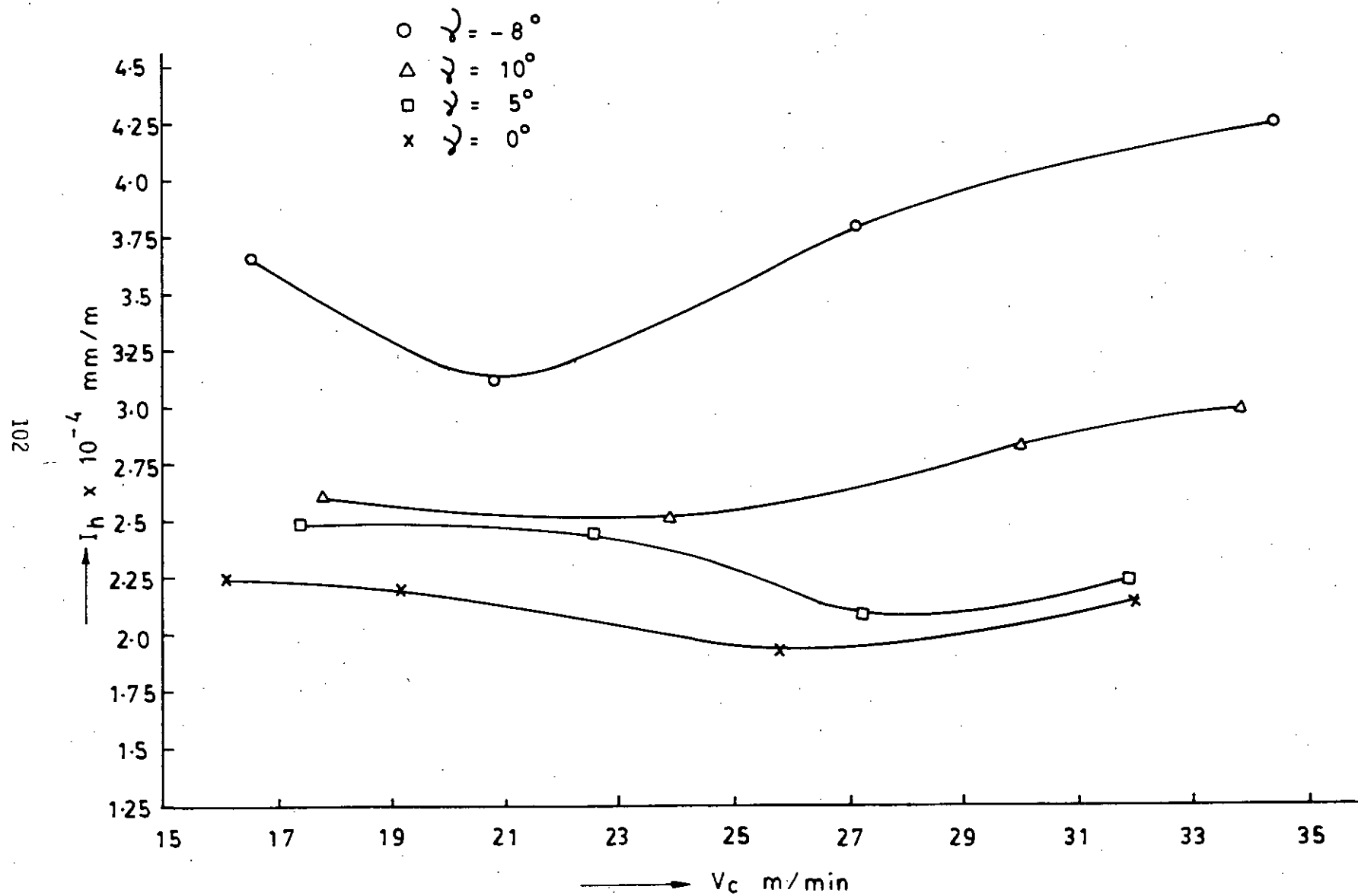


Figure-41
 Determination of optimum tool angle γ of cemented carbide cutting tool for stainless steel at constant $S=0.2$ mm/rev, $t=0.1$ mm $r=0$ and keeping fixed other angles ($\alpha=7^\circ$, $\alpha_1=7^\circ$, $\phi=50^\circ$, $\phi_1=25^\circ$, & $\gamma_1=0^\circ$)

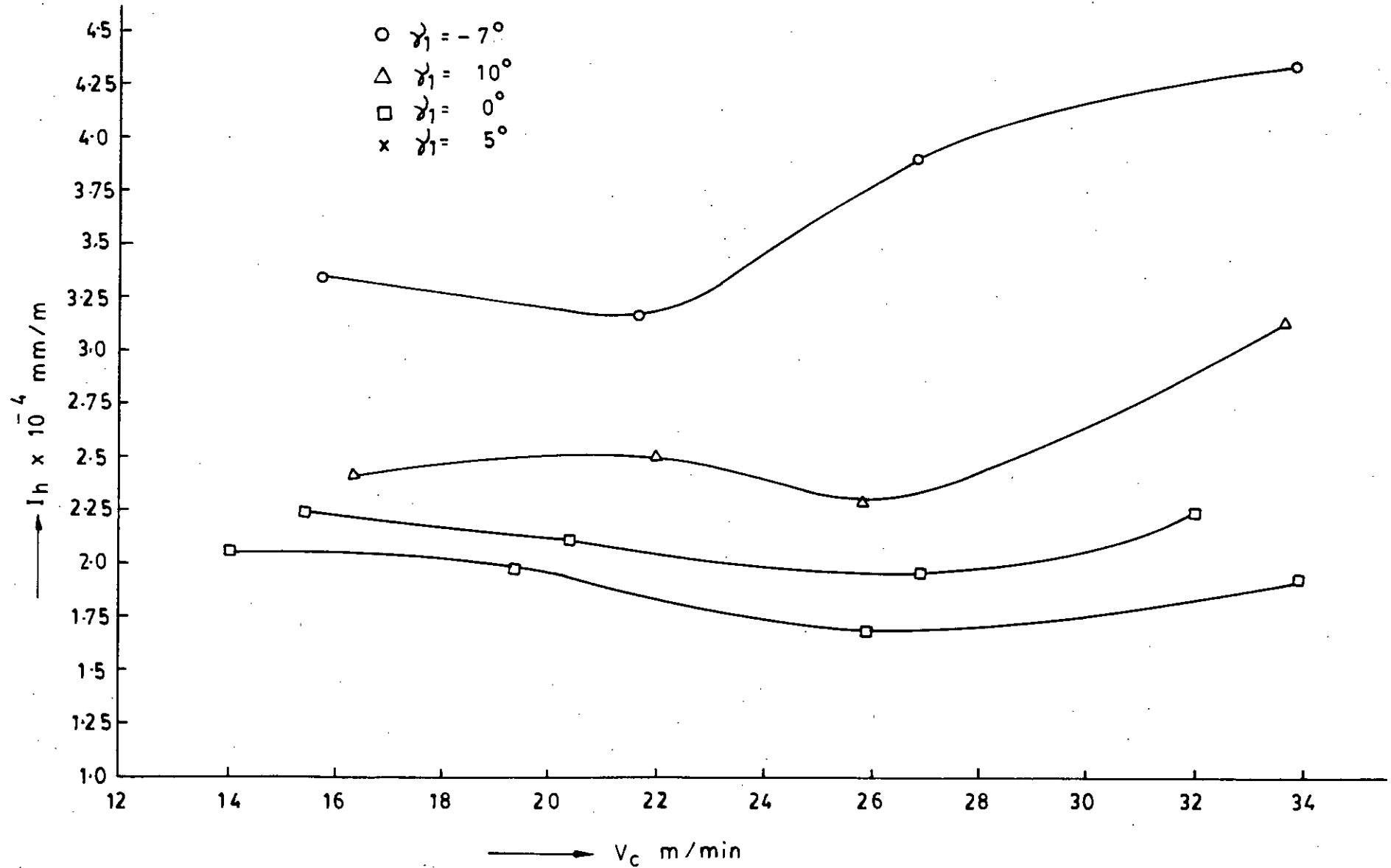


Figure-42

Determination of optimum tool angle γ_1 of cemented carbide cutting tool for stainless steel at constant $S=0.2$ mm/rev, $t=0.1$ mm $r=0$ and keeping fixed other angles ($\alpha=7^\circ$, $\alpha_1=7^\circ$, $\phi=50^\circ$, $\phi_1=25^\circ$, $\gamma=0^\circ$)

Considering cutting speed V_c m/min.	Tool geometry		Corresponding intensity of tool flank wear I_f mm/m
	Fixed angles	Variable angle	
17.5	$\alpha_1=6^\circ$, $\phi=45^\circ$ $\phi_1=20^\circ$, $\gamma=0^\circ$ $\gamma_1=0^\circ$	$\alpha=5^\circ$	4.3625
		$\alpha=7^\circ$	3.1625
		$\alpha=9^\circ$	2.9500
		$\alpha=11^\circ$	3.4625
22	$\alpha_1=6^\circ$, $\phi=45^\circ$ $\phi_1=20^\circ$, $\gamma=0^\circ$ $\gamma_1=0^\circ$	$\alpha=5^\circ$	5.5125
		$\alpha=7^\circ$	3.6125
		$\alpha=9^\circ$	3.6750
		$\alpha=11^\circ$	4.1500
26	$\alpha_1=6^\circ$, $\phi=45^\circ$ $\phi_1=20^\circ$, $\gamma=0^\circ$ $\gamma_1=0^\circ$	$\alpha=5^\circ$	5.2875
		$\alpha=7^\circ$	2.7750
		$\alpha=9^\circ$	3.6375
		$\alpha=11^\circ$	2.4750
30	$\alpha_1=6^\circ$, $\phi=45^\circ$ $\phi_1=20^\circ$, $\gamma=0^\circ$ $\gamma_1=0^\circ$	$\alpha=5^\circ$	5.4875
		$\alpha=7^\circ$	3.5375
		$\alpha=9^\circ$	4.3250
		$\alpha=11^\circ$	4.6625
17	$\alpha=7^\circ$, $\phi=45^\circ$ $\phi_1=20^\circ$, $\gamma=0^\circ$ $\gamma_1=0^\circ$	$\alpha_1=5^\circ$	2.9667
		$\alpha_1=7^\circ$	3.0000
		$\alpha_1=9^\circ$	3.5168
		$\alpha_1=11^\circ$	3.9375
22	$\alpha=7^\circ$, $\phi=45^\circ$ $\phi_1=20^\circ$, $\gamma=0^\circ$ $\gamma_1=0^\circ$	$\alpha_1=5^\circ$	3.2227
		$\alpha_1=7^\circ$	2.7875
		$\alpha_1=9^\circ$	3.6375
		$\alpha_1=11^\circ$	4.2250
26	$\alpha=7^\circ$, $\phi=45^\circ$ $\phi_1=20^\circ$, $\gamma=0^\circ$ $\gamma_1=0^\circ$	$\alpha_1=5^\circ$	2.8750
		$\alpha_1=7^\circ$	2.4375
		$\alpha_1=9^\circ$	3.3375
		$\alpha_1=11^\circ$	3.8185
30	$\alpha=7^\circ$, $\phi=45^\circ$ $\phi_1=20^\circ$, $\gamma=0^\circ$ $\gamma_1=0^\circ$	$\alpha_1=5^\circ$	2.9875
		$\alpha_1=7^\circ$	2.6000
		$\alpha_1=9^\circ$	3.7750
		$\alpha_1=11^\circ$	4.1373

Data Sheet # 4 : Study data from Fig. 37-42

Considering cutting speed V_c m/min.	Tool geometry		Corresponding intensity of tool flank wear I_h mm/m
	Fixed angles	Variable angle	
17	$\alpha=7^\circ, \alpha_1=7^\circ$ $\phi_1=20^\circ, \gamma=0^\circ$ $\gamma_1=0^\circ$	$\phi=30^\circ$	3.5875
		$\phi=40^\circ$	2.9750
		$\phi=50^\circ$	2.5875
		$\phi=60^\circ$	3.0813
22	$\alpha=7^\circ, \alpha_1=7^\circ$ $\phi_1=20^\circ, \gamma=0^\circ$ $\gamma_1=0^\circ$	$\phi=30^\circ$	3.8563
		$\phi=40^\circ$	2.8041
		$\phi=50^\circ$	2.5500
		$\phi=60^\circ$	3.0650
27	$\alpha=7^\circ, \alpha_1=7^\circ$ $\phi_1=20^\circ, \gamma=0^\circ$ $\gamma_1=0^\circ$	$\phi=30^\circ$	3.7875
		$\phi=40^\circ$	3.3250
		$\phi=50^\circ$	2.3704
		$\phi=60^\circ$	2.6813
32	$\alpha=7^\circ, \alpha_1=7^\circ$ $\phi_1=20^\circ, \gamma=0^\circ$ $\gamma_1=0^\circ$	$\phi=30^\circ$	4.1675
		$\phi=40^\circ$	3.8450
		$\phi=50^\circ$	2.6105
		$\phi=60^\circ$	3.1163
18	$\alpha=7^\circ, \phi_1=7^\circ$ $\phi=50^\circ, \gamma=0^\circ$ $\gamma_1=0^\circ$	$\phi_1=15^\circ$	2.7063
		$\phi_1=25^\circ$	2.6323
		$\phi_1=35^\circ$	3.3000
		$\phi_1=45^\circ$	3.3732
23	$\alpha=7^\circ, \alpha_1=7^\circ$ $\phi=50^\circ, \gamma=0^\circ$ $\gamma_1=0^\circ$	$\phi_1=15^\circ$	2.5000
		$\phi_1=25^\circ$	2.0812
		$\phi_1=35^\circ$	2.9813
		$\phi_1=45^\circ$	3.5875
26	$\alpha=7^\circ, \alpha_1=7^\circ$ $\phi=50^\circ, \gamma=0^\circ$ $\gamma_1=0^\circ$	$\phi_1=15^\circ$	2.4693
		$\phi_1=25^\circ$	2.1750
		$\phi_1=35^\circ$	3.1375
		$\phi_1=45^\circ$	3.4938
30	$\alpha=7^\circ, \alpha_1=7^\circ$ $\phi=50^\circ, \gamma=0^\circ$ $\gamma_1=0^\circ$	$\phi_1=45^\circ$	2.6125
		$\phi_1=45^\circ$	2.5125
		$\phi_1=45^\circ$	3.2750
		$\phi_1=45^\circ$	3.5625

Data sheet # 4 : Study data from fig. 37-42

Considering cutting speed V_c m/min.	Tool geometry		Corresponding intensity of tool flank wear I_h mm/m
	Fixed angles	Variable angle	
18	$\alpha=7^0, \alpha_1=7^0$ $\phi=50^b, \phi_1=25^0$ $\gamma_1=0^0$	$\gamma = -8^0$	3.4500
		$\gamma = 0^0$	2.2025
		$\gamma = 5^0$	2.4750
		$\gamma = 10^0$	2.6063
22	$\alpha=7^0, \alpha_1=7^0$ $\phi=50^b, \phi_1=25^0$ $\gamma_1=0^0$	$\gamma = -8^0$	3.2000
		$\gamma = 0^0$	2.0750
		$\gamma = 5^0$	2.4500
		$\gamma = 10^0$	2.5375
26	$\alpha=7^0, \alpha_1=7^0$ $\phi=50^b, \phi_1=25^0$ $\gamma_1=0^0$	$\gamma = -8^0$	3.6500
		$\gamma = 0^0$	1.9250
		$\gamma = 5^0$	2.1750
		$\gamma = 10^0$	2.6000
30	$\alpha=7^0, \alpha_1=7^0$ $\phi=50^b, \phi_1=25^0$ $\gamma_1=0^0$	$\gamma = -8^0$	4.0000
		$\gamma = 0^0$	2.0500
		$\gamma = 5^0$	2.1500
		$\gamma = 10^0$	2.8321
16	$\alpha=7^0, \alpha_1=7^0$ $\phi=50^b, \phi_1=25^0$ $\gamma=0^0$	$\gamma_1 = -7^0$	3.3250
		$\gamma_1 = 0^0$	2.1688
		$\gamma_1 = 5^0$	2.0500
		$\gamma_1 = 10^0$	2.3875
21	$\alpha=7^0, \alpha_1=7^0$ $\phi=50^b, \phi_1=25^0$ $\gamma=0^0$	$\gamma_1 = -7^0$	3.1875
		$\gamma_1 = 0^0$	2.0918
		$\gamma_1 = 5^0$	1.9125
		$\gamma_1 = 10^0$	2.4988
26	$\alpha=7^0, \alpha_1=7^0$ $\phi=50^b, \phi_1=25^0$ $\gamma=0^0$	$\gamma_1 = -7^0$	4.0375
		$\gamma_1 = 0^0$	1.9750
		$\gamma_1 = 5^0$	1.6800
		$\gamma_1 = 10^0$	2.2995
31	$\alpha=7^0, \alpha_1=7^0$ $\phi=50^b, \phi_1=25^0$ $\gamma=0^0$	$\gamma_1 = -7^0$	4.2250
		$\gamma_1 = 0^0$	2.1563
		$\gamma_1 = 5^0$	1.7875
		$\gamma_1 = 10^0$	2.7500

Data sheet # 4 : Study data from fig.37-42

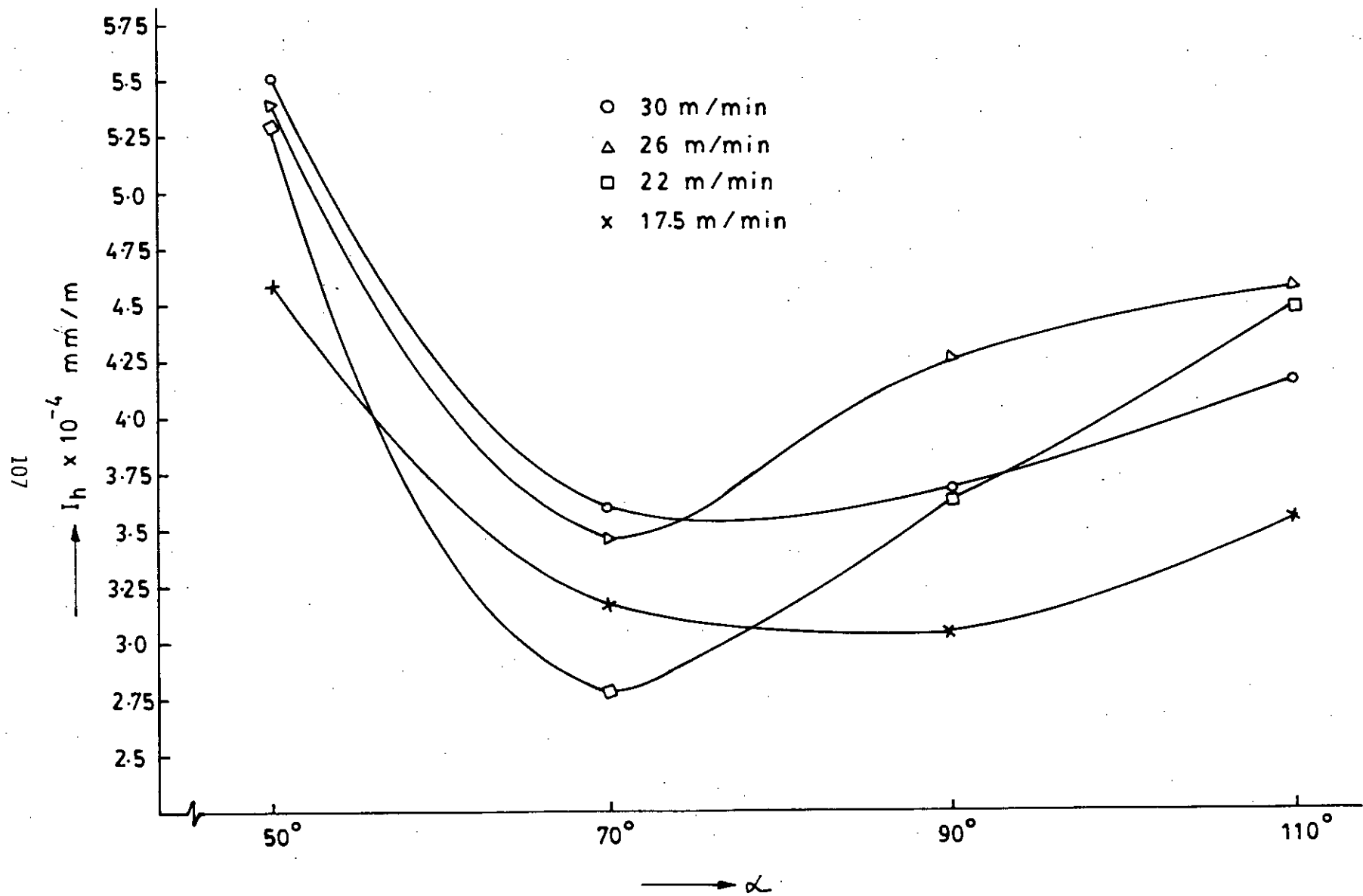


Figure-43
 Relationship between intensity of tool flank wear, I_f , and variable cutting angle, α keeping other angles fixed ($\alpha_1=6^\circ$, $\phi=45^\circ$, $\phi_1=20^\circ$, $\gamma=0^\circ$ & $\gamma_1=0^\circ$)

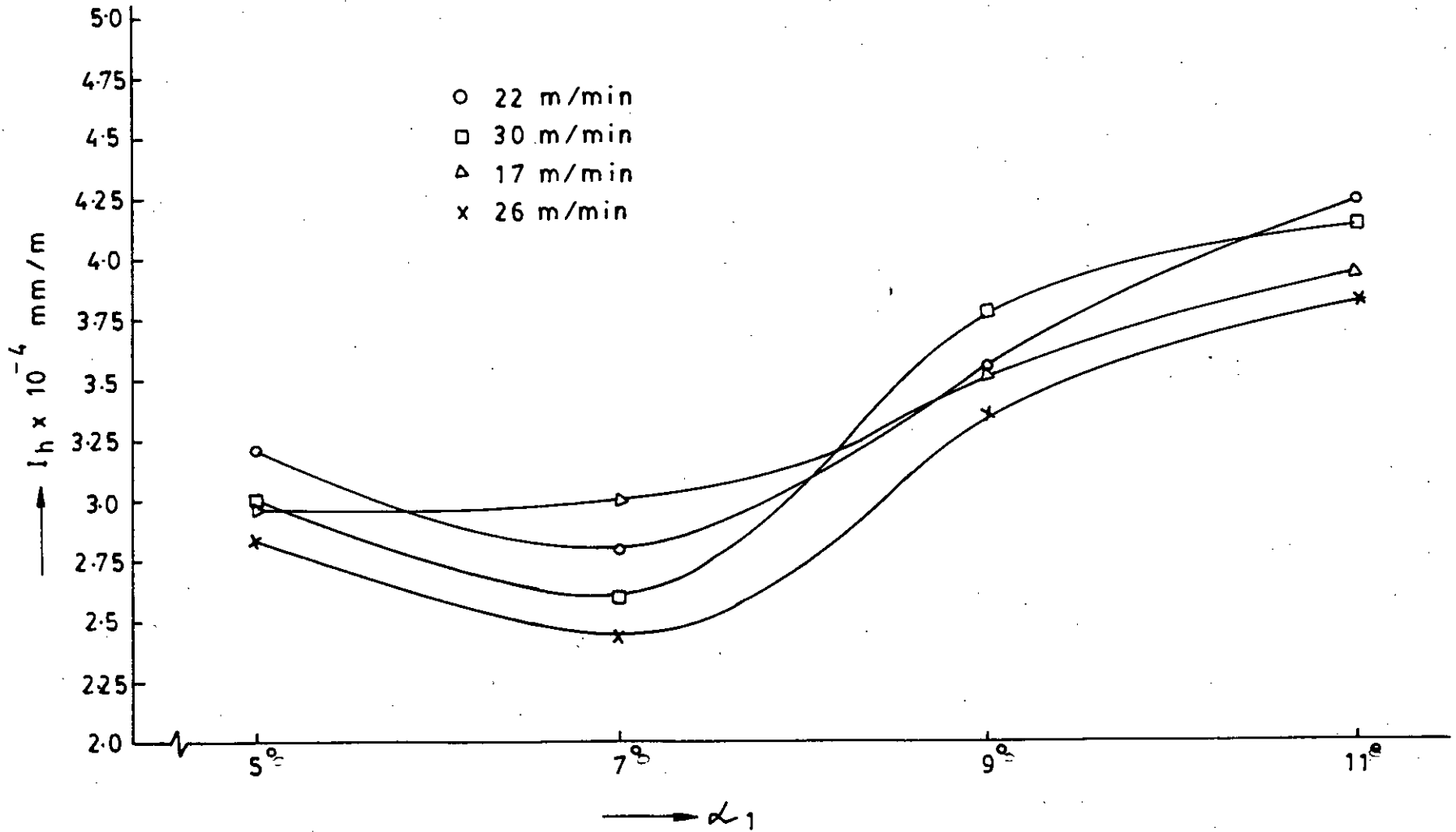


Figure-44
 Relationship between intensity of tool flank wear, I_h
 and variable cutting angle, α_1 keeping other angles
 fixed ($\alpha=7^\circ$, $\phi=45^\circ$, $\phi_1=20^\circ$, $\gamma=0^\circ$ & $\gamma_1=0^\circ$)

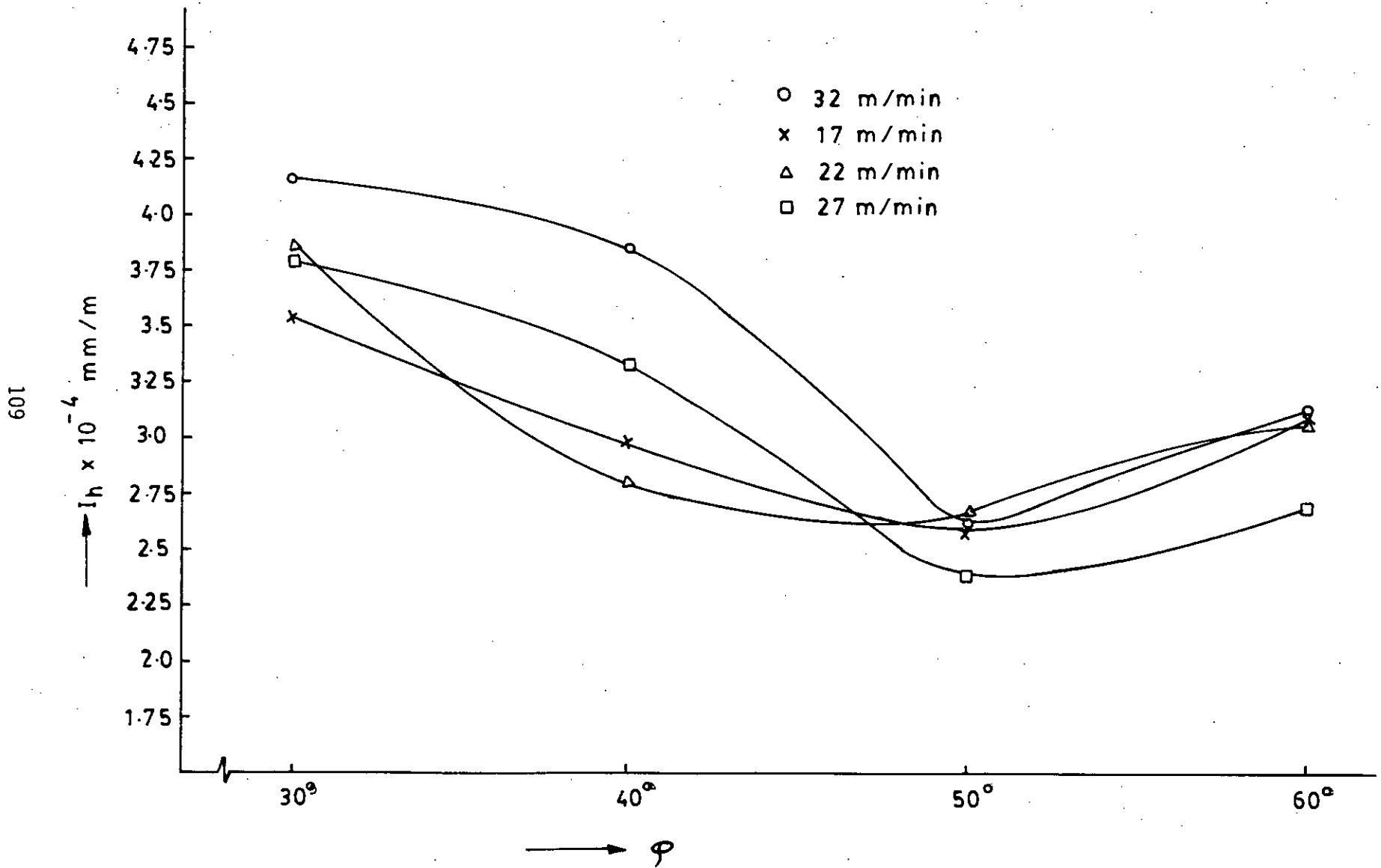


Figure-45
 Relationship between intensity of tool flank wear, I_f , and variable cutting angle, ϕ keeping other angles fixed ($\alpha=7^\circ$, $\alpha_1=7^\circ$, $\phi_1=20^\circ$, $\gamma=0^\circ$ & $\gamma_1=0^\circ$)

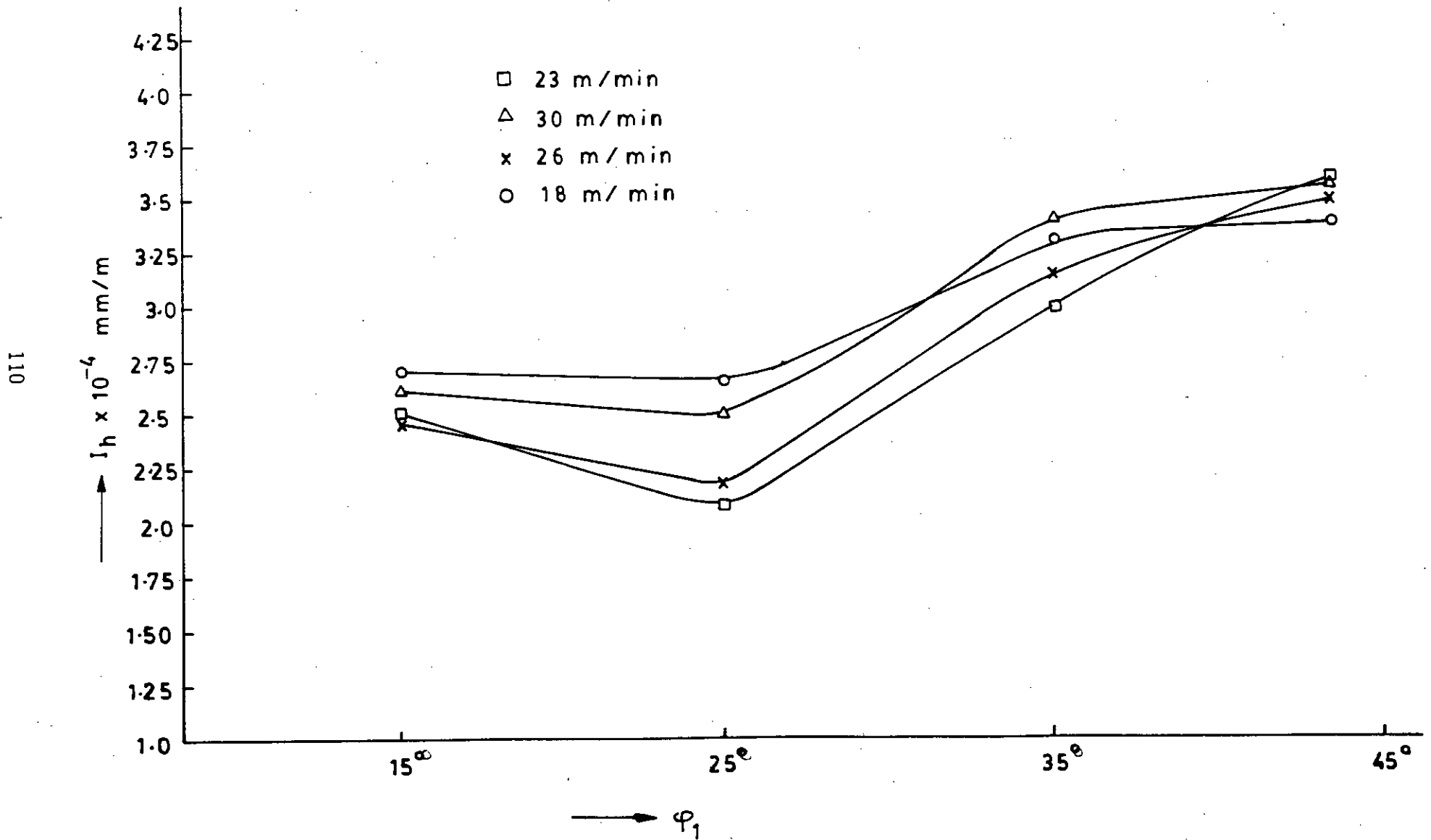


Figure-46
 Relationship between intensity of tool flank wear, I_h and variable cutting angle, ϕ_1 keeping other angles fixed ($\alpha=7^\circ$, $\alpha_1=7^\circ$, $\phi=50^\circ$, $\gamma=0^\circ$ & $\gamma_1=0^\circ$)

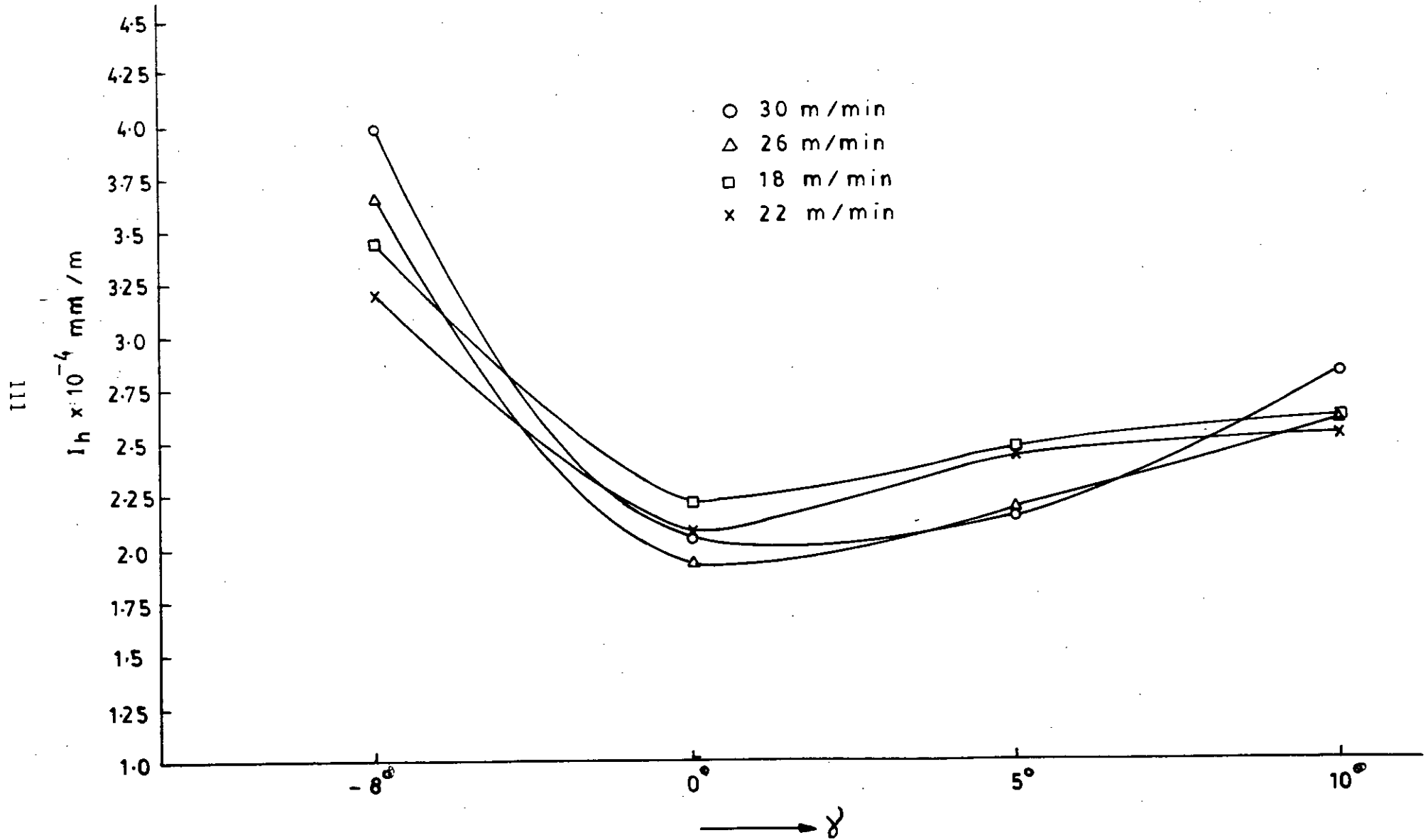


Figure-47
 Relationship between intensity of tool flank wear, I_h
 and variable cutting angle, γ keeping other angles
 fixed ($\alpha=7^\circ$, $\alpha_1=7^\circ$, $\phi=50^\circ$, $\phi_1=25^\circ$ & $\gamma_1=0^\circ$)

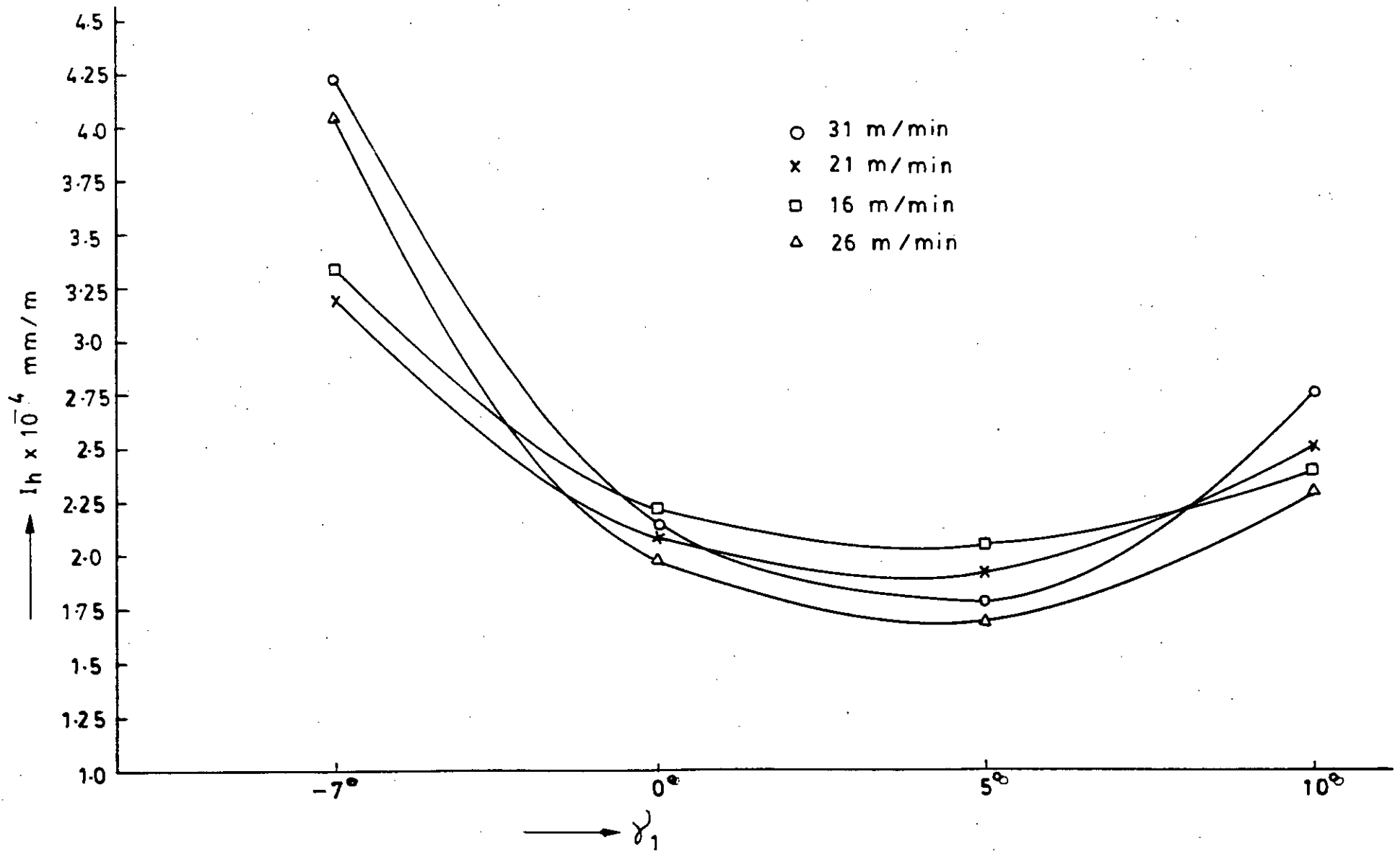


Figure-48
 Relationship between intensity of tool flank wear, I_h , and variable cutting angle, γ_1 , keeping other angles fixed ($\alpha=7^\circ$, $\alpha_1=7^\circ$, $\phi=50^\circ$, $\phi_1=25^\circ$, $\gamma=0^\circ$).

Table - 4
Determined values of minimum intensity of tool
flank wear for particular cutting speed
at different tool geometry

Particular cutting speed V_c m/min	Tool geometry		Minimum intensity of wear $I_h \times 10^{-4}$ mm/m
	Fixed angles	Variable angles	
17.5	$\alpha_1=6^\circ, \phi=45^\circ$ $\phi_1=20^\circ, \gamma=0^\circ$ $\gamma_1=0^\circ$	$\alpha=9^\circ$	2.950
22		$\alpha=7^\circ$	3.610
26		$\alpha=7^\circ$	2.775
30		$\alpha=7^\circ$	3.538
17	$\alpha=7^\circ, \phi=45^\circ$ $\phi_1=20^\circ, \gamma=0^\circ$ $\gamma_1=0^\circ$	$\alpha_1=5^\circ$	2.967
22		$\alpha_1=7^\circ$	2.788
26		$\alpha_1=7^\circ$	2.438
30		$\alpha_1=7^\circ$	2.600
17	$\alpha=7^\circ, \alpha_1=7^\circ$ $\phi_1=20^\circ, \gamma=0^\circ$ $\gamma_1=0^\circ$	$\phi=50^\circ$	2.588
22		$\phi=50^\circ$	2.550
27		$\phi=50^\circ$	2.370
32		$\phi=50^\circ$	2.611
18	$\alpha=7^\circ, \alpha_1=7^\circ$ $\phi=50^\circ, \gamma=0^\circ$ $\gamma_1=0^\circ$	$\phi_1=25^\circ$	2.632
23		$\phi_1=25^\circ$	2.081
26		$\phi_1=25^\circ$	2.175
30		$\phi_1=25^\circ$	2.513
18	$\alpha=7^\circ, \alpha_1=7^\circ$ $\phi=50^\circ, \phi_1=25^\circ$ $\gamma_1=0^\circ$	$\gamma=0^\circ$	2.203
22		$\gamma=0^\circ$	2.075
26		$\gamma=0^\circ$	1.925
30		$\gamma=0^\circ$	2.050
16	$\alpha=7^\circ, \alpha_1=7^\circ$ $\phi=50^\circ, \phi_1=25^\circ$ $\gamma=0^\circ$	$\gamma_1=5^\circ$	2.050
21		$\gamma_1=5^\circ$	1.913
26		$\gamma_1=5^\circ$	1.680
31		$\gamma_1=5^\circ$	1.788

Table - 5
 Determined values of optimum tool geometry
 and related cutting speed in turning stainless steel
 with cemented carbide cutting tool

Values of optimum tool angle	Corresponding cutting V_c m/min	Minimum intensity of tool flank wear $I_h \times 10^{-4}$ mm/m
$\alpha = 7^\circ$	25.8	2.7058
$\alpha_1 = 7^\circ$	25.9	2.4358
$\phi = 50^\circ$	27.0	2.3704
$\phi_1 = 25^\circ$	22.8	2.0778
$\gamma = 0^\circ$	25.8	1.9224
$\gamma_1 = 5^\circ$	25.9	1.6799

Table - 6
Determined values of optimum tool geometry
and related cutting speed in turning stainless steel
with cemented carbide cutting tool

Actual cutting speed V_c m/min	Optimum tool angle	Minimum intensity of tool flank wear $I_h \times 10^{-4}$ mm/m
26	$\alpha = 7^\circ$	2.7750
26	$\alpha_1 = 7^\circ$	2.4375
27	$\phi = 50^\circ$	2.3704
23	$\phi_1 = 25^\circ$	2.0812
26	$\gamma = 0^\circ$	1.9250
26	$\gamma_1 = 5^\circ$	1.6800

Table - 7
Individual Optimum values of different tool angles

Optimum tool geometry	$\alpha = 7^\circ, \alpha_1 = 7^\circ, \phi = 50^\circ,$ $\phi_1 = 25^\circ, \gamma = 0^\circ, \gamma_1 = 5^\circ$
-----------------------	---

values of minimum intensity of tool flank wear for particular cutting speed at different tool geometry is listed in table-4.

Intensity of tool flank wear vs. tool angle curves were plotted from data sheet-4 in Fig. 43, 44, 45, 46, 47 & 48 and optimum tool geometry was determined from Fig. 43-48 by considering minimum intensity of tool wear. The minimum values of intensity of tool flank wear I_h , respective cutting speed and optimum tool geometry are listed in table-6.

CHAPTER FOUR

RESULTS AND DISCUSSION

4.1 Results:

The critical cutting speeds of stainless steel at $S=0.2$ mm/rev., $t=0.1$ mm, $r=0$ and tool geometry $\alpha=5^\circ$, $\alpha_1=6^\circ$, $\phi=45^\circ$, $\phi_1=20^\circ$, $\gamma=0^\circ$ & $\gamma_1=0^\circ$ were found 18.6 m/min and 26.5 m/min this two critical cutting speeds was due to double carbide cemented carbide cutting tool. The optimum cutting speeds is less or equal to critical cutting speed i.e. $V_{op} \leq V_c^{23}$. In this case $V_{op1} \leq V_{c1}$ and $V_{op2} \leq V_{c2}$. Cutting speed range considered was 15 m/min to 30 m/min for stainless work material & cemented carbide cutting tool to suit the available rpm range and diameter of workpiece.

Optimum tool angle α is found from turning operation using $S=0.2$ mm/rev. $t=0.1$ mm, $r=0$, tool geometry, $\alpha_1=6^\circ$, $\phi=45^\circ$, $\phi_1=20^\circ$, $\gamma=0^\circ$, $\gamma_1=0^\circ$ keeping fixed and α variable, the values of α was 5° , 7° , 9° & 11° . The intensity of tool flank wear for $\alpha=5^\circ$ were 4.2849×10^{-4} , 5.5×10^{-4} , 5.4467×10^{-4} and 6.2784×10^{-4} mm/m at cutting speeds of 16.1, 21.7, 26.8, 30.3 and 33.9 m/min respectively. From the above calculations, it is seen that the intensity of tool flank wear I_h are not uniform along the cutting speed range, the curve I_h vs. V for $\alpha=5^\circ$ in Fig. 12 shows the two lower values of I_h also the other curves

of Fig.12 in same nature. It is for double carbide cutting tool, the minimum intensity of wear $I_h = 4.2849 \times 10^{-4}$ mm/m occurred for $\alpha = 5^\circ$ at 16.1 m/min also min $I_h = 2.7906 \times 10^{-4}$ mm/m for $\alpha = 7^\circ$ at 25.8 m/min.

Min $I_h = 2.9303 \times 10^{-4}$ mm/m for $\alpha = 9^\circ$ at 17.3 m/min and min $I_h = 3.1085 \times 10^{-4}$ mm/m at 15 m/min. i.e. absolute minimum value of $I_h = 2.7906 \times 10^{-4}$ mm/m for $\alpha = 7^\circ$ 25.8 m/min which is the optimum tool angle of α .

In case of α_1 , the absolute minimum value of $I_h = 2.4358 \times 10^{-4}$ mm/m for $\alpha_1 = 7^\circ$ at 25.9 m/min. For ϕ absolute minimum value of $I_h = 2.3704 \times 10^{-4}$ mm/m for $\phi = 50^\circ$ at 27 m/min. Absolute min value of $I_h = 2.0778 \times 10^{-4}$ mm/m for $\phi = 25^\circ$ at 22.8 m/min also for γ , absolute minimum value of $I_h = 1.9224 \times 10^{-4}$ mm/m for $\gamma = 0^\circ$ at 25.8 m/min and for $\gamma_1 = 5^\circ$ at 25.9 m/min. It is clear from the above results that there is a substantial effect of tool geometry I_h in turning operation. It means that the intensity of tool flank wear I_h varies quite appreciably with tool geometry and also cutting speeds.

It is observed that the intensity of tool flank wear I_h decrease gradually to the optimum tool angles setting and also the cutting speeds within a very short range.

From the experiment and the above result, it can be concluded that for double carbide tool, there are two critical cutting speeds and optimum cutting speeds range. Optimum tool geometry is $\alpha=7^\circ$, $\alpha_1=7^\circ$, $\phi=50^\circ$, $\phi_1=25^\circ$, $\gamma=0^\circ$ and $\gamma_1=5^\circ$ for stainless steel work material and cemented carbide cutting tool.

4.2 Discussion

Experiments have been performed in Mechanical workshop, BUET with conventional method, which is very simple and easy.

The considered parameter for the experiment are tool material, work material, cutting speed, nose radius and cutting tool angles α , α_1 , ϕ , ϕ_1 , γ and γ_1 . Used T₅K₁₀ type cemented carbide cutting tool material, stainless steel as work material, nose radius $r=0$ is constant, cutting speed range is select by determining critical cutting speed and determined tool geometry. Although cutting fluid and temperature have considerable influence on cutting conditions, yet cutting fluid was not used and temperature was not considered also feed and depth of cut was unchange during cutting operation i.e. feed and depth of cut were kept fixed during all the experiments.

Conventional method of calculation was used to determine the critical cutting speed. Chip-shrinkage calculation was done by

very simple method, but the chip lengths was difficult to measure. But was measured very carefully.

Fig.13-36, shows that the initial wear is higher than stable wear. This is due to the fact that the tool was not given initial wear by grinding but it is obvious that the wear is always higher for a sharp edge. However, initial wear was avoided in calculating the intensity of tool wear. It was also observed that the wear rate is not the same of all cutting sections for each cutting speed. It was not possible to maintain particular cutting speeds for different tool geometry due to unavailability of speeds for the remaining diameter of the workpiece and rpm available in the machine tool, also different cutting length of each section for the same reason, though the above factors did not effect the results, because the result obtained with respect to intensity of tool flank wear with related cutting speeds.

In Fig. 37-42 it was observed that at low cutting speeds, intensity of tool flank wear is low at most of the cutting tool angles. It is seen that with the increase in cutting speeds, intensity of tool flank wear increases in most all cases. For different tool geometry, some curves were not of the same nature. All curves in Fig. 37-42 showed symmetrical Characteristics i.e. intensity of tool flank wear is low at cutting speeds range 24 m/min to 29 m/min for different tool geometry. The factors such as chips, work material, vibration and other some parameters contribute to extremely low wear

rate of the tool in the above mentioned cutting speeds range. Optimum tool geometry, α was determined by comparing the curves of Fig. 37. Similarly, other geometrical parameters were determined in the same way from Fig. 38-42. The technique of finding the optimum tool geometry is so simple that it needs no adequate technical knowledge and expensive instruments. Having given a through idea about this technique, any technical person can predict the optimum tool geometry by using this method.

4.3 Limitation:

For more accurate control of tool geometry upto date tool grinding facilities should be made available in BUET. Though all possible efforts had been made to hold the tool geometry within a high precision level by using the facilities available, it is not unlikely that some errors in imparting the right geometry might have removed. The microscope by which the readings were taken is not a sophisticated one. Some errors may be incorporated during wear recording by that microscope, also some manual errors could be recorded during observing tool wear.

The determined tool geometry may deviate slightly during practical applications due to its various limitations of experimental facilities. Though the experimental data has been measured carefully.

Inspite of the small deviation of the results of proposed geometry from expected results, the approach has succeeded to show the way of achieving the final goal to optimize the tool geometry more precisely. Even the same approach may given better results providing the most sophisticated technological facilities.

CHAPTER FIVE
CONCLUSION, RECOMMENDATION
AND PROSPECT

5.1 CONCLUSION

From the results of the experiment, the following conclusion can be drawn.

1. There exists certain relationship between co-efficient of chip shrinkage, K and critical cutting speed, V_c . The maximum value of k corresponds to critical cutting speed, V_c .
2. It has been affirmed that for a pair of comented carbide cutting tool and stainless steel work matarial at a particular cutting speed the intensity of tool flank wear varies with the tool geometry.
3. There is a particular cutting tool angle at which the intensity of tool flank wear is minimumm for a particular cutting tool and work matetial for a given cutting condition. This particular cutting tool angle is known as optimum tool angle for the tool and work material.

4. Cutting speed has a significant effect on tool wear, because the temperature and vibration during cutting operation depend on cutting speed.
5. It has been established that for a cemented carbide cutting tool and stainless steel work material, the intensity of tool flank wear minimum when tool angles are $\alpha=7^{\circ}$, $\alpha_1=7^{\circ}$, $\phi=50^{\circ}$, $\phi_1=25^{\circ}$, $\gamma=0^{\circ}$, $\gamma_1=0^{\circ}$

5.2 RECOMMENDATION

Following suggestions are made to overcome the drawbacks which have been observed in the experimented work:-

1. This study had been conducted with a particular type of tool, tool material and work piece material. Further work can be performed varying the tool type, tool material and workpiece material.
2. This research had been conducted without using cutting fluid though cutting fluid has considerable effect as coolant during turning operation. There is a scope of study of the wear characteristics by using cutting fluid during cutting operations.
3. In this experiment a selected value of nose radius was used. Though this is the recommended value, there is

scope of further study by changing the value of nose radius to confirm the experimental results.

4. The experiment were performed by varying only one cutting angle. There is a scope of further study by varying two or more angles at a time. In that case more effective values could be determined.

5. A pair of cemented carbide cutting tool and stainless steel work material was used in the experiment due to the limitation of time. For the same reason it was not possible to change the feed, depth of cut, length of cut etc. Although the test results confirms the theoretical ideas, yet there is a scope of further study by changing the above conditions.

The experiment was conducted competely in the "laboratory Condition" and the proposed conventional method was developed on the basis on only these experimental results. Any change in "experimental condition" may change the values of test results, though in our opinion, the general pattern of the curves developed from the test results will hold good under changed conditions.

5.3 PROSPECT

This type of research work has a wide prospect in Bangladesh. If the concept of optimum tool geometry in the economical cutting conditions, adopted by the machine building industry including different engineering workshops they are bound to be economically benefitted. These industries and workshops are playing a vital role in our national development and the improvement of their competitive edge in the age of market economy is the pre-conditions of the socio-economic development of our country.

Thus, the present study has been made with a view to enriching the technical knowledge in the field of metal cutting operations.

There is wide fluctuation of the quality and price of the imported goods with the local products, the present study was undertaken to reduce the production costs and improve the quality of products in the international market. Thus, it has become necessary and it has practical importance determining the optimum cutting conditions. Therefore, there is a bright prospect of this research work.

REFERENCES

1. Ernst. H. : "Economics of Machining" Publication No. M-1955, Cincinnati Milling Machine Co., Cincinnati Ohio.
2. Armarego, E.J.A & Russel, J.K. : "Maximum profit rate as a criterion for selection of machining condition", International journal of Machine Tool Design & Research, vol. 6, no.1, March 1966.
3. Bjork, Yvind : "Mathematical Models for calculation of cutting data in rough training, "Paper at C.I.R.P. General Assembly, 1968.
4. Bakes, Jan. B : "Calculation of optimum cutting conditions", S.N.T.L. Technical Digest, vol.9, No.3, March 1967.
5. Basu, S.K. : "A New Approach for Optimum Solution in Metal Cutting Experiments", proceedings first M.T.D.R. conference, India, Jadavpur University, 1967.
6. Talantov., N.V. : "Contact process and wear of tool surface : Improvement of the cutting process and accuracy of machine tools", Ejevsk, USSR, 1969.
7. Kronenberg. M. : "Machining science and Application : Theory and Practice for Operation and Development of Machining Process," first English Edition, 1966.

8. Brewer, R.C. : "On the economic of the Basic turning operation", vol. 80, No.7, 1958.
9. Ernst, H., Merchant, W.E. & Kranacher : "Radio active cutting tools for rapid tool life testing, A.S.M.E, Cincinnati, June 1952.
10. Talantov, N.V., Cheriomoshnikov, N.P., Kurchenco. A.I., : "Influence of cutting speed on different characteristics of metal cutting process and tool wear". Technology of machine building and automation of production process, Volgograd 78, P-29-49.
11. Tresca, H. : "Memories Sur le Rabotage des Metaux", Bulletin De la Societe d' encouragement pour Lindustric national, 1973."
12. Mallock, A., : "The action of cutting Tools", proceedings of the Royal Society of London, England, vol-33, no.1, 1981.
13. Taylor, F.W. : "On the Art of Cutting Metals" Transaction of the ASME, vol.28, no.119, 1907.
14. Ernst, H. and Martellotti, M. : "The formation of built-up-edge", Mechanical Engineering, vol.57, no.2, 1938.
15. Ernst, H. : "Physics of Metal Cutting", Machining of Metals in 'Machining Metal', American Society for Metal, Cleveland, Ohio, 1938.

16. Ernst, H. and Marchant M.E. : "Surface friction of clean metals - A Basic Factor in the Metal Cutting process", Proceedings of a special Summer Conference on friction and surface finish, Massachusetts Institute of Technology, Cambridge, Mass, 1940.
17. Zorev, N.M. : "Investigation of Mechanical aspects of Metal Cutting Process", Moscow, Mashgiz, 1952.
18. Laladze, T.N. : "Metal Cutting Toolwear", Moscow, Mashgiz, 1958.
19. Makarov, A.D. : "Tool wear and Tool-life, Moscow, "Machine Building", 1966.
20. Nadai, K.A. : "Plasticity and Fracture of Solid Bodies", Moscow, Mir publication, vol.2, 1965.
21. Reznikov, A.N. : "Heat Physics in Metal Cutting", Moscow, Machine Building, 1969.
22. Time, I.A. : "Resistance of Metal and Wood during Cutting", St-Peterburg, Russia, 1970.
23. Sankar Roy : "Experimental determination of Optimum cutting conditions in turning low alloyed steel with cemented carbide tool", 1984, IPE, BUET.
24. Md. Khalilur Rhaman : "An experiment study of wear characteristics during cutting V-threads", IPE, BUET, 1988.
25. Md. Gullur Rahman : "Study of the existing manufacturing process and quality of local manufactured cemented carbide tool", IPE, BUET, 1991

26. Abu Hanifa : "Investigation of the effect of cutting speed on chip tool contact process and tool wear for steel of unknown composition, IPE, BUET, 1987.
27. Amin, A.K.M. : "Investigation of Laws of Chatters formation during metal Cutting and their influences on tool wear", Ph.D. thesis, Volgograd, 1982.
28. Amin, A.K.M.N. : "Experimental determination of optimum cutting conditions in turning low alloyed steel with cemented carbide tool", Journal of Science Research 5.1, Dhaka, 1987.
29. James G. Bralla : "A Principal Guide to Low-cost production"
: "Tool and Manufacturing Engineers Hand Book", Society of Manufacturing Engineers, 3rd Edition, 1976.
30. Laladge, T.N., : "Chip formation during Metal Cutting Process", Moscow, Mashgiz, P-200, 1952 (Translated From Russian into English)
31. Rozenberg, A.M. and Eremin, A.N., : "Elements of Theory of Metal cutting", Mashgiz, Moscow, 1956.
32. Clushin, T.N., : "Metal cutting process", Moscow, Mashgiz, P-356, 1958 (Translated from Russian into English)

33. Zorev, N.M., Gronovskiy, G.I., Larina, I.N., Tritiakov, I.P., : "Development of the science of Metal cutting", Moscow, Machine building publication P-416, 1967 (Translation from Russian into English)
34. Bhoothroyd, G., Eagle, J.M., and Chisholm, A.W.J., : "Effect of tool flank wear on the temperature generated during Metal cutting", Advances in machine tool Design Research, P667, 1967
35. Babrov, V.F., : "Productions of theory of metal cutting", Publication machine building, Moscow, P-344, 1975. (Translation from Russian into English)
36. Eckersley H. and Trent E.M., : "Manufacturing and application of sintered carbides" P-349-377, I.P.E. vol. 26 1 - 12, 1947
37. Rafiqui Islam : "A new method for testing quality of cemented carbide tools and a comparative study of different cemented carbide and high speed steel tools available in the local market", nov. 1989 IPE, BUET.

